CYTOSOLIC PROTEIN INTERACTION WITH THE VOLTAGE DEPENDENT ANION CHANNEL OF THE MITOCHONDRIAL OUTER MEMBRANE CONTROLS CELLULAR RESPIRATION

by

Kely L. Sheldon

A dissertation submitted to Johns Hopkins University in conformity with the requirements for the degree of Doctor of Philosophy

Baltimore, Maryland

December, 2013

ABSTRACT

The voltage dependent anion channel (VDAC) is a beta-barrel protein that spans the mitochondrial outer membrane and serves as the passageway for the flux of metabolites responsible for mitochondrial function. It was discovered in 2008 that the cytosolic protein dimeric tubulin interacts with VDAC causing highly reversible blockages of the channel (Rostovtseva and Bezrukov 2008). It was later shown that this tubulin-blocked state of VDAC is impermeable for ATP (Gurnev, Rostovtseva et al. 2011; Noskov, Rostovtseva et al. 2013), suggesting that this protein-protein interaction may be responsible for the regulation of respiration. Here, we expand on the current understanding of VDAC demonstrating a possible control mechanism of this tubulin-VDAC interaction. We show that when VDAC is phosphorylated *in vitro* by both protein kinase A (PKA) or glycogen-synthase kinase (GSK) and reconstituted into a planar lipid bilayer the on-rate of tubulin-VDAC interaction is increased by over two orders of magnitude. Our results were confirmed in subsequent whole cell experiments using microtubule stabilizing or destabilizing agents to alter the concentration of free tubulin in the cytosol. The increase and decrease of local tubulin concentration altered mitochondrial potential ($\Delta\Psi$) as measured by tetramethylrhodamine methyester (TMRM). Moreover, when cells were treated with small synthetic peptide protein kinase inhibitor (PKI) inhibiting the activity of PKA, $\Delta\Psi$ was increased, even after treatment of cells with microtubule destabilizing agent cholchicine. To explore the role that each VDAC isoform plays in the modulation of mitochondrial potential, samples of single VDAC isoforms were isolated from HepG2 cells treated with siRNA against two VDAC

isoforms and reconstituted into planar lipid bilayers. Remarkably, although the VDAC isoforms displayed similar single channel characteristics, each isoform exhibited markedly different sensitivities to both voltage induced gating, with VDAC2 being the most voltage sensitive, followed by VDAC1 and VDAC3, respectively, and to tubulin interaction, with VDAC1 and VDAC2 having tubulin-VDAC on-rates nearly two orders of magnitude higher than VDAC3. Taken together, we speculate that cellular respiration may be influenced by the local tubulin concentration, the expression rates of each VDAC isoform, the phosphorylation state of VDAC, and the potential across the MOM.

PREFACE

The work outlined in this dissertation was carried out in the Department of Molecular Microbiology and Immunology, Bloomberg School of Public Health, Johns Hopkins University, and the Program of Physical Biology, National Institute of Child Health and Human Development, National Institutes of Health over the period from August 2009 to December 2013 under the mentorship of Dr. J. Marie Hardwick and Dr. Sergey M. Bezrukov. This dissertation is the result of my work and includes nothing which is the outcome of work done in collaboration by others, except for a few instances which are clearly defined in the text.

ACKNOWLEDGEMENTS

I am grateful to my Johns Hopkins University supervisor, J. Marie Hardwick, for her enduring support of both my education and research. I would like to thank her for invaluable lessons about the importance of scientific rigor and for the freedom she granted to me to explore my scientific interests.

I am also indebted to my NIH supervisor, Sergey M. Bezrukov, who in addition to dealing with my bouts of scientific frustration was able to teach me the true meaning of science. The lessons he taught will be forever inscribed in me.

I am grateful of the mentorship of Tatiana K. Rostovtseva, who taught me the foundations of which this thesis is based.

To Dan Sackett, the 'Tubulin-Guru', who taught me the importance of understanding the science behind protocol. Your wealth of knowledge will forever give me something to strive towards.

I would like to thank each of my Thesis Committee members for their insight and continued support of my research: Pete Pedersen, Sean Prigge, Bary Zirkin and my two alternates Rob Jensen and Anthoney Leung.

Special thanks are due to Brenda Hanning, Director, Office of Education at NICHD for her encouragement, endurance, and expert assistance during the many years of my IRTA Fellowship at the NIH.

I would like to collectively thank all of my colleagues in ‘Building 9’ whose support and guidance over the years was invaluable to my research: Philip Gurnev, Oscar Teijido Hermida, Katya Nestorovich, Ralph Nossal, Shay Rappaport, Don Rau, Nina Sidorova, and Michael Weinrich.

Additionally, I want to thank Dr. Marco Colombini who provided me with advice, expertise, and all things VDAC.

And to the two people responsible for taking care of all of the paperwork, keeping me on track, ensuring my role as a student and IRTA fellow, and providing me more support than either will ever know, Gail O’Connor and Erlinda Inejosa-Ortanez.

I would like to extend a very large thank you to both of my parents, Jerry and Laurie Sheldon. I am an amalgam of my Father’s intellect and Mother’s curiosity. Without your continued support, words of wisdom, love and encouragement, I do not think I would be where I am today.

Finally, I would like to thank my family, and friends for their continued support: Cory and Jennifer Sheldon, Blake and Makenna Henry, Peko Tsuji, Kazuyuki Kitatani, Russell Jenkins, Dr. Yusuf Hannun and Dr. Lina Obeid, Cameron G. Roberts and Jillian Legault.

FUNDING

My work and studies were supported by the National Institutes of Health, IRTA Program, Individual Graduate Partnership Program, and the Dr. J. Harold Drudge Scholarship.

TABLE OF CONTENTS

TABLE OF FIGURES

CHAPTER 1: INTRODUCTION

PART I. CURRENT UNDERSTANDING OF THE VOLTAGE DEPENDENT ANION CHANNEL

Although there has been a steady shift in health in industrialized countries towards age-related and metabolic diseases, the role of mitochondrial respiration in the development and progression of disease has only recently begun to be appreciated (Wallace 2005). According to the American Diabetes Association, in 2007 there were an estimated 17.5 million Americans living with diagnosed type 1 or type 2 diabetes (Herman 2013). Analysis of the 2010 United States Census Report estimated that about 5.1 million Americans are currently suffering from the neurodegenerative disorder Alzheimer's disease, not including those that may be afflicted, but undiagnosed (Hebert, Weuve et al. 2013). Parkinson's disease, a chronic neurodegenerative disease, is estimated to have about a 0.3% prevalence (roughly 1 million people) in the United States, with an estimated doubling in diagnoses by 2040 (Kowal, Dall et al. 2013). Cancer, a major public health concern in the United States, is estimated to be responsible for one out of every four deaths (Siegel, Naishadham et al. 2013). These are only a few of the diseases impacting the United States and other developed parts of the world, each having a plausible link to some form of energy disorder.

Mitochondria are present in every mammalian cell excluding red blood cells, which during cell maturation rid the cell body of these organelles. Mitochondria are dynamic,

double-membrane organelles that are thought to be a result of the arrival of the first eukaryote, according to the proposed endosymbiotic theory (Margulis 1975). The mitochondrial inner membrane houses the components of the electron transport chain, and allows for the establishment of a proton gradient that drives ATP-synthase to produce ATP, the major source of energy for cellular metabolism. ATP-synthase is located on the inner mitochondrial membrane and requires respiratory substrate flux through the mitochondrial outer membrane (MOM) to maintain proper function. Although when first uncovered, the MOM was thought to play little role in mitochondrial function, it has been known since 1957 that the MOM shows selective permeability, allowing for the flux of small molecules like sucrose between the cytosol and inner mitochondrial space, but restricting the flux of polysaccharides greater than 50 kDa (Werkheiser and Bartley 1957). Eight years later, it was established that the MOM isolated from plant cells contained large channels with a diameter of roughly 2.5 to 3 nM as detected by negative staining and subsequent electron microscopy (Parsons, Bonner Jr et al. 1965), that were thought to be responsible for the regulation of metabolite flux. It was not, however, until reported in 1976 that the first voltage dependent anion channel (VDAC) was isolated from the mitochondrial fraction of *Paramecium aurelia* and reconstituted into a planar lipid bilayer, where it produced unique conducting channels that were both voltage dependent and highly selective for the anion chloride (Schein, Colombini et al. 1976). Since then, there has been a large effort to elucidate both the 3-dimensional structure and the function of VDAC.

VDAC structure

The first attempt at defining the structure of VDAC was published in 1989, where the authors utilized site-directed mutagenesis to probe which amino acids might be responsible for channel selectivity (Blachly-Dyson, Peng et al. 1989). The authors concluded that a lysine at position 61 to glutamic acid substitution altered channel selectivity as detected by channel reconstitution experiments, suggesting that this amino acid was located in the path of ions through the channel pore. One year later, 29 different residues were subjected to site-directed mutagenesis, and each construct was expressed in yeast, isolated biochemically, purified, and reconstituted into planar lipid bilayers (Blachly-Dyson, Peng et al. 1990; Mannella, Forte et al. 1992; Peng, Blachly-Dyson et al. 1992; Song, Midson et al. 1998; Angeles, Devine et al. 1999). Changes in channel selectivity were observed with the mutation of 14 of these amino acids, suggesting that these residues also were lining the channel pore. This allowed the authors to propose a structure of the open channel composed of 13 transmembrane beta-strands, and one transmembrane alpha-helix (Blachly-Dyson, Peng et al. 1990). Although the authors made a note suggesting the possibility that functional VDAC may be composed of a homodimer or n-mer of a larger channel complex, later worked verified that each ~30 kDa peptide was responsible for forming one unique VDAC channel (Peng, Blachly-Dyson et al. 1992).

During the early 1990s, emerging bioinformatics methods were used to compare the known biophysical properties of VDAC with other well-known bacterial channels thought to have similar beta-barrel structures. By using this comparative approach, the presence of anti-parallel beta-strands was detected using a comparative multiple alignment algorithm called the Gibbs sampler, but the number of possible beta-strands remained elusive, primarily due to the limitations of this predictive software (Mannella, Neuwald et al. 1996). When structure prediction software based on neural network-based predictors was used to study VDAC1 across many eukaryotic species, it was predicted that there were 16 anti-parallel beta-strands that spanned the membrane allowing for the development of a three-dimensional model of VDAC from *Saccharomyces cerevisiae* (Casadio, Jacoboni et al. 2002), which differed from the previously proposed model that contained only 13 beta-strands (Blachly-Dyson, Peng et al. 1990). Recent structural studies were paramount for the determination of the proper folding pattern of VDAC. Several papers were subsequently published predicting generally similar VDAC structures varying only by some minor differences between each of them.

The most recent solution structure of VDAC1 using nuclear magnetic resonance (NMR) was solved as a beta-barrel composed of 19 beta-strands, with the first and last strand meeting in parallel (Hiller, Garces et al. 2008). The authors did make mention of the need for cholesterol to obtain reconstituted recombinant VDAC1 channels that behaved in a similar fashion to native VDAC. Only a few months later, the structure of human VDAC1 was solved by both NMR spectroscopy and X-ray crystallography, also showing a beta-barrel composed of 19 beta-strands with the addition of an alpha-helix and with a

horizontal orientation at the midpoint of the channel lumen (Bayrhuber, Meins et al. 2008). Still one month after this report, the crystal structure of VDAC1 from mouse was solved at a 2.3 angstrom resolution again showing a beta barrel of 19 beta-strands, however with different predictions for the alpha-helix (Ujwal, Cascio et al. 2008). In this structure, The N-terminus was oriented against the interior wall leading to a constriction site at the center of the VDAC channel. Interestingly, only a few months later, a prominent investigator in the area of VDAC research published an opinion paper suggesting that these solved structures of VDAC1 most likely do not represent the "native" structure of VDAC, referring to all of the previous work dealing with biochemical analysis of the channel structure (Colombini 2009). Instead, Colimbini suggested that in place of 19 beta-strands seen in the crystal structures, the native or properly folded structure has 13 strands, and proposed that there are large loops (5 loops on one face and 1 loop on the other face) formed by these other beta-strands predicted to be buried in the membrane by previous structures and models. Even though the exact structure has yet to be verified, it is encouraging that the field took a tremendous leap towards elucidation of the proper structure of VDAC.

VDAC isoforms

The first indication that VDAC may exist in multiple unique isoforms was in 1990 when highly purified MOM was subjected to two-dimensional gel electrophoresis followed by isoelectric focusing experiments which suggested the presence of at least three unique VDAC isoforms (Pavlica, Hesler et al. 1990). VDAC exhists as three isoforms, each

VDAC being coded for by a different gene. Though research on VDAC spans more than 40 years, it was only in the last decade that the need for differentiation between the three mammalian isoforms – VDAC1, VDAC2, and VDAC3 – has become evident. Therefore, the majority of the published work on "VDAC" most probably concerns VDAC1, which is generally the most abundant isoform in the fractions being studied (Yamamoto, Yamada et al. 2006; Poleti, Tesch et al. 2010). The immediate questions arise: how much of the current data pertains to VDAC1 and how much is still unknown about VDAC2 or VDAC3? There is a strong sequence homology between all three mammalian VDAC isoforms, which suggests that their structures are most probably quite similar. For example, if the mouse VDAC1 X-ray structure is utilized as a guide for VDAC2 and VDAC3, each isoform can be modeled to form similar structures (19 beta-strands and the N-terminus comprised of an alpha-helix) (De Pinto, Guarino et al. 2010). Although structure is a good indication of function, it is not enough to infer that all three isoforms serve the same purpose.

All three mammalian isoforms of VDAC have been expressed and purified from yeast, and reconstituted into planar lipid bilayers showing differences among the three channels (Xu, Decker et al. 1999). All three isoforms form similar channels displaying a conductance around 4 nS in 1 M KCl. In addition, each channel seems to close or "gate" into lower conducting states upon the application of high transmembrane potentials (>50 mV), though VDAC3 was noted to be more difficult to insert into planar lipid bilayers (*see Chapter 3*). Mammalian VDAC1 has been purified from many different tissues while VDAC2 has only been isolated from spermatozoa (Menzel, Cassara et al. 2009).

Mammalian VDAC3 has yet to be isolated, purified, and reconstituted. However, as described in this thesis, isoform-specific siRNA treatment of HepG2 cells has permitted the study of individual isoforms of VDAC and their reconstitution into planar lipid bilayers. For the first time, functional differences between all three isoforms were possible, revealing that VDAC1 and VDAC2 voltage gate at lower potentials than VDAC3 (*see Chapter 3)*. Additionally, we found that the sensitivity of each isoform to tubulin binding varies greatly: VDAC1 and VDAC2 are highly sensitive to tubulin interaction, while VDAC3 remains virtually tubulin-insensitive (*see Chapter 3*). This adds strong support for the functional differences among the three channels.

Interestingly, the expression of the three VDAC isoforms varies greatly depending on the tissue type. In general, the expression of each isoform is ubiquitous as detected by mRNA and gel electrophoresis followed by subsequent detection by isoform-specific antibodies (Sampson, Lovell et al. 1997; Anflous, Blondel et al. 1998; Rahmani, Maunoury et al. 1998; Massa, Marliera et al. 2000). While VDAC1 and VDAC2 seem to generally be the most abundantly expressed out of the three isoforms, there are a few exceptions. In testis, VDAC3 is largely expressed as well as VDAC2, and to a minor extent VDAC1 (Sampson, Lovell et al. 1997; Rahmani, Maunoury et al. 1998) whereas in HepG2 cells, VDAC1 and VDAC2 make up the majority of the expressed VDAC (roughly 90% between the two isoforms) followed by about ~10% of VDAC3 (*see Chapter 3*) (Maldonado, Patnaik et al. 2010). The differences in tissue expression of the three isoforms add support for the differing roles of each isoform. Additionally, it was noted that the transcript levels of VDAC2 and VDAC3 are highly influenced by the other

VDAC isoforms, suggesting a probable cross-talk between VDAC gene isoforms (De Pinto, Guarino et al. 2010).

Post-translational modifications of VDAC

Mitochondria are widely known as "the powerhouse of the cell" since being coined as such in 1957 (Siekevitz 1957). One of the primary functions of mitochondria is in the transformation of "food-energy" into usable energy for cellular processes, namely ATP. The mitochondrial outer membrane (MOM) provides a selective barrier between the cytosol and inner mitochondrial space. The MOM is studded with protein channels (e.g. TOM, VDAC) that allow for the flux of respiratory substrates, proteins, and other metabolites. VDAC is thought to contain large loops at the mouth of the channel, facing the cytosolic side of MOM. Interestingly, proposed loops are present in all solved structures, but are a bit more prominent, as defined by length, in the first proposed structure deduced from site-directed mutagenesis studies (Bayrhuber, Meins et al. 2008; Hiller, Garces et al. 2008; Ujwal, Cascio et al. 2008; Colombini 2009). It is these loops that are thought to facilitate protein-protein interaction.

There has been a recent focus on VDAC phosphorylation and the downstream effects due to the developing prominent role VDAC is thought to play in cellular respiration. Phosphorylation is typically seen as an "on-off" switch for many protein functions and is a versatile post-translational modification due to its reversibility. In studies that I completed before graduate school, I found that dimeric tubulin was shown to interact specifically and highly-reversibly with VDAC (Rostovtseva, Sheldon et al. 2008), and the

sensitivity of this interaction was greatly increased after phosphorylation of the VDAC channel, presumably on the channel loops (*see Chapter 2*). Additionally, it has been reported that there are many cellular kinases that target mitochondria and specifically VDAC, leading to phosphorylation (Distler, Kerner et al. 2007; Kerner, Lee et al. 2012). For the majority of these phosphorylation events, the outcome is still largely unknown. However, glycogen-synthase-kinase 3-beta and protein kinase C have been shown to localize near the mitochondria, and the cross-talk between the two kinases and subsequent phosphorylation of VDAC is thought to modulate hexokinase-VDAC interaction (Pastorino and Hoek 2008).

VDAC has also been shown to be a target of acetylation, both N-terminal and lysine epsilon acetylation, though the function of this post-translational modification is still unknown (Distler, Kerner et al. 2007; Kerner, Lee et al. 2012). Astoundingly, it is thought that over 85% of human proteins (as detected in HeLa cells) may be candidates for N-terminal acetylation (Zhang, Ye et al. 2011). Although previous work linked N-terminal acetylation to protein function/assembly and intracellular location (Van Damme, Arnesen et al. 2011; Zhang, Ye et al. 2011), recent evidence has linked acetylation to regulation of cellular metabolism and sensitization of the cell to apoptosis (Yi, Pan et al. 2011). Concerning VDAC, all three isoforms have been shown to be targets of epsilon lysine acetylation: VDAC1 ($K^{28, 33, 41, 42, 122, 132, 234, 237}$), VDAC2 ($K^{32, 75, 121}$) and VDAC3 ($K^{20, 28, 61, 63, 109}$) (Kerner, Lee et al. 2012). In each of these cases, the functional consequences of the acetylation are still unknown; however post-translational

modifications are common markers of cell-signaling events, implying that VDAC may play a larger role in cell signaling events.

Even though VDAC is the most abundant protein in the MOM, little is known as to the regulation of this protein channel. Remarkably, all three VDAC isoforms have been shown to be the targets of post-translational modifications, namely phosphorylation and acetylation. Likely, more post-translational modifications of VDAC will be uncovered in the near future. Even with the currently known sites, there is a disconnect between phosphorylation/acetylation and the outcome of these events, evermore complicated by the presence of three isoforms whose expression levels are dependent on other cell signaling events.

VDAC and its role in apoptosis

There is a major misunderstanding in the field that arose when VDAC was implicated as a component of the permeability transition pore (PTP), a large protein complex thought to form linking the inner and outer mitochondrial membranes leading to cytochrome *c* release and the progression of apoptosis (Szabo, De Pinto et al. 1993; Szabo and Zoratti 1993; Crompton, Virji et al. 1998). However, with evidence suggesting that even in the absence of VDAC1, VDAC2 or VDAC3, or all three isoforms the cells maintain the ability to form the PTP, this view has largely been discredited (Krauskopf, Eriksson et al. 2006; Baines, Kaiser et al. 2007). Nevertheless, there is strong evidence supporting the role that VDAC may play in the cellular events leading to apoptosis.

Mitochondrial outer membrane (MOM) permeability plays a major role in apoptotic signaling, whereby the release of cytochrome *c* from the inner mitochondrial space activates subsequent apoptotic signaling. Although VDAC itself is too small for the flux of cytochrome *c*, it is permeable to monovalent and divalent ions. When in the open state, VDAC is slightly anion selective displaying a reversal potential in a 10x gradient of KCl of about -19 mV for VDAC isolated from mouse liver suggesting a preference for negatively charged metabolites such as ADP (Rostovtseva, Tan et al. 2005). Surprisingly, in the VDAC open state, Ca^{2+} is still able to flux through the channel even with the open state anion selectivity. However, when VDAC gates or closes into lower conducting states, the selectivity of the channel changes from anion selective to cation selective, and the flux of Ca^{2+} through the channel is estimated to be about 10-fold higher than in open state (Tan and Colombini 2007). This apparent preference of the VDAC closed state for calcium flux may be involved in cellular calcium homeostasis. Although mitochondria are important calcium stores, excessive permeation of calcium into the mitochondria leads to mitochondrial swelling, permeability transition and apoptotic signaling. However, the question of what mechanisms modulate VDAC open and closed states remains. The name "voltage-dependent" anion channel is a bit of a misnomer. True, at high transmembrane potentials, VDAC will begin to gate or close into lower conducting states; however, the best estimates of MOM potential only fall between 10-15 mV to as high as 60 mV (Lemeshko 2006). Potentials much greater than 20-30 mV are required to cause VDAC to gate into lower conducting states, so most probably, there is

cooperation between transmembrane voltage and other cytosolic factors that modulate channel VDAC closure.

The MOM is thought to serve as a platform for the orchestration of apoptotic events, including protein interaction with VDAC. After stimulation of apoptosis, cytochrome *c* is released from the mitochondria into the cytosol where it further activates caspases eventually leading to cell death. Bcl-2 family of proteins are widely thought to regulate MOM permeability for cytochrome *c* during apoptosis, however recent evidence suggests that the Bcl-2 family proteins also have other important cellular roles, i.e., in mitochondrial morphology and subcellular localization of these organelles (Hardwick, Chen et al. 2012; Hardwick and Soane 2013). While Bax and Bid (tBid) are proapoptotic and promote the release of apoptogenic factors, Bcl-2 and Bcl-xL prevent this release (Rostovtseva, Antonsson et al. 2004). Originally, it was thought that the Bcl-2 family protein Bax interacted directly with VDAC leading to the release of cytochrome *c* and apoptosis (Shimizu, Narita et al. 1999; Shimizu, Shinohara et al. 2000; Tsujimoto and Shimizu 2000). It was proposed that the association of Bax with VDAC leads to the formation of a larger pore complex involving Bax and VDAC, resulting in the release of cytochrome *c* (Shimizu, Narita et al. 1999; Shimizu, Ide et al. 2000). However, it was later shown that Bax induces no changes to VDAC reconstituted into a planar lipid bilayer (Rostovtseva, Antonsson et al. 2004). Moreover, cytosolic Bax is usually present in a monomeric state, which is incapable of forming channels (Hsu and Youle 1998). Conversely, the oligomeric form of Bax does indeed have channel activity on mitochondrial outer membranes and these channels have sensitivity to both voltage and

pH (Desagher, Osen-Sand et al. 1999). However, extensive research has indicated that VDAC interaction with either monomeric or oligomeric Bax is not responsible for cytochrome *c* release. Bax expressed in VDAC-deficient yeast is still able to promote cytochrome *c* release and induce apoptosis in a similar fashion when VDAC1 is present (Priault, Chaudhuri et al. 1999; Gross, Pilcher et al. 2000). Recent evidence suggests that there may be other cytosolic components required for Bax channel formation on the MOM, which postulates that Bax, in unison with membrane remodeling factors (MRFs), work together to stress the outer membrane leading to the formation of a lipid containing pore (Basanez, Soane et al. 2012). Additionally, it was shown that Bax is able to form channels of multiple conducntances in the mitochondrial outer membrane, however, the majority of these channels are too small for the release of cytochrome *c* (Jonas, Hardwick et al. 2005). Further, the authors speculated that these Bax channels may serve an addition function not involved in cell death pathways, however, that the rare incidence of larger Bax channels may be representative of activated Bax involved in cell death pathways.

The BH3-only protein of the core Bcl-2 family, Bid, has been shown to directly interact with VDAC leading to channel closure, but only after being cleaved or truncated (tBID) by caspase-8 (Brustovetsky, Dubinsky et al. 2003; Rostovtseva, Antonsson et al. 2004; Rostovtseva and Bezrukov 2008; Ott, Norberg et al. 2009). Full-length Bid is dispersed throughout the cytosol, but after cleavage, translocates to mitochondria leading to the release of cytochrome *c* by either directly activating Bax or by inhibiting Bcl-xL, thus transmitting the signals from the plasma membrane to the mitochondria (Li, Zhu et al.

1998). It has been reported that tBid is able to greatly decrease VDAC open probability in both reconstituted single and multichannel experiments (Rostovtseva, Antonsson et al. 2004). A reduction in open probability suggests VDAC closure and a reduction on MOM permeability.

In brief, there are two proposed models of cellular events leading to cytochrome *c* release: (1) Bcl-2 family protein-protein interaction leading to MOM permeabilization and subsequent cytochrome *c* release, and (2) inhibition of VDAC, leading to an over-accumulation of metabolites and substrates in the mitochondria, which causes matrix swelling and eventual membrane rupture to release cytochrome *c*. It is now apparent that VDAC is also not required for the formation of the permeability transition pore, and while some proapoptotic proteins interact specifically with VDAC, it is believed that others act in concert with unknown factors leading to MOM permeabilization and the release of cytochrome *c*.

VDAC and hexokinase

Hexokinase is an enzyme responsible for the conversion of glucose into glucose-6-phosphate (G6P) in glycolysis by facilitating the phosphorylation of the sixth carbon on glucose, thereby inhibiting its flux out of the cell through glucose transporters. In mammals, there are four isoforms of hexokinase, HK1, HK2, HK3, and HK4, which is also known as glucokinase. Both HK1 and HK2 bind to mitochondria, however HK3 lacks the hydrophobic region of the N-terminus, which may explain its more perinuclear

localization (Wilson 2003). Interestingly, there has been strong evidence for the role of HK2 in cancer metabolism (Mathupala, Ko et al. 2006; Mathupala, Ko et al. 2009; Wolf, Agnihotri et al. 2011; Patra and Hay 2013; Patra, Wang et al. 2013). The levels of HK2 are greatly up-regulated in cancer cells, which is thought to support increased energy production via glycolysis (Pastorino and Hoek 2008).

Classically, the Warburg Effect describes the phenotype of many tumor cancer cells to undergo glycolysis as their primary mode of energy production, even in the presence of oxygen (Pedersen 2008). It is important to note that while there are tumors that exhibit high glycolytic rates, tumor cells do not rely solely on glycolysis. In fact, the mitochondria from cancer cells are still functional – e.g. when isolated still maintain a proper functional electron transport chain and respire; energy production via oxidative phosphorylation however, is toned down (Pedersen 2007). VDAC has been proposed as the docking site for HK2, based on coimmunoprecipitation studies (Chiara, Castellaro et al. 2008) and recently by two-color STED microscopy (Neumann, Buckers et al. 2010). Nevertheless, there is a large discrepancy in the field concerning the outcome of this interaction. Studies showing that bound HK causes VDAC to close was detected by reconstituted VDAC experiments (Azoulay-Zohar, Israelson et al. 2004). However, as described in Chapter 4, we have found that both single and multichannel level that although HK does indeed interact with VDAC, the binding of HK to VDAC does not induce channel closure. These data support another hypothesis in the field, where HK binds to VDAC, maintaining the channel in its open state, and, therefore, gaining preferential access to ATP fluxing out of VDAC to the cytosol (Pedersen 2007; Guzun,

Gonzalez-Granillo et al. 2012). As mentioned above, closing VDAC hinders mitochondrial potential, and eventually leads to cell death, the opposite of how cancer cells are thought to be programmed.

VDAC and neurodegenerative disease

Accumulating evidence supports the important role that cellular energy plays in many neurodegenerative disorders, e.g. Alzheimer's disease, Parkinson's disease, and stroke. Because of increasing understanding of VDAC and its role as that of the gateway controlling respiratory metabolite flux, there is a growing interest in VDAC as the major player in these energy-dependent neurological diseases.

Alzheimer's disease (AD) is defined as a late-onset and age dependent neurodegenerative disease that is followed by changes in behavior and a decrease in active memory (Aliev, Obrenovich et al. 2013). Among the early events of AD progression is mitochondrial oxidative damage, however this mitochondrial dysfunction is still largely not understood (Manczak and Reddy 2012). It was shown in mouse models that expression of amyloid-beta soluble peptides characteristic of AD was able to induce overexpression of VDAC1 in neurological tissues (Cuadrado-Tejedor, Vilarino et al. 2011). In another study, it was shown that the N-terminus of human VDAC1 contains a classical GxxxG motif that shares corresponding sequences with the amyloid peptides unique to AD, which the authors concluded interacted with the plasma membrane VDAC1 and kept the channel in its open conformation (Thinnes 2011). It should be noted that the presence of VDAC on

the plasma membrane or anywhere besides the MOM remains a topic of much controversy. However, there have been studies suggesting that VDAC may be present in membranes other than the MOM (Bahamonde, Fernandez-Fernandez et al. 2003; Bahamonde and Valverde 2003; Elinder, Akanda et al. 2005; De Pinto, Messina et al. 2010).

Parkinson's disease (PD), like other neurodegenerative disorders, has no effective treatment except amelioration of symptoms, rather than the underlying and still unknown cause (McGhee, Royle et al. 2013). Two proteins have been identified as important housekeepers for damaged mitochondria, Parkin and PINK1. Heritable mutations in throughout Parkin or PINK1 can lead to the progression of PD (Morrison 2003; Bradbury 2004). It was shown that parkin is recruited to the MOM by all three VDAC isoforms, VDAC1, VDAC2, and VDAC3, where in the absence of VDAC, parkin is not recruited to the MOM of defective mitochondria and mitophagy is hindered (Geisler, Holmstrom et al. 2010; Sun, Vashisht et al. 2012). Thus, the accumulation of dysfunctional mitochondria is a mainstream hypothesis to explain PD. One common hallmark of PD is the rapid accumulation of the small neurological peptide alpha-synuclein, whereby it has been shown that overexpression of this peptide in rat brains leads to the peptide targeting the mitochondria and is enough to induce PD-like symptoms (Lu, Zhang et al. 2013). Even so, little is known about its function. Recent evidence has shown that alpha-synuclein specifically interacts with VDAC reconstituted into planar lipid bilayers, causing rapid channel closure thought to be a product of the peptide translocation through

the inner lumen of the VDAC pore (*Gurnev, P., NIH, unpublished*). Much work remains in ascertaining the direct events leading to PD development.

VDAC and its role in cancer

One primary indication of VDACs role in cancer progression was in the discovery that all VDAC isoforms are over expressed in cancerous cells (Mathupala and Pedersen 2010). It was reported that in many mammalian cell lines, the expression of VDACs is much higher in tumor cells verses non-tumor cells (Shinohara, Ishida et al. 2000; Simamura, Hirai et al. 2006; Simamura, Shimada et al. 2008), though this should be viewed with some skepticism, as distinguishing between cancerous and noncancerous cultured cells is not a trivial task, and appropriate definitions have yet to be established.

As previously mentioned, one of the characteristics of many cancers is the overexpression of hexokinase (HK), namely hexokinase-2, responsible for the conversion of glucose to glucose-6-phosphate to support upregulated glycolysis. Primarily, it is thought that only HK1 and HK2 can bind to MOM – specifically to VDAC (Azoulay-Zohar, Israelson et al. 2004; Pedersen 2007; Abu-Hamad, Zaid et al. 2008; Pastorino and Hoek 2008; Shoshan-Barmatz, Zakar et al. 2009). However, the role of HK attachment to the MOM or VDAC is still a topic of debate. Generally, HK2 overexpression and MOM attachment is thought to be in support of shunting cancerous cells into obtaining more energy from glycolysis, producing lactic acid as a byproduct, which was suggested to prepare the surrounding tissue for invasion (Mathupala, Ko et al. 2006). As disscused in Chapter 1 Section II, we have found that the interplay between dimeric tubulin and

VDAC in cancerous human hepatoma cells modulates mitochondrial respiration as detected by cell permeant mitochondrial potential indicator, Tetramethylrhodamine methyl ester (TMRM) uptake (Maldonado, Patnaik et al. 2010). Moreover, it has also been shown that this interaction is tightly regulated by the phosphorylation state of VDAC (*see Chapter 2*), suggesting that modulation of cellular respiration involves upstream signaling events that lead to the targeting of VDAC, altering the channel sensitivity to blockage by tubulin, and thus influencing metabolite exchange and respiration. Interestingly, it was shown that mitochondrial potential can be directly influenced by cell treatment with common microtubule targeting chemotherapeutic agents such as taxol and colchicine (Maldonado, Patnaik et al. 2010). This strongly suggests that possibly some of the side-effects of chemotherapeutic treatments targeting microtubules may in fact be caused by the inhibition of mitochondrial respiration, leading to cell death.

Future directions for VDAC research

There is much work to be done concerning VDAC and its role in cellular events. With plausible links to cancer and neurodegenerative diseases, VDAC may prove a viable target for directed therapeutics. Although one plausible structure has been solved for VDAC1, VDAC2 and VDAC3 structures have yet to be elucidated. Structure is linked to function, and uncovering the correct structures of each isoform will prove to be invaluable, not only for understanding VDAC channel functioning, but also for understanding VDAC-protein interactions. Importantly, only recently have the three

isoforms of VDAC come into the spotlight. Emerging evidence suggests that although similar in structure, the three VDAC isoforms may dramatically differ in function (*see Chapter 3*). This will hopefully provide a unique tool for studying the functional characteristics unique to each isoform. Additionally, the role of VDAC in apoptosis is undeniable. There is still much work to be done in verifying which proteins are responsible for specifically interacting with VDAC, leading to either pro-apoptotic or anti-apoptotic events. Gaining an understanding of the exact mechanisms that finely control cellular respiration will not only provide an advanced picture of the cellular signaling events, but also deliver insight as to possible targets for future therapeutics.

PART II. BACKGROUND WORK COMPLETED BEFORE MATRICULATION ON TUBULIN INTERACITON WITH THE VOLTAGE DEPENDENT ANION CHANNEL THAT CAUSES CHANNEL CLOSURE AND MAY MODULATE CELLULAR RESPIRATION

Introduction

Mitochondria are characterized as having an inner membrane (MIM) and an outer membrane (MOM). While the MIM has been the subject of much research, it has only been in about the last twenty years that the MOM has become a focus. Primarily, according to the current understanding, it serves two functions: (1) as a platform for the orchestration of many apoptogenic proteins (Hoppins and Nunnari 2012) and (2) as a regulator of the flux of respiratory substrates into and out of the mitochondria (Vander Heiden, Chandel et al. 2000). This second function is controlled primarily by the most abundant protein of the MOM, the voltage-dependent anion channel (VDAC), which spans the length of the membrane and serves as the passageway for small molecules, namely ATP/ADP between the cytosol and mitochondria. As the name VDAC implies, at relatively high trans-membrane potentials (>30 mV), VDAC begins to "gate" or close into lower conducting states. Although initially, this mechanism was proposed for control of the flux of metabolites, the best estimates of MOM potential are around 10-20 mV (Lemeshko 2006).

One of the unique properties of mitochondria and the MOM is the tight association with microtubules (Guerrero, Monge et al. 2010) and dimeric tubulin respectively (Carre, Andre et al. 2002). Interestingly, in respirometry experiments with isolated mitochondria, the K_m for exogenously added ADP is almost 10-fold lower than in permeabilized cells (Saks, Kuznetsov et al. 1995; Appaix, Kuznetsov et al. 2003). This difference between respiration rates of isolated mitochondria as compared to whole cells may in fact be attributed to MOM permeability and thus VDAC. Interaction of dimeric tubulin with VDAC may cause a decrease in the permeability of the MOM, restrict the flux of metabolites, and thus hinder oxidative phosphorylation (OxPhos). Indeed, permeabilized cells exposed to a gentle trypsin treatment known to target tubulin, have a restored K_m for ADP nearly matching that of isolated mitochondria (Saks, Kuznetsov et al. 1995).

Tubulin was an attractive candidate for VDAC modulation namely due to its long-known interaction with mitochondria (Bernier-Valentin and Rousset 1982; Saetersdal, Greve et al. 1990). Immunoprecipitation of mitochondrial proteins (isolated mitochondria) with an antibody to alpha-tubulin showed that when alpha-tubulin is pulled down using protein G agarose beads, VDAC is a component of the band suggesting *in vivo* interaction. Conversely, when incubated with an antibody against VDAC, alpha-tubulin is found associated (Carre, Andre et al. 2002). Additionally, radio-labeled tubulin was found in highly purified mitochondrial membrane extracts where the authors made a point to use

plasma membrane fractions as a control due to the known contamination of mitochondrial fractions with plasma membrane (Bernier-Valentin and Rousset 1982).

Dimeric tubulin is a heterodimer of an alpha and beta monomer, each monomer having a distinct C-terminal tail (CTT). Each dimer binds to another in the formation of a higher structured ring, which then polymerizes to form a hollow cylinder with the CTTs facing out resembling a 'brush'. It is interesting to note, that the primary reason that most microtubules are depicted as smooth tubes (lacking the CTTs) is due to the published structure. When the structure was solved, the authors made note of the high variability of the last 6-11 amino acids that comprise the CTTs explaining why their model lacked these regions (Nogales, Wolf et al. 1998). Interestingly, it was these CTTs that were the most attractive candidates for interaction with VDAC. Each tail has a large net negative charge, where even though the tails only comprise about 3% of the total tubulin subunit, they are responsible for over 40% of the subunit net charge (Sackett, Bhattacharyya et al. 1985; Priel, Tuszynski et al. 2005).

Investigating the plausible link between cytosolic proteins and control of cellular respiration, we studied the functional interaction between dimeric tubulin and mitochondrial channel VDAC and showed that nanomolar concentrations of dimeric tubulin induce voltage-sensitive reversible closures of VDAC reconstituted into planar lipid bilayers. Moreover, the interaction between dimeric tubulin and VDAC is highly dependent on both the globular tubulin body and the negatively charged CTTs. Finally, evolutional studies revealed the highly conserved tubulin CTT length and charge in species requiring mitochondria for respiration. Species not dependent on mitochondria

display highly variable tubulin CTT lengths and charges suggesting an ancient interaction between these two proteins.

Materials and Methods

VDAC Purification. VDAC was isolated from rat liver or *Neurospora crassa* mitochondrial outer membrane fractions. *N. crassa* and rat liver mitochondrial fractions were a generous gift from Marco Colombini. We then used these fractions and isolated VDAC from the membranes using a modified approach described in (Blachly-Dyson, Peng et al. 1990) to optimize protein yield. Membranes were spun for 30 min in a refrigerated centrifuge (4^{o}C) at 14,000 G until the membranes were pelleted in the bottom of a 1.5 mL microtube. The supernatant was removed. The cell pellet was resuspended in 1 mL solubilizing buffer (2.5% Triton X-100, 15% DMSO, 50 mM KCl, 10 mM Tris HCl, and 1 mM EDTA at pH 7.0). The sample was left on ice and every 5 min was vortexed for ~ 1 min. It was very important not to let the sample overheat, so all possible steps were done on ice. After 30 min, the sample was spun for 30 min in a refrigerated centrifuge (4^{o}C) at 14,000 G. During this spin, a column was prepared in a long tip glass Pasteur pipette. The tip of the pipette was filed off leaving ~ 10 mm diameter tip. The column was then packed with enough glass cotton to measure 1 cm from the bottom of the pipette. The column was then packed with 1:2 by weight Hydroxyapatite and Celite roughly 10 cm for every 0.1 mL of sample to be run. The supernatant was then applied to the dry column. This was followed by one solubilizing buffer of the same volume as the sample applied. Fractions of ~50 μL were collected, labeled, and stored at -20^{o} C until use.

Electrophysiological Recordings. Artificial lipid bilayers were formed from lipid monolayers made from 1% (wt/vol) solutions of lipid in pentane on a ~70 μm diameter aperture in a thin Teflon membrane separating two ~2 mL chambers. The aperture was treated with a mixture of petroleum gel suspended in petroleum ether. Lipid solutions were composed of either diphytanoyl phosphatidylcholine (DPhPC) or the soybean lipid mixture asolectin and cholesterol (10:1 wt:wt). All lipids were purchased from Avanti Polar Lipids, and dry cholesterol was purchased from Sigma. VDAC reconstitution was achieved by adding ~0.1-1.0 μL of isolated VDAC in Triton X-100 buffer to 1.5 mL buffer (1M KCl, 5 mM HEPES pH 7.4) to the *cis* side of the chamber under constant stirring for 1 min. All potentials were defined as positive when they were greater at the side of the chamber where VDAC was added (*cis)*, Fig. i. After insertion, channels were monitored for basic channel parameters, and tubulin was added to one or both sides of the membrane under constant stirring for 1 min. Kinetic analysis was preformed by using Clampfit 9.2 (Axon Instruments).

Results

Tubulin Induces Highly-Reversible Reduction in Current Through VDAC Reconstituted into Planar Lipid Bilayers. Fig. iiA shows the characteristic current record through a single VDAC channel at a potential of 50 mV. As previously stated, the channel begins to "gate" into multiple lower conducting states at high applied potentials. Some of these lower conducting states will have lifetimes on the order of mins, while

other lower conducting states will stay closed until the potential is zeroed in order to fully re-open the channel and reapplied. Fig. iiB depicts the same channel with the addition of 50 nM tubulin to the *cis* side of the membrane, which induces fast and highly reversible channel current fluctuations at a much lower potential of 25 mV. It should be noted that in tubulin-free solution VDAC will stay open and fully conducting if left at a potential of 25 mV for the life of the membrane (usually on the order of hours). Indeed, voltage gating and tubulin interaction with VDAC are both voltage dependent processes, however the features of these two processes vary greatly. The addition of tubulin increases the voltage sensitivity of the channel, and the nature of the current fluctuations is markedly different. With tubulin present, channel closure is to one characteristic closed state, which is about 60% closure or 40% residual channel conductance as seen in Fig. iiC. Additionally, the off-times, or the time the channel stays in the closed state, when tubulin is present can be fit with two exponentials. One off-time ($\tau 1$) is on the order of milliseconds and one off-time ($\tau 2$) is on the order of seconds as seen in Fig. iii. These two off-times may be explained by the interaction with the alpha CTT verses the beta CTT, whereby both charge and length of the tail would impact residency time in the channel. Tubulin added to the opposite side of the channel (*trans)* interacts with the same kinetics as the *cis* side of the channel, suggesting that the tubulin binding site(s) in the VDAC channel pore is accessible for the tubulin tail from both sides of the channel. Without tubulin, channel closure times can span from several mins to being "trapped" or stuck in a closed state indefinitely until the potential is zeroed and reapplied. Additionally, without tubulin, the distribution of the closed state conductance has a much wider distribution.

Fig. iiC depicts a representative amplitude histogram showing one uniquely defined open state with a conductance of about 4.2 nS. It is important to notice that the histogram of voltage induced closed states of VDAC from *N. crassa* has a wide distribution. Recently, we discovered that with VDAC from rat liver, although the histogram of voltage induced closed states has a wider distribution than with tubulin present, we see a preference for a characteristic 40% residual conductance closed-state typical to that of which we see with tubulin present. With tubulin present, in both VDAC from *N. crassa* or rat liver, the open state remains unaltered, and there is one uniquely defined closed state with 40% residual conductance.

Further studies will be conducted to conclude if this interaction is only a product of *in vitro* system, or if tubulin interaction with VDAC in the control of respiration is indeed physiological. As seen in Fig. iv, work published by our collaborators on cell cultured human hepatoma cells (HepG2) in the presence of tetramethylrhodamine ethyl ester (TMRE) to monitor mitochondrial potential before and after the treatment of cells with either a microtubule de-stabilizer or microtubule stabilizer showed that altering the availability of free dimeric tubulin does directly affect mitochondrial potential giving additional support to the idea that the interaction between tubulin and VDAC has indeed physiological implications (Maldonado, Patnaik et al. 2010). Fig. ivA depicts the relative concentrations of free to polymerized tubulin after treatment of cells with microtubule targeting drugs. As seen in Fig. ivB, colchicine (Col) treatment of cells leads to an increase in free tubulin concentration and a subsequent mitochondrial depolarization.

Treatment of cells with paclitaxel (Ptx) induces microtubule stabilization, leading to a decrease in free tubulin concentration and a subsequent mitochondrial hyperpolarization. Taken together, these results strongly support our hypothesis that mitochondrial potential is modulated at least partially by tubulin interaction with VDAC.

The Role of the C-terminal Tails in Tubulin-VDAC Interaction. As previously noted, both the alpha and beta CTTs of tubulin are highly negatively charged. We postulated that these tails may be responsible for interaction with VDAC, where they may permeate into the positively charged inner lumen of the VDAC channel causing the characteristic channel blockage and reversal of channel selectivity we see when tubulin is present. To test this, we developed two tubulin constructs. First, both CTTs were proteolytically cleaved off the tubulin body (Tub-S) by treatment with subtilisin, a serine protease. As seen in Fig. vA, even at two times the concentration of tubulin required for interaction, Tub-S does not cause the characteristic closures seen with full length tubulin. Tub-S does certainly cause noise of the current through VDAC, which may be explained by interaction of the tubulin body with some part of the mouth of the channel placing the body in the path of the ions through the channel; however this interaction is markedly different from that seen with full length tubulin.

This was followed by testing for interaction of just the CTTs with VDAC. Both the alpha and beta CTT sequences from mammalian brain tubulin were commercially synthesized, and as seen in Fig. vA, even at the hundred times larger concentration than used for intact tubulin, both peptides showed no interaction with VDAC, suggesting that each peptide

may not interact with the channel, or that each peptide may translocate through the VDAC channel faster than detectable with our system (<0.1 ms time scale).

Taken together, this allowed us to conclude that both the tubulin body as well as the CTTs are needed for the characteristic tubulin blockages seen in Fig. vB. While the size of the alpha and beta CTTs is small enough to fit into the channel lumen, the bulky tubulin body with dimensions of roughly 8 nm X 4.5 nm X 6.5 nM serves as an anchor restricting the translocation of the CTTs completely through the VDAC channel with a 2.5-3.0 nM diameter and in turn, creating the characteristic channel blockage.

It is interesting to note that Tub-S does indeed interact with VDAC isolated from rat liver as seen in Fig. vi. However, the interaction with Tub-S is quite different than with full length tubulin. Certainly, Tub-S interaction is both concentration and voltage dependent as seen with full length tubulin. However the off-times of Tub-S are much shorter than with full length tubulin, and the distribution of closed state conductance is much wider, but still maintains a large peak at 40% residual conductance. The wider range in closed state conductance may be explained by the variable cleavage lengths of the tails that the Tub-S population is comprised. Or, the protein-body interactions with VDAC may be a conserved interaction between mammalian VDAC and the mammalian tubulin body. VDAC is thought to have several loops at the mouth of the channel that lay on the membrane, and these loops may also be responsible for interaction with the tubulin body. Indeed, in later research, we concluded that altering the phosphorylation state of VDAC by phosphorylating these cytosolic loops greatly increases the on-rate of tubulin binding,

suggesting a second component of interaction between the body of tubulin and the loops of VDAC. Future work will focus on the question if phosphorylation of these VDAC loops increases the on-rate of Tub-S binding, which will help support our understanding of the mechanism of interaction between the tubulin body and the loops of VDAC.

All previous experiments were conducted on VDAC from either *N. crassa* or rat liver and tubulin isolated from bovine brain. To check for the species specificity of the interaction, we decided to test tubulin isolated from two protozoan parasites *Leishmania tarentolae* and *Leishmania amazonensis*. Although *Leishmania* have a beta tubulin sequence that is roughly 82% similar to *homo* sapiens, their tubulin is markedly different from bovine brain tubulin due to many post-translational modifications (PTMs) including branching of the CTTs (Fong and Lee 1988). Branching is one possible PTM of the CTT, which occurs at either a glycine or glutamic acid residue (Janke and Kneussel 2010). The branching usually happens at a fixed location on the tail and never happens at the ends of the tails. Most tend to think that branching of the CTTs is responsible in some way for modifying microtubule associated protein (MAP) interaction with microtubules. Our aim was to see if branching of the CTTs would in someway influence tubulin interaction with VDAC. Qualitatively, *Leishmania* tubulin does indeed interact with VDAC in a way remarkably similar to bovine brain tubulin. However, quantitatively, there seems to be some difference in the interaction in addition to the distribution of closed state conductance being wider than seen with bovine brain tubulin (*data not shown*). This may be explained by the high branching of the CTTs of *Leishmania* tubulin where branched CTTs would sterically hinder complete permeation of the tail into the channel, which

could be reflected in either altered off-times or a decrease in the closed-state conductance. It is important to note that while the CTTs are flexible and able to move locally, branching could also lead to possible CTT-tubulin body interactions, causing the tail to associate tightly with the tubulin body which may be enhanced after any PTM that adds a charged residue to the tail. There are many charged domains on the tubulin body that are thought to be in reach of the tails, and modifying the charge or length of these tails by branching may induce interaction of the CTTs with the body of tubulin (Craddock, Tuszynski et al. 2012).

Microtubules are known to interact via the CTTs with many MAPs (Amos and Schlieper 2005). To answer the question if polymerized tubulin interacts with VDAC, tubulin was treated with the microtubule stabilizing agent taxol after inducing polymerization. The fractions were spun to separate polymerized microtubules from dimeric tubulin leaving a heterogeneous fraction of differing lengths of microtubules. When added to VDAC, we did see some interaction (*data not shown*), but the interaction was almost one-hundred times less than that of dimeric tubulin. And, this basal interaction could be explained by sample contamination with dimeric tubulin, where even at 5 – 10% contamination, could explain the interaction seen. However, *in vivo*, microtubule interaction of CTTs with VDAC seems unlikely. Microtubules have external diameter or about 25 nM while a mitochondrion (though quite variable) roughly has a diameter of about 500 nM. Assuming the entire surface of the mitochondria was studded with VDAC, you would need a tight and highly organized lattice work of microtubules around mitochondria to begin interacting with enough channels; even then there would be probably not enough

interacting channels to influence respiration. The more likely interaction between mitochondria and microtubules is with transport and distribution of mitochondria throughout the cell (Heggeness, Simon et al. 1978). Upon disruption of microtubules, mitochondria distribution in the cytosol varied considerably.

Actin, another structural protein with an acidic body that is roughly the size of tubulin, was used to test for similar interaction. Approximately, the dimensions of an actin subunit are about 5.5 nm X 5.5 nm X 3.5 nm, and like tubulin subunits, they polymerize into higher ordered filaments, however, they lack the long, flexible CTT of tubulin (Dominguez and Holmes 2011). There is evidence that suggests an association of actin and actin filaments with mitochondria, however this is usually through the association of actin related proteins (Krendel, Sgourdas et al. 1998; Ligon and Steward 2000). As shown in Fig. vA, actin interacts with VDAC in a manner similar to Tub-S. Addition of the protein causes an excess of current noise again indicating possible protein-channel interaction, however even at much higher concentrations, actin does not induce the characteristic channel blockages that full length tubulin induces. This adds additional support to a previous study that reported actin interaction with VDAC isolated from *Neurospora crassa* (Xu, Forbes et al. 2001). This also adds evidence supporting the specificity of the interaction between dimeric tubulin and VDAC, and once again displays the importance of CTTs of tubulin for channel blockage.

Future work will aim to classify which of the two tails are responsible for tubulin interaction. Currently, a construct is being made attaching a single alpha CTT or a single

beta CTT to human serum albumin (HSA), a protein that has a similar bulky acidic body to that of tubulin. There are some potential pitfalls, including the possibility of neglecting how important the native tubulin body may be in tubulin-VDAC interaction. If the first step of interaction is the body interacting with the channel, then the HSA construct will likely show little to no interaction, but this will not be due to lack of CTT/VDAC interaction. There is the possibility of making a construct for recombinant tubulin with truncated CTTs, however many papers have argued that the structure of recombinant refolded tubulin is far from that of native tubulin and that recombinant tubulin once refolded, will not polymerize into microtubules, a hallmark of proper folding of subunits (Shah, Xu et al. 2001).

Dimeric Tubulin Decreases the Respiration Rate of Mitochondria Isolated from Brain and Heart. Our results thus far have suggested that tubulin interacts with VDAC causing highly reversible channel closures, and thus may be able to regulate respiration by controlling the flux of metabolites between the mitochondria and the cytosol. To test this, our collaborators conducted experiments on intact mitochondria isolated from either brain or heart tissue. Oxygen consumption was measured in response to subsequent doses of ADP using an Oroboros oxygraph. The K_m for ADP corresponds to the accessibility of ADP for the adenine nucleotide transporter (ANT) located in the MIM, to stimulate OXPHOS. Without the coupling of ATP and ADP exchange, the electron transport chain is halted and aerobic respiration slows. The accepted K_m value for isolated mitochondria is around 10 – 20 μM (Vignais 1976), and while the first measured component was 7 +/- 2 μM, addition of 1 μM of tubulin resulted in the appearance of a

second component of respiration with a K_m of 169 +/- 52 μM as seen in (Rostovtseva, Sheldon et al. 2008). This allowed us to conclude that in isolated mitochondria both from brain and heart tissue, tubulin addition reduces the availability of exogenous ADP, resulting in hindered respiration. Interestingly, even after the addition of tubulin, the first component of respiration persisted (the component seen in the control). One possible explanation at the time was the possibility of the three VDAC isoforms displaying different sensitivities to tubulin binding. Today, we know that to be true, where VDAC1 and VDAC2 are highly sensitive to tubulin binding, while VDAC3 is almost tubulin-insensitive. Future work will focus on mitochondria isolated from cells treated with siRNA targeting two of the three VDAC isoforms in order to isolate a single isoform enriched population of mitochondria. If correct, VDAC3 enriched mitochondria should fail to display a second component of respiration after addition of tubulin, suggesting that VDAC1 and VDAC2 are primarily responsible for regulation by tubulin.

Discussion

Tubulin has generally been classified as a structural protein, polymerizing and depolymerizing in dynamic instability to serve as scaffolding for the cell. We proposed for the first time, that there may be another role of tubulin, more than just supporting the cell and serving as "molecular highways" for carrier proteins. Nanomolar to micromolar concentrations of dimeric tubulin interact with VDAC inducing highly reversible channel blockages at relatively low membrane potentials. These blockages are to one characteristic closed state and this closed state has a reversed selectivity, changing from

anionic in the open state, to cationic in the blocked state. This interaction is highly dependent on both the concentration of tubulin and the potential across the MOM. Moreover, for interaction, both the CTTs and tubulin body are required for the characteristic channel blockage. Noise from Tub-S interaction is indicative of protein-channel interaction suggesting there may be some interaction of the body with the loops of the channel; however without the tails tubulin is unable to induce the characteristic block.

Almost 250 eukaryotic tubulin sequences are known and the conservation between each sequence is striking (Tuszynski, Carpenter et al. 2006). However, while the sequence comprising the body is relatively unaltered between species, there is great sequence variation in the region of the CTTs. Interestingly, although the CTT amino acid sequences may change, there seems to be conservation of both CTT length (9.9 +/- 1.6 for alpha and 19.2 +/- 2.8 for beta) and charge (-7.2 +/- 1.4 for alpha and -10.3 +/- 1.5 for beta) compiled for over 86 different species for alpha and over 132 species for beta, that require mitochondria for respiration as seen for the beta-tail in Fig. viiA and B (Rostovtseva, Sheldon et al. 2008). However, in species that are amitochondiral, both the charge and length of the CTTs begins to vary greatly as seen with CTT sequences of obligate intracellular eukaryotes. Tubulin is a particularly ancient protein found in all eukaryotes (Margulis, Chapman et al. 2006). The question remains, does this tubulin-VDAC interaction happen throughout the eukaryotic world as well? To begin to answer this, we used VDAC isolated from either *N. crassa* or rat liver and tubulin isolated from bovine brain and from *Leishmania.* As previously mentioned, the differences between the

species of VDAC are negligible and qualitatively the interaction of tubulin from different species is generally conserved. While we tested tubulin from *Leishmania* and the bacterial tubulin analog FitZ, future work should be conducted on tubulin isolated from many species of eukaryotes to verify the uncovered functional interaction.

Tubulin interaction with VDAC may begin to start answering the long standing questions of cellular respiration control. Hypothetically, respiration could be finely controlled simply by altering the local concentration of free tubulin. This immediately raises the question as to how cell respiration is linked to cellular processes that cause dramatic cytoskeletal rearrangement such as mitosis. Additionally, this functional interaction has implications in the many therapies that use microtubule targeting chemotherapeutics to alter polymerization rates. Yes, generally these drugs interfere with cell cycle progression, which lead to cell death; however, our results suggest that administration of these therapeutics may also promote or inhibit mitochondrial respiration leading to an increased or hindered energy output. Future work will need to be conducted to understand if these drugs do indeed impact mitochondrial respiration.

i

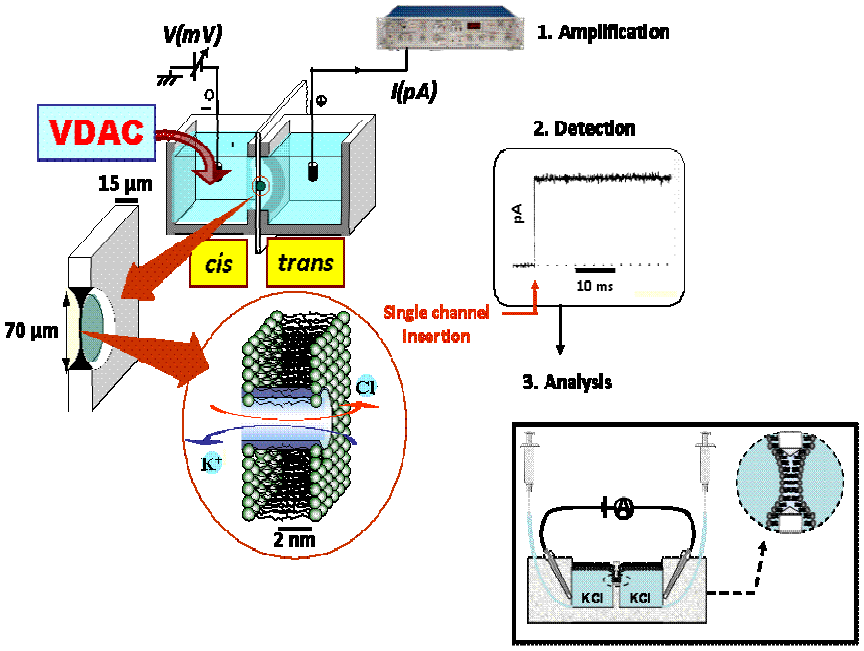

Experimental set-up for functional reconstitution of channel-forming proteins into planar lipid bilayers. A two compartment chamber is separated by a thin Teflon partition roughly 15 µm in thickness, with contains a tiny aperture roughly 70 µm in diameter from which a lipid bilayer is formed over. Each compartment contains roughly 1.5 mL of buffer solution (1M KCl, 5 mM hepes, pH 7.4). An electrode is placed into each compartment which is attached to an Axon amplifier for signal detection. This work was preformed prior to my thesis work.

ii

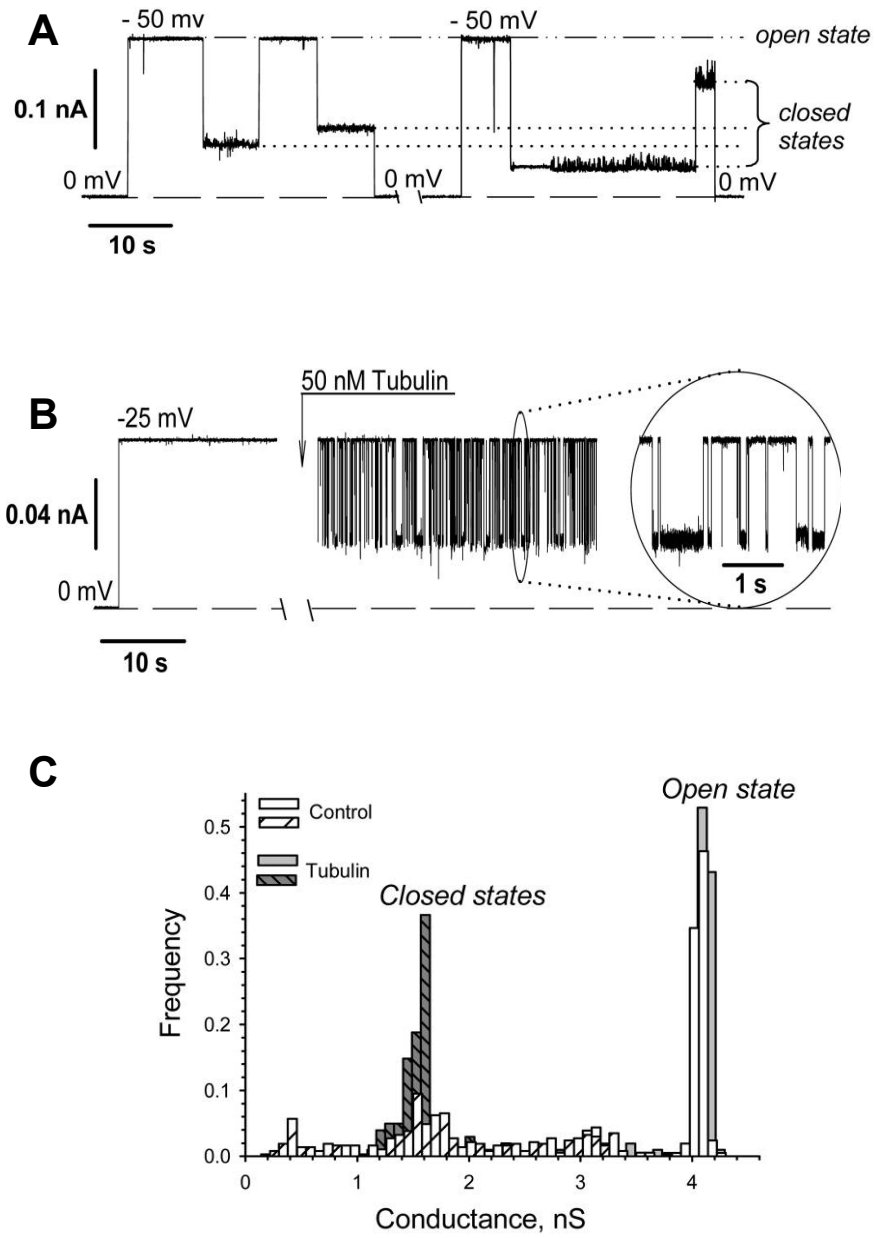

Dimeric tubulin interacts with VDAC causing characteristic channel blockages. (A) A representative current trace through a singe VDAC channel isolated from *N. crassa*. Under high transmembrane potentials (< 50 mV) VDAC with "gate" or close to multiple lower conducting states. (B) The addition of nanomolar concentrations of tubulin

induces highly reversible channel closures at 25 mV. This interaction is characterized by one unique closed state conductance (~40 % residual conductance) as depicted in the amplitude histogram (C). Adapted from (Rostovtseva, Sheldon et al., 2008). This work was preformed prior to my thesis work.

iii

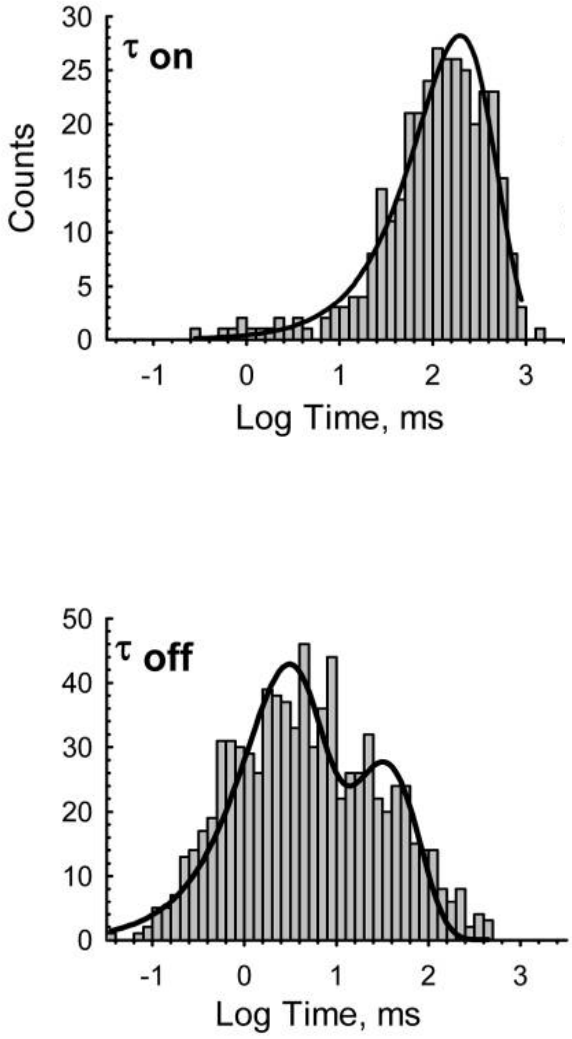

Tubulin interaction with VDAC is characterized by one unique open time and at least two closed times. Statistical analysis of multiple tubulin induced closure events (~ 400 events) produce one unique open time, or characteristic time the channel remains open between individual closure events (τon). The off-time (τoff) defining the duration that the channel stays in its blocked state is fit with at least two exponentials. Adapted

from (Rostovtseva, Sheldon et al., 2008). This work was preformed prior to my thesis work.

iv

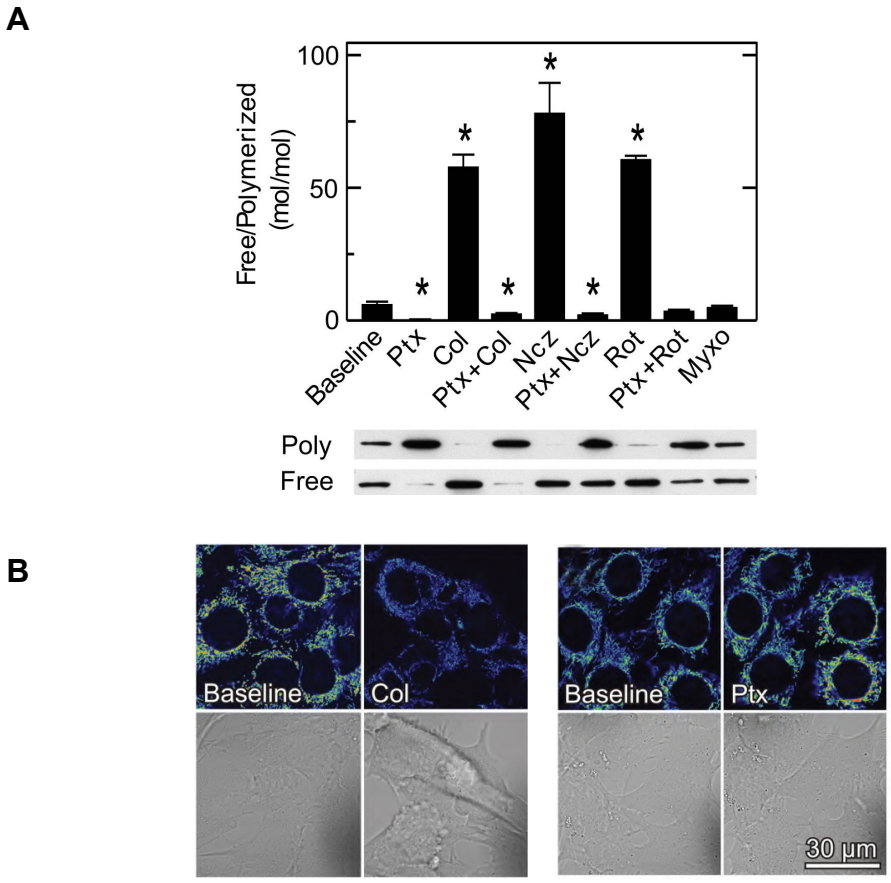

Microtubule targeting drugs influence local tubulin concentration affecting mitochondrial potential as measured by TMRM. Our collaborators supported our findings by showing tubulin interaction with VDAC modulates mitochondrial potential. (A) Relative concentrations of polymerized microtubules to free dimeric tubulin after HepG2 cell treatment with multiple microtubule targeting drugs. (B) Specifically, colchicine treatment of cells increase the concentration of free tubulin leading to mitochondrial depolarization. Conversely, paclitaxel treatment stabilizes polymerized microtubules leading to a decrease in free tubulin and a subsequent mitochondrial hyperpolarization. Figure taken from (Maldonado, Patnaik et al., 2010).

v

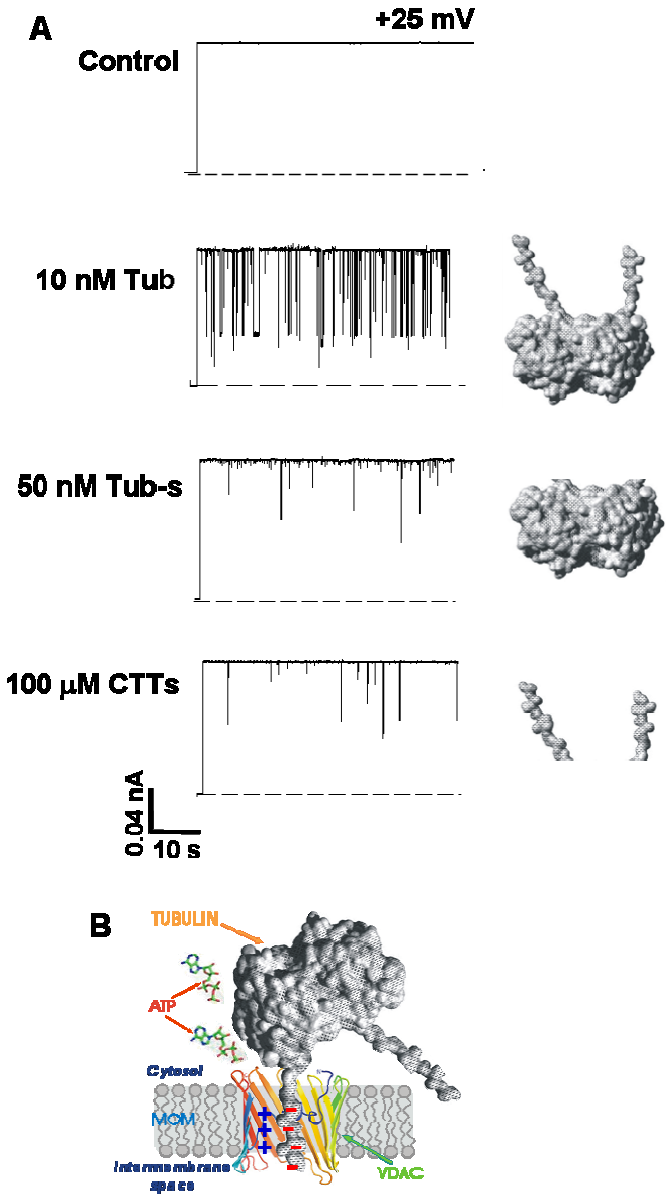

Both the bulky body and c-terminal tails of tubulin are required for tubulin interaction with VDAC. (A) Current traces through single VDAC channels in the presence of tubulin (10 nM), Tub-s (50 nM), and a mix of synthetic alpha and beta c-terminal tail peptides (100 µM). Taken together, we propose a model of tubulin-VDAC interaction (B) in which the highly negatively charged CTTs of tubulin permeate into the

positively charged inner lumen of VDAC leading to the characteristic channel blockage. Adapted from (Rostovtseva, Sheldon et al., 2008). This work was preformed prior to my thesis work.

vi

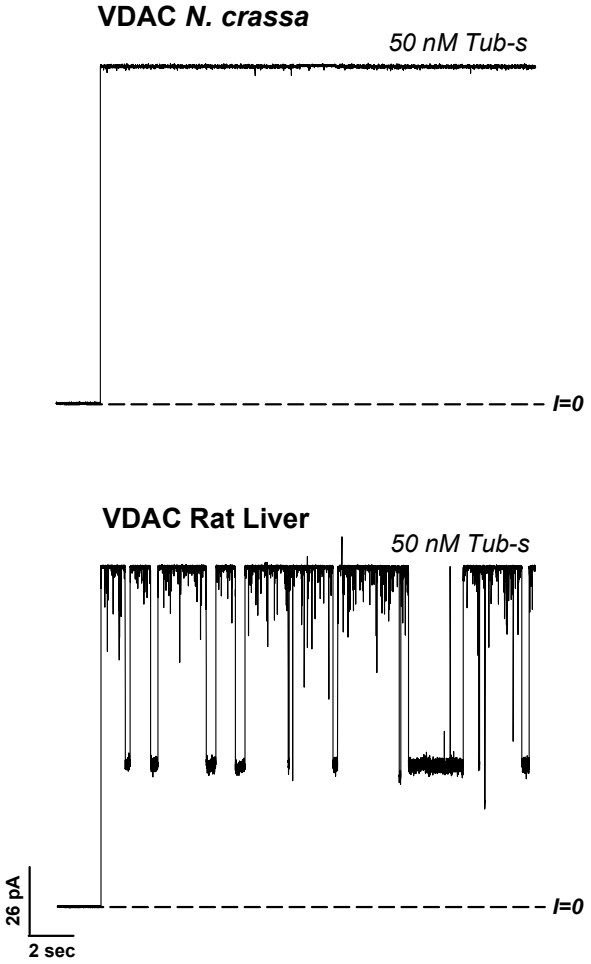

Tubulin S interaction with VDAC is dependent on VDAC species. Tubulin-s has little interaction with VDAC isolated from *N. crassa*, even at high concentrations (50 nM) with high transmembrane potentials (30 mV). The same concentration of tubulin-s causes the generation of noise seen in the fast, short events, and also induces channel closure to about 60%. This work was performed prior to my thesis work.

vii

A **Sequence alignments of beta-tubulin CTT**

Eukaryotes with mitochondria	
Homo sapiens	ATADEQGEFEEEGEDEA
Gallus gallus	ATANDGEEAFEDDEEEINE
Danio rerio	ATADDEADFGEEGE
Xenopus laevis	ATADEQGEFEEEEDEA
Drosophila melanogaster	ATADEDAEFEEEQEAEVDEN
Homarus americanus	ATADDEAEFEEEGEVEGEYA
Zea mays	ATAEEYDEEEQDGEEEHD
Schizosaccharomyces pombe	AGIDEGDEDYEIEEEKEPLEY
Brugia malyi	ATADEEQDLQEGESEYIEQEE
Tetrahymena thermophila	ATAEEEGEFEEEEGEN
Leishmania tarentolae	ATVEEEGEYDEEEEPT
Eukaryotes lacking mitochondria	
Guillardia theta	AKMDNDAFEDQDLY
Enterocytozoon bieneusi	SQVGGY
Encephalitozoon cuniculi	ATIEDADDFLVN
Bacteria	
Prosthecobacter dejongeii (BTubB)	---
Prosthecobacter dejongeii (BTubA)	SQAEAAVQDSAGDTQMEAAAA- GVSDDAEGSMSLADLVDRRR

B **Summary of alpha and beta CTT properties**

	Alpha (n = 86)	Beta (n = 132)
Charge [1]	**-7.2 ± 1.4**	**-10.3 ± 1.5**
Length (residues) [1]	**9.9 ± 1.6**	**19.2 ± 2.8**

1. Values are mean ± s.d.

Evolutional conservation of tubulin CTTs is characteristic of any organism that depends on mitochondria. (A) Displays the sequence alignments of the beta-tubulin CTT from eukaryotes with mitochondria, eukaryotes lacking mitochondria, and bacteria. Acidic residues are colored red while basic residues are colored blue. (B) Summary of both the alpha and beta CTT properties of 86 organisms for the alpha tail and 132 organisms for the beta tail. Both CTT length and charge are highly conserved for any

organism that is dependent on respiration via mitochondria. (Rostovtseva, Sheldon et al., 2008) This work was preformed prior to my thesis work.

CHAPTER 2: PHOSPHORYLATION STATE OF CYTOSOLIC LOOPS OF THE VOLTAGE DEPENDENT ANION CHANNEL MODULATES ITS INTERACTION WITH TUBULIN

Introduction

Mitochondria are now understood to have a role not only in aerobic energy production, but also in calcium signaling and the promotion of apoptosis by the release of cytochrome *c*. In addition, there has been a recent focus on how mitochondria are involved in cell signaling pathways (Duchen 1999; Tait and Green 2012). The voltage-dependent anion channel (VDAC) is the primary protein in the mitochondrial outer membrane (MOM) and it serves to facilitate the flux of small ions and respiratory substrates between the inner mitochondrial space and the cytosol (*see Chapter 1*). Previously, we showed that the subunits of polymerized microtubules, tubulin dimers, interact with VDAC causing rapid and highly reversible blockages of the channel current (Rostovtseva, Sheldon et al. 2008). Even though the residual conductance of a blocked channel is relatively high (~40%), the selectivity of the channel is changed from anion-selective in the open state to cation-selective in the blocked state (Rostovtseva, Sheldon et al. 2008). Moreover, this tubulin-blocked state is impermeable for ATP (Gurnev, Rostovtseva et al. 2011). However, there are up to micromolar concentrations of dimeric tubulin in the cytosol of a "typical" non-dividing cell (Gard and Kirschner 1987). If sub-nanomolar concentrations of tubulin are sufficient to induce channel closure, then this would suggest that all VDAC would be

closed. Therefore, we postulate that there must be additional control or regulation of the tubulin interaction with VDAC.

Recent work has elucidated potential amino acid residues of the three VDAC isoforms that are targets of phosphorylation as detected by site-directed mutagenesis, immunohistochemistry, or mass spectrometry (Distler, Kerner et al. 2007; Martel, Allouche et al. 2013). Phosphorylation of proteins typically modulates protein function, and in layman's terms, can be thought of as an "on-off" switch for many cell pathways. Although numerous sites on VDAC have been predicted or proven as targets of phosphorylation, the outcome of phosphorylation for many of these residues remains elusive. One interesting observation to note is that the majority of these phosphorylatable sites are clustered near the mouth of the channel, as predicted from the solved crystal structure of VDAC1 (Bayrhuber, Meins et al. 2008; Ujwal, Cascio et al. 2008). Although there is still much debate about whether the available VDAC1 structures represent the native conformation of VDAC1 in the MOM (Colombini 2009), both the predicted native conformation and the solved 3D structures currently proposed maintain cytosolic loops with a cluster of tentative phosphorylation sites near the mouth of the VDAC channel, regardless of the proposed structure. Much work has centered around two protein kinases that have been shown to interact with VDAC: protein kinase A (PKA) and glycogen-synthase kinase three beta (GSK3β) (Bera, Ghosh et al. 1995; Banerjee and Ghosh 2006; Pastorino and Hoek 2008).

Eukaryotic protein kinases PKA and GSK3β are part of a large superfamily of homologous proteins that act specifically on target proteins by phosphorylating serines (Ser) or threonines (Thr) (Hanks and Hunter 1995). PKA phosphorylation of VDAC has been implicated in the regulation of MOM permeability during ethanol-induced stress (Lemasters, Holmuhamedov et al. 2012), and has also been shown to increase the probability of the closed state of the channel in reconstitution experiments (Bera and Ghosh 2001). Although the primary roles of PKA are related to cell growth and differentiation, there is mounting evidence that implicates PKA in many cancer pathways (Tortora and Daniele 2006). For instance, over-expression of the catalytic subunit of PKA is a hallmark of breast cancer promoting increased cell proliferation of normal breast tissue as well as promoting transformation of normal breast tissue into malignant tissue (Miller 2002). Additionally, evidence suggests that PKA and its signaling pathways are linked to progression of prostate cancer (Wang, Jones et al. 2006).

GSK3β is primarily described as being involved in glycogen metabolism, however there is growing evidence suggesting that GSK3β inhibition may prove to be a viable treatment for many energy-dependent diseases like cancer, diabetes, and Alzheimer's disease (Martinez, Alonso et al. 2002; Martinez, Castro et al. 2002). Specific to its phosphorylation of VDAC, GSK3β is said to have a larger role in promoting mitochondrial dysfunction whereby phosphorylation of VDAC leads to hexokinase (HXK) detachment from VDAC leading to ischemia and reperfusion injury of cardiac tissue (Pastorino and Hoek 2008).

Here I show that the functional interaction of tubulin with mammalian VDAC reconstituted into planar lipid bilayers is highly dependent on the state of VDAC phosphorylation. My work described below shows that VDAC phosphorylation by PKA or GSK increases the on-rate of tubulin binding to VDAC by over two orders of magnitude, while basic channel properties such as single channel conductance and selectivity remain unaltered. This suggests that PKA and GSK phosphorylation sites may reside on the exposed VDAC loops at the mouth of the VDAC channel. Moreover, phosphorylated VDAC is more sensitive to tubulin interaction, but only when tubulin is added to the same side as the addition of VDAC (the *cis* side) allowing us to determine, for the first time, the channel orientation in our experimental set-up. Additionally, in cultured human hepatoma cells, mitochondrial potential of the mitochondrial inner membrane (MIM) can be modulated by altering kinase activity with a PKA inhibitor. Taken together, we postulate an intricate control mechanism of cellular respiration governed by (1) the local tubulin concentration and (2) the phosphorylation state of the cytosolic loops of VDAC.

Materials and Methods

Protein purification

Dr. Marco Colombini (University of Maryland College Park) is a foremost authority on purified native VDAC. Therefore, I obtained frozen mouse MOM fractions from his laboratory to isolate and purify VDAC for the experiments that follow. I isolated VDAC from MOM using a previous published method (Blachly-Dyson, Peng et al. 1990) with

minor modifications. Membranes were run on a hydroxyapatite-celite (2:1) column following the method described in (Palmieri and De Pinto 1989) (*see Chapter 1*). Tubulin isolated from bovine brain was purchased from Cytoskeleton (Denver, CO) and tubulin from rat brain was isolated and purified according to the methods described in (Wolff, Sackett et al. 1996) and was a munificent gift from Dan Sackett (NICHD, NIH). PKA purified from bovine heart was purchased from Promega (Madison, WI) and Calbiochem, EMD. GSK3β from rabbit skeletal muscle and alkaline phosphatase from calf intestine were both purchased from Calbiochem, EMD (Gibbstown, NJ). Recombinant human protein phosphatase 2A (PP2A) was purchased from Cayman Chemical (Ann Arbor, MI).

Phosphorylation and detection

VDAC was phosphorylated by two methods: (1) ~1.0 mg isolated mitochondrial membranes were treated with ~1000 units of GSK3β or PKA in the presence of 10 μL of kinase buffer (25 mM Hepes pH 7.4, 150 mM NaCl, 25 mM β-glycerophosphate, 1 mM DTT, and 10 mM $MgCl_2$). Each sample had an abundance of MgATP (~50 μM) and was incubated for 30 min at 37^{o}C with phosphatase inhibitors (Pierce). (2) 10 μL of purified VDAC from rat liver (*see chapter 2)* was incubated according to the above protocol at 32^{o}C, which my assay for optimization determined was the optimal temperature for the highest yield of phosphorylated VDAC. Dephosphorylation was conducted on ~1.0 mg of mitochondrial membrane fraction incubated with 100 units of alkaline phosphatase (AP) or PP2A in 5 μL Tris-HCl at pH 8.0 at 37^{o}C for 30 min, followed by VDAC purification as previously described. Detection of the phosphorylation level was first

conducted by using a panel of antibodies specific for recognition of phosphorylated consensus sequences from Cell Signaling (Danvers, MA). Marco Colombini kindly provided us with a proprietary anti-VDAC antibody, specific for VDAC detection. Both phosphorylated and dephosphorylated samples were separated by SDS-PAGE, and stained with commercially available Pro-Q Phosphorylation Detection Stain following manufacturer's instructions (Invitrogen). VDAC bands were imaged at 532 – 560 nm excitations on a Fuji Gel Scanner and the difference in intensities was measured using Multi Gauge V3.0 software used on un-manipulated images. Graphs displaying differences in band intensities are the averages of at least three different independently conducted experiments. For reconstitution experiments, VDAC was phosphorylated freshly according to method (2) before being immediately used for single channel studies.

Channel reconstitution experiments

Planar lipid bilayer membranes were formed over a ~70 μm diameter aperture in a ~15 μm thick Teflon partition that separates two chambers filled with aqueous buffer as previously described (Rostovtseva, Kazemi et al. 2006). Lipid monolayers used to form bilayers were composed from 5 mg/mL solution of diphytanoyl phosphatidylcholine (DPhPC) purchased from Avanti Polar Lipids (Alabaster, AL) in pentane. Monolayers were formed on the surface of aqueous solutions of 1 M KCl buffered with 5 mM HEPES at pH 7.4. ~0.1 – 1.0 μL of isolated VDAC in Triton X-100 buffer (2.5% Triton X-100, 15% DMSO, 50 mM KCl, 10 mM Tris, 1 mM EDTA, pH 7.0) was added to the *cis* side of the chamber under constant stirring for 1 min. Potential is defined as positive when it is greater on the side of VDAC addition, referred to as the *cis* side. All current

recordings were performed as previously described in (Rostovtseva, Kazemi et al. 2006) using an Axopatch 200B amplifier from Axon Instruments (Foster City, CA) in the voltage clamp mode. Single channel data were filtered by a low-pass 8-pole Butterworth filter, model 9002 from Frequency Devices (Haverhill, MA) at 15 kHz and directly saved into the computer memory with a sampling frequency of 50 kHz. Clampfit 9.2 was used for data analysis after all recordings were filtered by a digital 8-pole Bessel low pass filter set at 500 Hz. Statistical analysis was completed by using nine different logarithmic probability fits to logarithmically binned histograms of at least 150 blockage events as described (Sigworth and Sine 1987).

Cell Imaging

All cell imaging was done by our collaborators at the Medical University of South Carolina, in Charleston South Carolina as described in (Sheldon, Maldonado et al. 2011).

Results

Detection of phosphorylation level of VDAC samples. To avoid protein dilution due to isolation and purification, phosphorylation and dephosphorylation of VDAC were carried out on whole mitochondrial membranes prior to purification of VDAC. The presence of VDAC in our samples was first verified by Western blot analysis using an antibody specifically designed to target mammalian VDAC1 (Fig. 1A). Concurrently, untreated, PKA-phosphorylated, GSK-phosphorylated, and PP2A- VDAC samples were separated by SDS-PAGE, followed by subsequent staining with commercially available non-

specific phospho-detection dye, Pro-Q. Compared with the untreated control, both PKA and GSK treated VDAC samples appeared to have increased levels of phosphorylation (Fig. 1B), though PKA tended to have a greater effect than GSK. All phosphorylation protocols were optimized for both time and concentration of kinase to ensure saturation of the purified VDAC samples. PKA induced a VDAC phosphorylation signal over two-times that of the control, whereas GSK only increases the signal just under two-times that of the control (Fig. 1C). PP2A treatment tended to decrease the signal from that of the control, it is likely that the untreated VDAC has a basal level of phosphorylation that is to some extent higher than the dephosphorylated samples. Additionally, there was a large variability of phosphorylation state of the untreated sample which is consistent with and provides a possible explanation for previously published results displaying differing sensitivities to tubulin when VDAC was isolated from different mitochondrial fraction preparations. A possible explanation could be that if indeed VDAC is a target of upstream signaling leading to phosphorylation, the states of VDAC phosphorylation could vary depending on the mouse. The low phospho-signal observed in the PP2A-dephosphorylated samples may be explained by phosphatase specificity or the putative phosphorylation sites located in the inner lumen of the channel that are inaccessible to PP2A, which may be phosphorylated as a post-translational modification during protein synthesis.

One final note should be made about the detection of phosphorylation of VDAC used for single-channel reconstitution. While it would be of interest to treat VDAC with kinases and phosphatases following incorporation of VDAC into planar membranes, the quantity

of kinase needed in the bath of our bilayer experimental setup would be far too great for such an experiment. Additionally, VDAC recovered from the preps used for channel reconstitution is too dilute and contains too much detergent to detect proper phospho-signal by Pro-Q stain (detergent interferes with Pro-Q staining as stated by the manufacturer). To control for this, purified samples were treated according to the protocol listed in the materials section, and subjected to a cold chloroform-methanol treatment to both concentrate the VDAC and remove any trace of detergent allowing for optimal Pro-Q staining and signal.

The on-rate of tubulin binding to VDAC is highly dependent on VDAC phosphorylation state. To study the effect of PKA or GSK phosphorylation of VDAC on tubulin interaction with the channel, VDAC isolated from mouse liver mitochondrial fractions was incubated with PKA or GSK in the presence of an excess of MgATP for 1 hour at room temperature to ensure maximum phosphorylation of the purified VDAC. Immediately following phosphorylation, VDAC was reconstituted into planar lipid membranes followed by the addition of dimeric tubulin to the bath to either the *cis* side or both *cis* and *trans* sides. We discovered that both kinases greatly sensitize VDAC to tubulin as shown by the representative traces of ion current through a VDAC channel (Fig. 2B PKA, GSK *not shown*). PKA phosphorylation of VDAC increased the frequency of channel closure in the presence of tubulin (Fig. 2B), while PP2A-dephosphorylated VDAC was similar to or slightly less senstivie to tubulin closure than control (Fig. 2C). In the absence of tubulin, ion current traces through phosphorylated and dephosphorylated VDAC are indistinguishable from untreated VDAC (Fig. 2A, B

and C), suggesting that these modified amino acid residues may be located out of the path of ions. It is important to note that dephosphorylated VDAC was much harder to reconstitute and it often produced noisy open states, which could potentially be explained by dephosphorylation of certain residues required for proper protein folding. Remarkably, the effect of phosphorylation is clearly seen with the addition of tubulin to the bath. The untreated trace displays the characteristic tubulin interaction at a potential of 25 mV with 20 nM of dimeric tubulin at the *cis* side (Fig. 2A). As seen in the trace of PKA-treated VDAC, the concentration of tubulin needed to induce channel closure is almost seven times less than needed for untreated VDAC (Fig. 2B). Conversely, dephosphorylated VDAC is less sensitive to tubulin interaction than untreated VDAC (Fig. 2C). On-rates for the three VDAC samples as calculated from statistical analysis of the times between successive tubulin-induced closure events (τ_{on}), are satisfactorily described by one single exponential fitting (Fig. 2D). This implies that the tubulin-VDAC interaction can be sufficiently represented by a simple first order reaction with an on-rate constant (K_{on}) defined as the inverse average τ_{on} normalized by tubulin concentration. At 25 mV, the K_{on} of phosphorylated VDAC is greater by nearly two orders of magnitude than the on-rate constant of untreated and dephosphorylated VDAC.

Initial plans were to phosphorylate VDAC after the channel was reconstituted into our planar lipid membrane system. However, due to the amount of kinase that would be required to reach its effective concentration, the experiment proved to be too expensive. This led us to the necessity of VDAC phosphorylation before reconstitution. Additionally, the phosphorylation state of the channels is hyper-sensitive to freeze-thaw

cycles. Sensitivity of phosphorylated VDAC to tubulin interaction is greatly diminished even after one freeze-thaw cycle, requiring that the VDAC be used immediately after phosphorylation and that the samples not be used for subsequent experiments. Likely, this can be explained by certain contamination of our samples with phosphatases remaining from the isolation of VDAC that cleave phosphate groups during sample storage. Alternatively and more probable is the hydrolytic cleavage of these phospho-groups during freezing as described previously (Schmidt-Mende, Hellstrom-Lindberg et al. 2000). According to these authors, subjecting samples to even one freeze-thaw cycle greatly increased intrinsic proteolytic activity.

Phosphorylated VDAC displays highly asymmetrical sensitivity to tubulin. A characteristic record of current through a single untreated VDAC channel at +/- 25 mV in the presence of 20 nM dimeric tubulin on both sides of the channel, *cis* and *trans* is symmetrical in tubulin interaction with VDAC (Fig. 3A). Astonishingly, after phosphorylation of VDAC by PKA, the sensitivity to tubulin binding increases greatly, but only at one side, the *cis* side of the channel (Fig. 3B). Compared with untreated VDAC, phosphorylated VDAC requires tubulin concentrations roughly one-hundred times less to induce similar effects observed with the untreated sample. However, this same low concentration (0.3 nM tubulin) had no effect when added only to the *trans* side (Fig. 3B). That is, VDAC requires the same concentration of tubulin used with the untreated sample to induce identical channel blockage on the *trans* side. The same is true for GSK-phosphorylated VDAC (Fig. 3C); however the sensitivity of the channel to tubulin, though greater than that of the untreated channel, is not as sensitive as seen with

the PKA-phosphorylated sample. Despite the large differences in the on-rates of each VDAC sample – phosphorylated and dephosphorylated – the slopes of the on-rates versus the applied potential remain similar (Fig. 4A). Additionally, the off-rate of channel blockage is described by at least two different characteristic times $\tau 1$ and $\tau 2$, which are not influenced by channel phosphorylation state (Fig. 4B). These two characteristic off times were previously reported, but their cause is yet to be determined (Rostovtseva, Sheldon et al. 2008).

Collectively, these findings allow us to predict that the candidate sites of phosphorylation reside outside of the water-filled lumen of VDAC. Presumably phosphorylation occurs on the loops facing the *cis* or cytosolic side of the channel. It should be noted that phosphorylation of isolated VDAC in detergent micelles may be responsible for inducing the asymmetry in tubulin sensitivity of the channel. If a portion of VDAC resides in the micelle, it would be inaccessible to phosphorylation by kinases. We controlled for this possibility by phosphorylating VDAC in broken mitochondrial membranes which should allow for both faces of the channel to be exposed to the bulk, and, therefore, accessible to kinase interaction. Even so, there was no difference between the asymmetry of tubulin binding to VDAC phosphorylated by either of the two protocols.

PKA-dependent phosphorylation influences mitochondrial membrane potential in HepG2 cells as detected by TMRM. To verify my previous work with phosphorylation induced VDAC-tubulin interaction on a cell level, we collaborated with the John Lemasters and his laboratory (Medical University of South Carolina). We aimed to see if

the striking effect that phosphorylation state of VDAC has on the sensitivity to tubulin in these in vitro experiments suggests that the interplay between kinase activity and tubulin concentration might regulate MOM permeability in cells, thus controlling the flux of metabolites into and out of the mitochondria and influencing mitochondrial potential ($\Delta\Psi$). To test this, we assayed mitochondrial potential as measured by tetramethylrhodamine methylester (TMRM) uptake in HepG2 cells using confocal microscopy as described in (Lemasters and Ramshesh 2007). For clarification, all work with cell culture as described in this section was conducted by our collaborators at the Medical University of South Carolina in Charleston, South Carolina and can be found in more detail in (Sheldon, Maldonado et al. 2011). Previous work had demonstrated that mitochondrial $\Delta\Psi$ is influenced by altering the concentration of free tubulin by treatment of HepG2 cells with cholchicine or paclitaxel to depolymerize or stabilize microtubules, respectively (Maldonado, Patnaik et al. 2010). By increasing the concentration of cytosolic dimeric tubulin, treatment of cells with cholchicine induced a sharp depolarization of mitochondria possibly by inactivating/closing VDAC channels (Maldonado, Patnaik et al. 2010). Conversely, treatment of cells with microtubule stabilizer paclitaxel decreased the concentration of dimeric tubulin in the cytosol and coincided with a hyper-polarization of mitochondria (Maldonado, Patnaik et al. 2010). These results could be explained by modulating MOM permeability by altering tubulin-VDAC interaction.

We proposed that due to the strong influence the phosphorylation state has on tubulin interaction with VDAC, the inhibition of PKA activity by H89 treatment should also

impede tubulin interaction with VDAC, thereby promoting polarization of mitochondria. Indeed, treatment of HepG2 cells by our collaborators with 1 μM of PKA inhibitor H89 increased mitochondrial TMRM fluorescence by ~60% (Fig. 5A). According to (Davies, Reddy et al. 2000), H89 used at this concentration, inhibits the action of PKA without influencing other cytosolic kinases. To further this study, we employed both H89 treatment with subsequent colchicine treatment. While treatment of cells with H89 increased $\Delta\Psi$, the subsequent treatment with colchicine failed to decrease $\Delta\Psi$. This is notable because in the absence of H89, colchicine treatment of HepG2 cells greatly depolarized mitochondria. Conversely, treatment of cells first with colchicine greatly reduces $\Delta\Psi$. Subsequent treatment with H89 hyperpolarizes mitochondria as seen by an increase in $\Delta\Psi$ (Fig. 5B). All fluorescence signals were averaged over multiple experiments and are quantified in Fig. 5C.

These experiments were also conducted with commercially available synthetic peptide protein kinase inhibitor (PKI), a peptide specific for PKA inhibition by mimicking the PKA protein substrate (Glass, Cheng et al. 1986; Pediaditakis, Kim et al. 2010), in place of H89, and the outcome was consistent with what was seen with H89. Taken together, these experiments strongly support our results with a single reconstituted VDAC channel and our claim that the phosphorylation of VDAC greatly influences VDAC interaction with dimeric tubulin.

Discussion

This is a growing list of kinases that has been implicated in direct phosphorylation of the three VDAC isoforms. Specifically, VDAC1 on Ser12 by CaM-II and GSK3, Thr51 by GSK3 (Pastorino, Hoek et al. 2005), Ser136 by PKC; VDAC2 on Tyr237 by INSR; and VDAC3 on Ser241 by CKI and PKA, and Thr33 by PKC (Distler, Kerner et al. 2007). Because generally in a healthy, non-dividing cell tyrosine phosphorylation only accounts for about 0.01% to 0.05% of the total phosphorylated amino acid content (Hunter 1995), we chose to focus our research primarily on two serine/threonine specific kinases that have been shown to interact with VDAC, PKA and GSK. To our surprise, untreated VDAC isolated from mouse liver displayed a basal level of phosphorylation, suggesting that VDAC probably undergoes post-translational modifications following protein synthesis. VDAC treated with non-specific protein phosphatases alkaline phosphatase or protein phosphatase-2A tended to display a decreased phospho-protein signal than the control, however even with the most dephosphorylated VDAC samples, there was still the presence of a slight signal, which could be attributed to phosphorylation of VDAC in the inner lumen of the channel, where three serine/threonine sites have been identified (Kerner, Lee et al. 2012). Additionally, it must be noted that there are protein kinases that reside in the inner-mitochondrial space, which may be specific for phosphorylating amino acid residues on the loops on the side of the channel that faces away from the cytosol, giving a possible additional form of VDAC control (Verdanis 1977).

Both the size of kinases and the unchanging selectivity of VDAC after phosphorylation suggest that VDAC phosphorylation by PKA and GSK likely takes place on the "loops" of the VDAC channel that connect the beta-sheets of the VDAC beta-barrel (Ujwal, Cascio et al. 2008), which are thought to form channel entrances. If the phosphorylation sites are located in the path of the flow of ions through the channel, it would be reflected by increasing the cationic selectivity of VDAC. According to the published 3D VDAC structure (Ujwal, Cascio et al. 2008), there is an asymmetry of the number of potential serine/threonine sites that may be targeted by cellular kinases. One face (*cis*) is enriched with five serine and eight threonine residues on the channel loops while the other side (*trans*) only has one serine and four threonines (Fig. 7). Although detection of specific sites by mass spectrometry is required to verify specific amino acid targets, the asymmetry of the clustering of accessible phosphorylatable sites fits nicely with the asymmetry of tubulin interaction we showed after VDAC phosphorylation, where after phosphorylation of VDAC only the *cis* side of the channel becomes sensitized to tubulin interaction. Moreover, this allows us for the first time to suggest channel orientation both in our experimental set up, and in the MOM.

Previously, we published the interaction of the highly negatively charged C-terminal tails (CTT) of dimeric tubulin permeating into the positively charged lumen of the VDAC pore (Rostovtseva, Sheldon et al. 2008). We showed that when you remove the CTTs, the bulky body of dimeric tubulin interacts with the mouth of the pore, as seen by the generation of high-frequency current noise that is typical of interaction. Our model suggested that tubulin interaction with VDAC was at the least a two-step process where

the tubulin body interacted with some portion of the channel – presumably the cytosolic loops – and the CTTs permeated into the channel pore causing the characteristic and highly reversible blockage of channel conductance. Now, we show that by altering the state of phosphorylation of these loops, we greatly alter the on-rate of tubulin binding. Although we originally thought that introducing negative charges to the mouth of the channel might decrease tubulin interaction due to the Coulomb repulsion of the negative tails, we now believe that these negative charges introduced by treatment with either PKA or GSK interact with some positively charged domain(s) of the tubulin body. This would be explained by the increase of the on-rate of tubulin binding while having no influence on the residence time of the tails in the channel pore.

The best estimates of the potential across the MOM range from as low as 10 mV (Lemeshko 2006), to between 15-20 mV (Cortese, Voglino et al. 1992), to as high as 46 mV (Porcelli, Ghelli et al. 2005). Although the last estimate of MOM potential seems to be inflated as it would only require picomolar concentrations of tubulin for sufficient blockage of VDAC. Fig. 6 displays the IC50 values for phosphorylated/dephosphorylated and untreated VDAC as a function of the applied potential displaying that interaction of tubulin with VDAC spans from micromolar to subnanomolar concentrations at voltages between 10 and 30 mV. This begins to answer a long standing question of our work (Rostovtseva, Sheldon et al. 2008) where nanomolar concentrations of tubulin were sufficient for interaction with VDAC. Under normal physiological conditions of a non-dividing cell, the concentration of cytosolic tubulin is on the order of micromoles, and changes from this value only slightly depending on cell

needs. It is only during cell division, under stress or apoptotic signaling, or during cell motility that the dynamic equilibrium of tubulin to microtubules changes significantly (Kirschner and Schulze 1986; Desai and Mitchison 1997; Rodionov, Nadezhdina et al. 1999). We now show that there are at least two additional components that control the interaction of tubulin with VDAC, (1) local dimeric tubulin concentration, and (2) the phosphorylation state of VDAC. Moreover, it implicates MOM permeability control as a function of upstream cellular signaling. Altering phosphorylation state of VDAC alters MOM permeability and hence the flux of metabolites between the cytosol and inner mitochondrial space, resulting in altered oxidative phosphorylation and energy production.

Our collaborators supported our results by showing that in HepG2 cells mitochondrial MOM permeability and, therefore, $\Delta\Psi$ are directly influenced by treatment of cells with microtubule targeting drugs that promote either polymerization of microtubules or depolymerization of microtubules into dimeric tubulin. Moreover, we show that the interaction of dimeric tubulin with VDAC is dependent on PKA activation, whereby when PKA is inhibited by either H89 or PKI, mitochondria remain hyperpolarized even when dimeric tubulin concentrations are increased by cell treatment with colchicine. Taken together with the findings on reconstituted VDAC, our work suggests that MOM permeability could be intricately controlled by upstream cell-signaling events. As seen in Fig. 7, the cytosolic loops of VDAC are accessible for post translational modifications including, but not limited to phosphorylation, which in turn modulates the interaction of VDAC promoting channel opening or closure.

Differences in phosphorylation level of VDAC isolated from mouse liver (*data not shown*) may be explained by either multiple target sites of phosphorylation or the possibility of kinase interaction with specific VDAC isoforms. Generally, mouse liver VDAC is primarily composed of VDAC1 and VDAC2 followed by lower levels of VDAC3 (Blachly-Dyson and Forte 2001; Krauskopf, Eriksson et al. 2006). Future work will need to be conducted to phosphorylate individual populations of VDAC1, VDAC2, and VDAC3 to gain a deeper insight into specific phosphorylation control of tubulin-VDAC interaction.

Figure 1

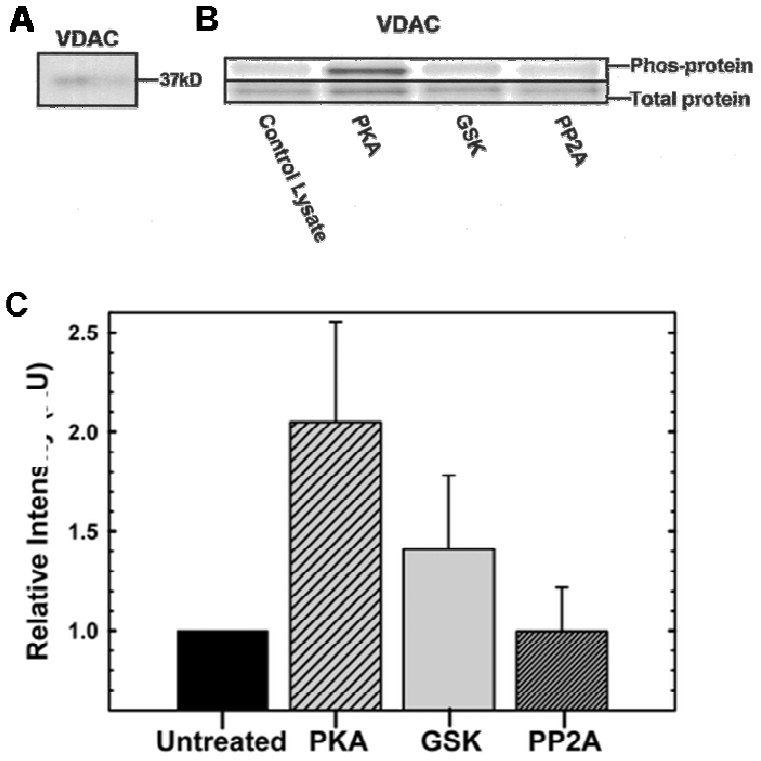

VDAC isolated from mouse liver undergoes phosphorylation by cytosolic kinases protein kinase A (PKA) and glycogen synthase kinase 3 beta (GSK3). (A) Isolated VDAC run on SDS page and blotted for VDAC displays a band at about 36 kD. VDAC samples treated with either PKA, GSK3, or a non-specific phosphatase were run on SDS page and stained with a phospho-specific dye (B). When the signals were quantified over 3 independent experiments (C), both kinase treated VDAC samples displayed higher band intensities than the untreated and phosphatase treated samples. (Sheldon, Maldonado et al., 2011)

Figure 2

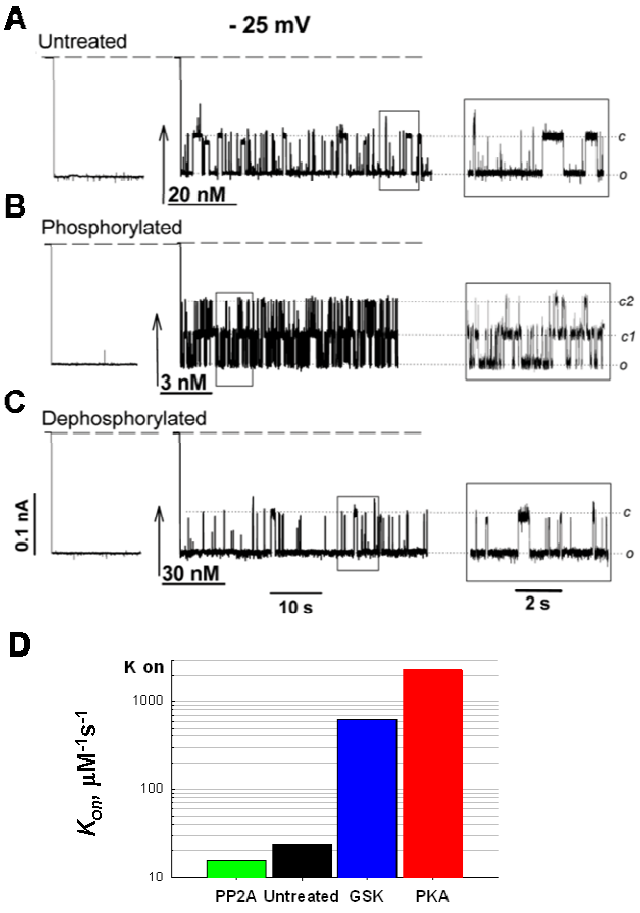

VDAC phosphorylation enhances its blockage by tubulin. Current records through two VDAC channels are shown: (A) untreated VDAC in the presence of 20 nM tubulin, (B) PKA phosphorylated VDAC in the presence of 3 nM tubulin, (C) dephosphorylated VDAC in the presence of 30 nM tubulin. Each inset displays the open channel state, one channel blocked state (c1) and two channel blocked state (c2). (D) Quantification of the on-rates of tubulin binding for each sample showing an increase of tubulin binding more than two orders of magnitude for both kinase treated VDACs. (Sheldon, Maldonado et al., 2011)

Figure 3

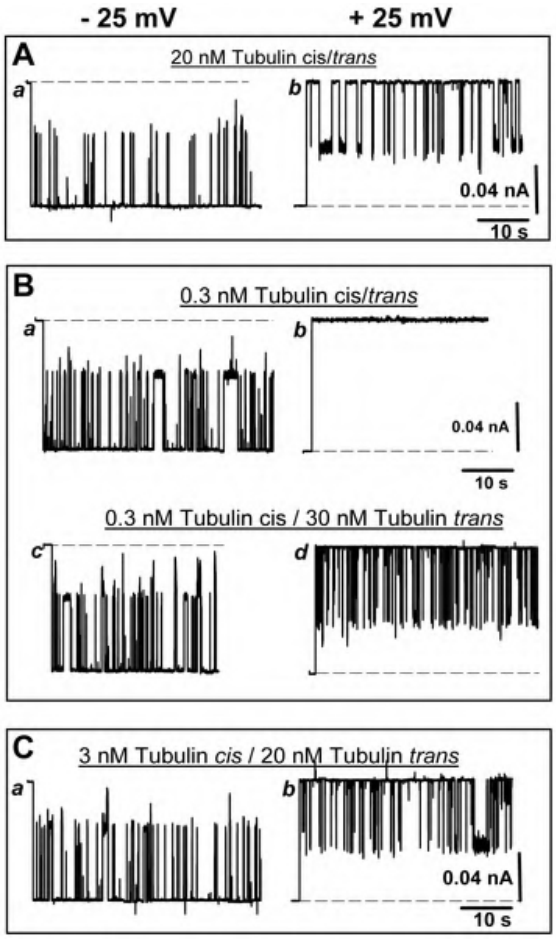

VDAC phosphorylation increases tubulin binding only at the cytosolic face of the channel. Current traces through one single VDAC channel: (A) untreated VDAC with 20 nM tubulin on both the cytosolic (*cis*) side and the inner-mitochondrial (*trans*) side of the channel. (B) PKA phosphorylated VDAC becomes sensitive to tubulin interaction only requiring 0.3 nM tubulin to induce channel closure (a), where the same concentration on the *trans* side has not interaction (b). Increasing the concentration of tubulin on the *trans* side to concentrations used with the untreated VDAC shows channel interaction. (C) GSK3 phosphorylated VDAC also induces asymmetry of tubulin

sensitivity of VDAC, but to a lesser extent than PKA treated VDAC. (Sheldon, Maldonado et al., 2011)

Figure 4

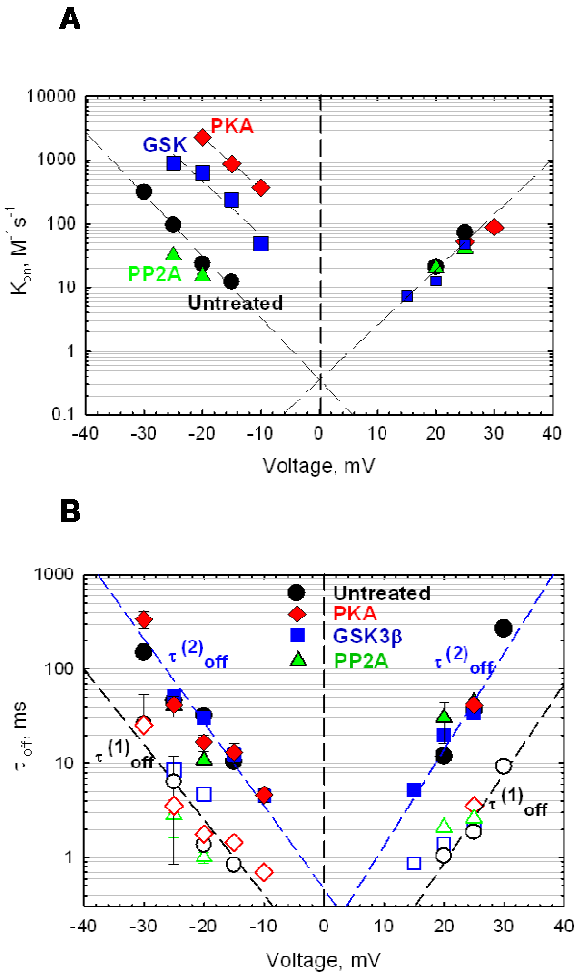

On-rates of tubulin interaction display high asymmetry of interaction for all phosphorylated VDAC samples while the off-rates remaining unaltered. On-rates for both the PKA (red) and GSK (blue) treated VDAC samples display an increase of K_{on} nearly two orders of magnitude greater than untreated VDAC samples, but only on the *cis* side of the channel. All *trans* side on-rates collapse to the same line. Off-times for tubulin-VDAC interaction can be describe by two fits (τ1 black and τ2 blue dashed lines). All τ1 off-times collapse to the same black line regardless of phosphorylation state or side of the channel. This is also true for all τ2 off-times which collapse to the same blue line. (Sheldon, Maldonado et al., 2011)

Figure 5

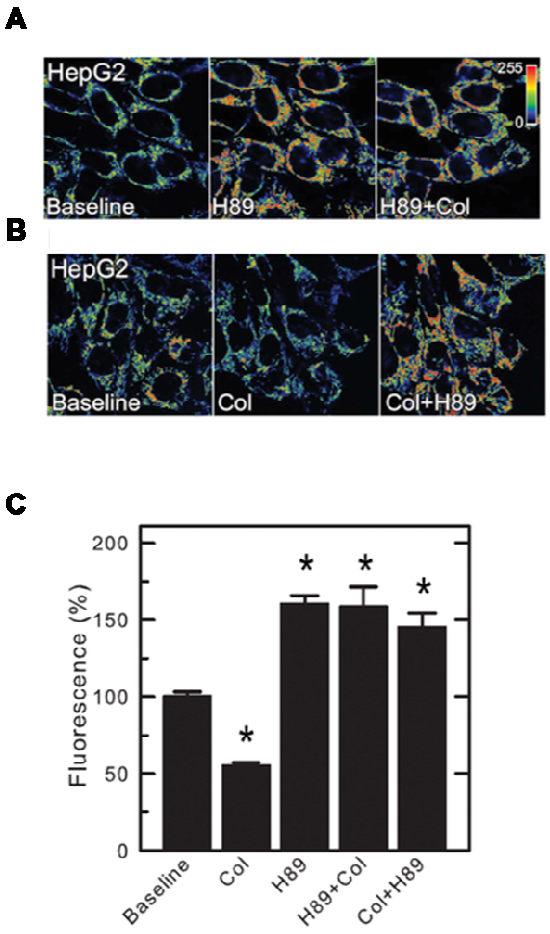

Mitochondrial potential is modulated by VDAC-tubulin binding. Our collaborators showed that (A) treatment of HepG2 cells with PKA inhibitor H89 hyperpolarizes mitochondria where even after subsequent treatment with microtubule destabilizer colchicine, potential remains unaltered. (B) Treatment of HepG2 cells first with colchicine decreased mitochondrial potential as previously shown. Subsequent treatment of cells with H89 reestablishes mitochondrial potential. (C) Quantification of fluorescence displays that compared to baseline potential, treatment of cells with colchicine leads to mitochondrial depolarization, however following this treatment with

PKA inhibitor H89 not only leads to restoration of potential, but also a slight hyperpolarization. (Maldonado, Sheldon et al., 2013)

Figure 6

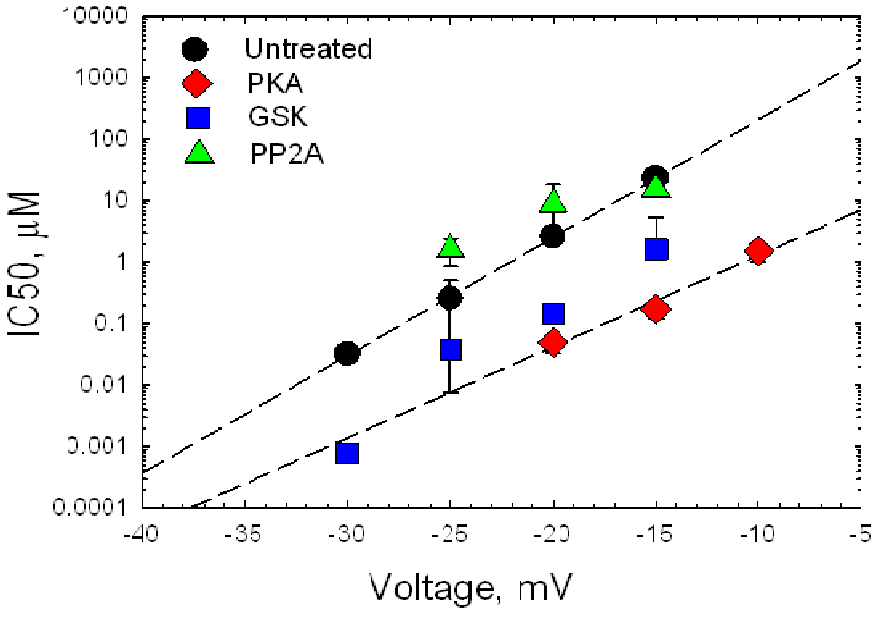

Tubulin inhibitory concentration depends on both applied potential and VDAC phsophorylation state. The IC50 values are obtained from statistical analysis of 5-8 independent experiments where the dashed lines represent linear regressions through the data of untreated and GSK treated VDAC samples. IC50(V) = IC50(0)exp(nVF/RT), where V is the applied potential and n is the effective gating charge n = 11.2 and n = 12.2 respectively. (Sheldon, Maldonado et al., 2011)

Figure 7

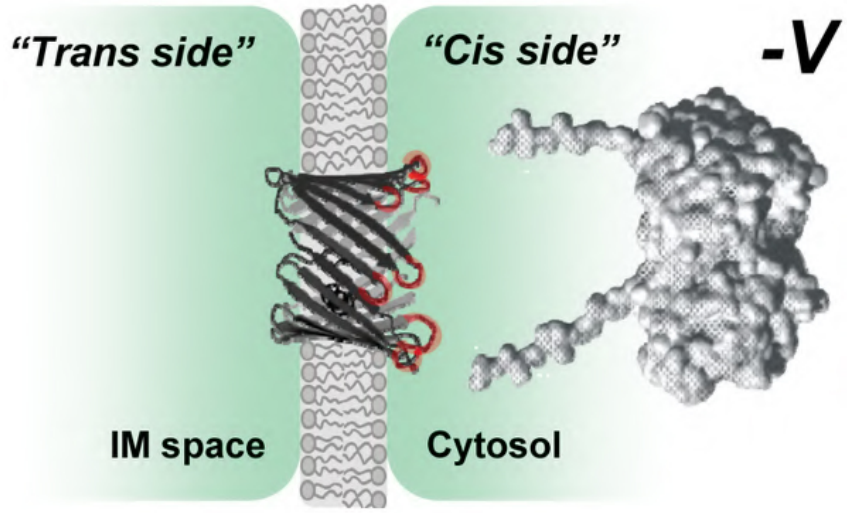

Potential phosphorylation sites on VDAC loops are exposed on the *cis* (or cytosolic) face of the channel. A scheme of VDAC interaction with phosphorylated VDAC depicting the *cis* loops of VDAC highlighted in red to indicate potential phosphorylation domains. Application of negative potentials drives tubulin towards the mouth of the channel. The VDAC beta-barrel protein is adapted from (Ujwal, Cascio et al., 2008). The loops in red are enriched with five Ser and eight Thr residues. The model of the tubulin dimer was adapted from (Priel, Tuszynski et al., 2005). (Sheldon, Maldonado et al. 2011)

CHAPTER 3: CHARACTERIZATION OF THE UNIQUE CHANNEL PROPERTIES OF THE THREE MAMMALIAN VDAC ISOFORMS ISOLATED FROM HUMAN HEPATOMA CELLS

Introduction

It has been known since the late 1920s that aerobic cancer cells display a greatly increased rate of energy production via glycolysis, markedly different than that of non-proliferating non-cancerous tissues under the same conditions which typically rely more heavily on mitochondrial-dependent oxidative respiration (Warburg, Wind et al. 1927; Warburg 1956; Pedersen 1978). This cancer phenotype, described by a shift in energy production from oxidative phosphorylation (OxPhos) to glycolysis, has been a hallmark of the Warburg phenomenon. Though originally thought to result from a permanent loss in mitochondria function, today we understand that mitochondria isolated from most cancer tissues maintain functional respiratory chain potential in the presence of oxygen (Pedersen 2007; Hsu and Sabatini 2008; Zheng 2012). Indeed, glycolysis produces ATP less efficiently than could be generated by OxPhos, however, in addition to energy production, glycolysis provides both NADPH and the carbon needed for production of biomass to support cell growth and proliferation (Flamholz, Noor et al. 2013). This suggests that the Warburg phenomenon is likely caused by an adaptation (or mutation) of the cell to suppress mitochondrial respiration in favor of glycolysis, and it is this process of adaptation that remains poorly understood.

Ultimately, mitochondrial outer membrane (MOM) permeability is involved in the regulation of metabolite flux into and out of the mitochondria, thus controlling mitochondrial respiration. The voltage-dependent anion channel (VDAC) is a beta-barrel protein expressed in all studied Eukaryotes. It spans the mitochondrial outer membrane and functions as the primary passageway for adenine nucleotides and other respiratory substrates into and out of the mitochondria. Although there are three known mammalian isoforms, VDAC1, VDAC2, and VDAC3, it has been only recently appreciated that each may play a different and very distinct role in cell metabolism and cell signaling. Generally, tissue expression of each isoform is ubiquitous; however the expression levels of each can vary quite considerably depending on the tissue type. For instance, in human cervical cancer cells as detected by mRNA transcript levels, VDAC1 is abundantly expressed (one order of magnitude higher than VDAC2), followed by VDAC2 and finally VDAC3 which is expressed nearly two orders of magnitude less than that of VDAC1 (De Pinto, Guarino et al. 2010). Whereas in testes, the expression of VDAC1 is nearly absent while the expression of VDAC2 and VDAC3 is more robust (Sampson, Lovell et al. 1996).

Although the primary function of VDAC is to conduct metabolites (Rostovtseva and Colombini 1996; Rostovtseva and Colombini 1997; Rostovtseva and Bezrukov 1998), there is growing evidence that supports an additional function. VDAC has been reported to serve as a hub for other cell signaling events such as apoptosis (Rostovtseva, Tan et al. 2005), cardioprotective events (Schwertz, Carter et al. 2007; Das and Steenbergen 2012), and glycolysis where HK has been shown to bind VDAC (Shulga, Wilson-Smith et al.

2009; Wenner 2010). Moreover, our earlier work found that VDAC has a unique protein-protein interaction with dimeric tubulin (Rostovtseva, Sheldon et al. 2008), the subunit of microtubules, which reversibly binds and blocks VDAC. The binding is dependent on both the mitochondrial membrane potential and the local concentration of tubulin. Additionally, as described in Chapter 2, the interaction of tubulin and VDAC is greatly influenced by the phosphorylation state of the cytosolic mouth of the channel, whereby phosphorylation of VDAC by either protein kianse A or glycogen synthase kinase 3-beta increases the on-rate of tubulin binding by almost 2 orders of magnitude (Sheldon, Maldonado et al. 2011). Furthermore, in this tubulin blocked state VDAC selectivity switches from anionic to slightly cationic and restricts the flux of ATP (Gurnev, Rostovtseva et al. 2011; Noskov, Rostovtseva et al. 2013).

In addition, it has been shown that by altering the concentration of free tubulin in the cytosol of HepG2 cells, mitochondrial potential can be dramatically changed, as measured by TMRM uptake (Maldonado and Lemasters 2012; Maldonado, Sheldon et al. 2013). Knockdown of individual VDAC isoforms by siRNA suggests that while VDAC1 and VDAC2 may be the most abundantly expressed isoforms in HepG2 cells, VDAC3 plays a key role in the modulation of mitochondrial potential through tubulin interaction (Maldonado, Sheldon et al. 2013).

Erastin is a small molecular weight compound reported in 2003 to selectively target and kill engineered human tumor cells (Dolma, Lessnick et al. 2003). However, erastin was reported more recently to interact directly with mitochondria through VDAC, causing an

accumulation of reactive oxygen species that leads to the non-apoptotic cell death (Yagoda, von Rechenberg et al. 2007). This same group showed that VDAC2 was specifically targeted by erastin as confirmed by using a radio-labeled filter binding assay. It was later demonstrated that erastin promotes the open state of recombinant VDAC2 as measured by NADH uptake of VDAC when isolated, refolded, and reconstituted into liposomes (Bauer, Gieschler et al. 2011).

Here, we characterize the basic channel properties of each VDAC isoform isolated from HepG2 cells treated with siRNA targeting two of the three isoforms. We find that while single channel conductance in 1M KCl and selectivity of each channel are relatively unchanged, both voltage sensitivity and tubulin sensitivity vary greatly between the isoforms. Additionally, in multichannel membranes with VDAC purified from HepG2 cells, erastin depresses VDAC inhibition by tubulin, restoring channel conductance to that of control.

Materials and Methods

Cell culture and siRNA

Human hepatocytes (HepG2) cells were grown in RPMI supplemented with 10% fetal bovine serum in the presence of 5% CO_2 at 37^{o}C. Cells were split roughly every two days to avoid high confluence and cell overgrowth. For siRNA treatment, cells were grown to ~80% confluence and transfected with 5 nM siRNA targeting VDAC1, VDAC2, VDAC3 and a non-target serving as control, all of which were purchased from

Ambion (Austin, TX). VDAC1, VDAC2, and VDAC3 constructs were Silencer Select: VDAC1 (Catalogue #4390844), VDAC2 (Catalogue #4392420), and VDAC3 (Catalogue #4392420). siRNAs were reverse transfected using Lipofectamine RNAiMAX reagent from Invitrogen (Carlsbad, CA) according to the provided manufacturer's instructions. Previous work was conducted by our collaborators to optimize transfection for both time and concentration of siRNAs for each isoform, confirming knock-down by both real-time PCR and immunohistochemsitry (Maldonado, Patnaik et al. 2010).

Mitochondrial fraction isolation

HepG2 cells were subjected to mild trypsin treatment, and mitochondrial fractions were isolated at 4^{o}C with a BioVision Mitochondria/Cytosol Fractionation Kit (Catalogue #K256-25) according to manufacturer recommendations. All crude mitochondrial fractions were then stored at -20^{o} C for subsequent isolation and purification of VDAC; all other cell cytosolic fractions were discarded.

VDAC isolation and purification

VDAC isoforms were isolated from siRNA-treated HepG2 mitochondrial fractions according to the manufacturer's protocol. All fractions were thawed on ice for ~20 min and pelleted at 4^{o}C in a refrigerated centrifuge for 30 min at 14,000 g. Supernatants were removed and discarded and the mitochondrial pellets were resuspended in VDAC isolation buffer (2.5% Triton X-100, 15% DMSO, 50 mM KCl, 10 mM TRIS, 1 mM EDTA at pH 7.0). It was extremely important to do all isolation steps on ice to avoid sample heating, leading to rapid protein degradation and decreased sample yields. Each

sample was passed roughly 10X first through a Monoject hypodermic needle (0.9 mm X 38.1 mm) then 10X through a Becton Dickinson PrecisionGlide hypodermic needle (30G) to ensure maximal homogenization of mitochondrial fractions. Samples were then run on hydroxyappatite/celite ion exchange columns according to the protocol described in (Sheldon, Maldonado et al. 2011). Purity was verified by gel electrophoresis and subsequent treatment with VDAC isoform specific antibodies as previously described.

Channel reconstitution and analysis

Single channel reconstitution and analysis was conducted according to the methods listed in Chapter 1. Multichannel experiments were analyzed following protocols developed previously where VDAC gating is analyzed from the channel response to a slowly changing periodic voltage (+60 mV to -60 mV) at 5 mHz, as previously described (Colombini 1989; Zizi, Byrd et al. 1998). For single channel reconstitution experiments, VDAC was inserted according to the protocol mentioned above. Current recordings were conducted as previously described (Rostovtseva, Kazemi et al. 2006) using the Axopatch 200B amplifier in the voltage-clamp mode. Data were filtered by a low-pass 8-pole Butterworth filter at 15 kHz. Single channel data were sampled at a frequency of 50 kHz and directly collected and stored into the computer memory. For data analysis, Clampfit 9.2 was used and all records were filtered with an 8-pole Bessel low pass filter set at 500 Hz. Kinetic analysis was conducted according to previous methods as described in (Sigworth and Sine 1987).

Western blots

Western blots were conducted on whole cell fractions. Briefly, after siRNA treatment, cells (~$2x10^7$) were washed with 1 mL of cold PBS, scrapped and collected. Samples displayed a high content of large DNA polymers (as seen by the viscosity of the samples). To correct for this, all samples were treated by sonication for three 1 min intervals switching between sonication and resting in an ice-bath (Branson bath Sonifier 450). After sonication, samples were treated with loading buffer to a working concentration of 1X, boiled for 3 min, and separated on 4-12% NuPAGE Bis-Tris gels from Invitrogen and transferred onto polyvinylidene difluoride (PVDF) membranes using an XCell II Blot Module also from Invitrogen. PVDF blots were first blocked for ~ 1 hour using a blocking buffer (1X TBS, 0.1% Tween, with 5% w/v instant nonfat dry milk) followed by incubation with antibodies against VDAC1 from Santa Cruz Biotechnologies (SC-8828, Santa Cruz, CA), VDAC2 from Abcam (Ab-47104, Cambridge, MA), VDAC3 from MitoSciences (MSA03/E08326, Eugene, OR), and beta-actin from MP Biomedicals (691002, Solon, OH). All blots were then developed using secondary antibodies conjugated to peroxidase from Santa Cruz Biotechnologies. Detection was carried out using Supersignal Westpico Chemiluminiscent Substrate (Rockford, IL)

Results

siRNA knockdown of VDAC isoforms

There is little known about the functional distinction between the three isoforms of VDAC. Therefore, we began to probe the differences between each VDAC isoform by characterizing tubulin interaction with each of the three different VDAC isoforms. In order to isolate each isoform, our collaborators at the Medical University of South Carolina in the laboratory of John J. Lemasters used siRNA to transiently deplete the other two VDAC isoforms in HepG2 cells. They optimized siRNA transfection conditions to obtain a knock-down efficiency of ~95% as determined by both real time PCR and quantitative western blot analysis. After knock-down, cells were lysed, mitochondrial membranes were isolated, and one unique isoform of VDAC was purified according to the methods described in Chapter 1.

Each VDAC isoform displays a unique sensitivity to both transmembrane potential and tubulin interaction. One possible difference between the three VDAC isoforms might be through differences in their sensitivities to voltage (voltage-induced gating) and/or interaction with tubulin. To test for these possibilities, each siRNA double knock-down VDAC sample was tested. Specifically, VDAC1 fractions were treated with siRNA against VDAC2 and VDAC3, VDAC2 fractions were treated with siRNA against VDAC1 and VDAC3, and VDAC3 populations were treated with siRNA against VDAC1 and VDAC2.

Because siRNA knockdowns are incomplete, it was also important to evaluate the function of multiple channels in one experiment. For instance, if each fraction was tested on a single-channel, there is the slight possibility that the channel that inserts may be from the low-grade contamination of the VDAC population with the other isoforms. To correct for this possibility, experiments were first conducted on multichannel membranes with roughly an average of 50 channels inserted into one membrane. In doing so, the majority of the VDAC channels that insert into the membrane will be from the isoform population of interest. Even if the VDAC1 sample has a 5% contamination by incomplete knock-down of VDAC2 and VDAC3, VDAC2/3 will only account for about 2 or 3 channels out of the total 50, and these 2 or 3 channels would be averaged out during kinetic analysis. As seen in Fig. 15A which displays the response of at least 50 VDAC channels in a single membrane to the application of a slowly applied triangular voltage (5 mHz) from -60/+60 mV, channel closure at different potentials was expressed as conductance (G) normalized to the maximal conductance (G_{max}) in each period normalizing for the exact channel number. Surprisingly, both VDAC1 and VDAC2 displayed a dependence on applied potential nearly identical to that of VDAC isolated from untreated HepG2. However, VDAC3 purified from VDAC1/2 siRNA-treated cells displayed reduced voltage dependence, whereby VDAC3 channels maintained their open state even under the application of 60 mV. As previously mentioned in Chapter 1, the best estimates of mitochondrial transmembrane potential are around 10-20 mV, allowing us to conclude that VDAC3 channels isolated from VDAC1/2 double knock-down HepG2 cells are physiologically voltage-insensitive. Another important feature of this graph to note is the inherent asymmetry of all VDAC isoforms to the applied potential, a

characteristic previously described in Chapter 1. This strongly suggests that there is a strong lipid-dependent component in channel conformational energetics that induces the asymmetry of VDAC voltage gating (Rostovtseva, Kazemi et al. 2006). This asymmetry was inherent in all channel reconstitution experiments and adds further support that the channels are properly folded in our experiments.

The greatest functional difference between the three VDAC isoforms was revealed with the addition of nanomolar concentrations of dimeric tubulin (Fig. 8B). Under the same potential, in the presence of 10 nM tubulin applied to both the *cis* and *trans* side of VDAC, we can clearly see that VDAC1 is highly sensitive to the interaction and subsequent closure by tubulin, followed by VDAC2, while VDAC3 remained relatively tubulin insensitive. Even at tubulin concentrations 5 times that used for VDAC1 and VDAC2, VDAC3 still was almost completely tubulin insensitive (Fig. 8C). This raises a question as to what is responsible for the differences in sensitivity of each of the three isoforms to tubulin. Immediately, based on our previous work showing phosphorylation of VDAC increases the sensitivity of the VDAC channel to tubulin (Sheldon, Maldonado et al. 2011), it appeared that the phosphorylation state of the cytosolic loops might alter the regulation of different VDAC isoforms by tubulin. However, one key feature of *in vitro* phosphorylated and reconstituted VDAC is the induced asymmetry of tubulin binding, where one face of the channel becomes highly sensitive to tubulin interaction (determined to be the cytosolic face of the channel) while the opposite side of the channel remains unaltered (see Chapter 2). As shown in Fig. 8B, we see that the sensitivities of both the *cis* and *trans* side of VDAC seem to be quite similar. Of course, the possibility

of phosphorylation cannot be ruled out. The amino acid sequences of the cytosolic loops are quite different among all three isoforms and all previous phosphorylation work was conducted on VDAC isolated from mouse liver (a mix of VDAC1 and VDAC2 primarily) rather than pure VDAC isoform populations. The question remains: when VDAC isolated from mouse liver is treated with kinase and MgATP, do all isoforms become phosphorylated, or is there an isoform specificity of phosphorylation? Future work will be aimed at elucidating the phosphorylation level of each of the three VDAC isoforms expressed in HepG2 cells. Another possibility could be the difference between VDAC expressed in cancerous vs. non-cancerous tissue. There are intricate signaling pathways activated in cancers cells that could lead to the modification of VDAC by the previously mentioned phosphorylation of target amino acid residues located on the channel loops, or by acetylation at the N-terminus or on lysine side-chains as detected by mass spectrometry or site directed mutagenesis (Distler, Kerner et al. 2007). Additionally, although modification by acetylation of the cytosolic loops of VDAC has been reported, the impact of this modification on interactions with tubulin is unclear at present.

Differences between VDAC isoforms as studied by single-channel reconstitution are consistent with multi-channel data and suggest functional variation. The tentative structure of VDAC1 was first deduced from single amino-acid mutations to prove probable structures (Song, Midson et al. 1998), and more recently by NMR and X-ray crystallography (Ujwal, Cascio et al. 2008). However, there still remains much debate over the native folding pattern of the channel, primarily if the folding pattern of

artificially reconstituted channels is the same as the folding pattern of native channels. Moreover, the 3D structures for VDAC2 and VDAC3 remain elusive. Many researchers now agree that VDAC3 represents the most ancient form of VDAC, followed by VDAC2 and then VDAC1 which is thought to be a product of the latest evolutionary divergence (Messina, Reina et al. 2012). Due to the remarkable conservation of secondary-structure and function between all three isoforms, it is predicted that each isoform is similar in structure to VDAC1, which was concluded to be composed of 19 anti-parallel beta-strands with the only alpha-helical structure located at the N-terminus (Messina, Reina et al. 2012).

To address this long-standing question in the field concerning the functional similarities and differences of the three VDAC isoforms, I purified each isoform-enriched VDAC population from mitochondrial membranes provided by the Lemasters lab. I then reconstituted purified VDAC isoforms from knockdown cells into planar lipid bilayers and analyzed both the effects of transmembrane potential and tubulin at the single channel level. As described in earlier in this chapter, there was the possibility of low-grade contamination of the individual VDAC isoform populations due to incomplete knock-down in each preparation from target siRNA-treated cells, our collaborators verified both by immunohistochemistry and RT-PCR that the knock-down efficiency for each isoform was nearly 90%. To control for this possible 10% contamination, all single channel experiments were conducted at least six individual times for each isoform studied.

Interestingly, all three isoforms have an open-state conductance of about 4.2 nS in 1M KCl (Fig. 9A). Ease of channel insertion was markedly different between each isoform, where VDAC1 and VDAC2 inserted in the planar lipid bilayer quite easily, but VDAC3 required both a higher concentration of VDAC (ten times the concentration need for VDAC1 channel insertion and 5 times that of VDAC2 needed) added to the bath and a greater potential applied (20 mV for VDAC1 and VDAC2 insertion, and 100 mV for VDAC3 insertion. The exact mechanism of VDAC insertion into a planar lipid membrane from detergent micelles is unknown and it is possible that insertion rates could be a function of proper protein folding; however, the more likely explanation is differing VDAC concentrations of the isolated and purified samples. Both VDAC1 and VDAC2 are the highest expressed isoforms in HepG2 cells, together comprising nearly 90% of the total VDAC on the MOM (Maldonado, Sheldon et al. 2013). Even after siRNA knock-down of VDAC1 and VDAC2, the total concentration of VDAC3 remained unaltered. In fact, even though Western blot analysis determined a high purity of VDAC3 with almost no VDAC1/2 present, analysis of protein concentration by a Bradford assay shows that the total concentration of the VDAC3 sample after isolation and purification is nearly ten-times less than that of VDAC1 and VDAC2 (*data not shown*).

Interestingly, the voltage sensitivities of each of the three isoforms are markedly different. Under the application of 50 mV, each isoform shows a unique sensitivity to voltage-induced closure. While VDAC1/2 readily begin to gate at 50 mV (Fig. 9A/B), VDAC3 remains fully open (Fig. 9C). As explained in Chapter 1, the MOM potential is estimated to be between about 10-20 mV, suggesting that most probably, voltage induced

gating is only relevant for *in vitro* systems. However, these differences in sensitivities may allow us to begin to elucidate the exact mechanism behind voltage induced closures. Originally, Zizi et al. (Zizi, Byrd et al. 1998) published that the translocation of the voltage sensor from the inner lumen of the VDAC channel to the mouth of the channel was responsible for the decreased channel conductance and gating. Later work concluded that the N-terminus flexibility was essential for proper channel gating (Mertins, Psakis et al. 2012), which was largely discounted by analysis of a point-mutation in the inner lumen of VDAC designed to lock the N-terminus to the inside of the barrel and still was able to show proper channel gating (Teijido, Ujwal et al. 2012). Because the N-terminus was immobile and the channel still gated, it suggested that the N-terminus is not involved in the gating mechanism of VDAC.

To study tubulin interaction with each individual isoform, dimeric tubulin was added to either one or both sides of the channel. Remarkably, single channel interaction with dimeric tubulin is consistent with the results observed with multichannel membranes: VDAC1 was highly sensitive to tubulin (Fig. 9A), followed by VDAC2 (Fig. 9B), while VDAC3 remained tubulin insensitive (Fig. 9C). Even at tubulin concentrations 5-10 times of those needed for VDAC1 and VDAC2 interaction, VDAC3 remained open and unblocked (*data not shown)*. Statistical analysis confirmed that both VDAC1 and VDAC2 on-rates are nearly 3 orders of magnitude higher than that for VDAC3 (Fig. 9D). Additionally, it is important to note that although quite similar, VDAC1 and VDAC2 on-rates do differ slightly, where VDAC1 is more sensitive to tubulin biding than VDAC2. Even more remarkable is the conserved sensitivity on both sides of the channel.

One would assume that if phosphorylation was indeed responsible for the difference in channel sensitivities, then the VDAC isoforms should maintain a high asymmetry of tubulin interaction, whereby the *cis* or cytosolic face of the channel is sensitive to tubulin interaction, and the *trans* or inner mitochondrial space face remains unaltered. One of the possibilities is that in HepG2 cells there is an induced phosphorylation of the loops facing inside of the mitochondria. Another possibility is that the sensitivity to tubulin interaction is related more to the primary amino sequence and structure in the membrane. Future work will elucidate the mechanism by which VDAC isoforms isolated from HepG2 react to tubulin by specifically mutating candidate phosphorylation sites on the cytosolic loops. Moreover, mass spectrometry can be used to study if the possible post-translational modifications of each isoform are conserved or different.

These trends in isoform sensitivity to tubulin interaction were supported by work from our collaborators, who used TMRE uptake by mitochondria in HepG2 whole cell studies, to determine the contribution of each isoform to mitochondrial potential. We concluded that in HepG2 cells, VDAC3 was the isoform that contributed most to the modulation of mitochondrial potential. In experiments conducted by our collaborators and seen in Fig. 10A, as concluded by relative mRNA levels, both VDAC1 and VDAC2 are the highest expressed isoforms in HepG2 cells. Each siRNA knock down was greater than 90% effective as seen in the lower graph. Knock down was also confirmed by using antibodies against each isoform (Fig. 10B). After siRNA knock-down of both VDAC1 and VDAC2, mitochondrial potential was slightly altered as compared with the control.

However, knock-down of VDAC3 caused the greatest depolarization of mitochondria as seen in Fig. 10C. Additionally, in VDAC1/2 double knock-down cells, altering the amount of free tubulin did not influence mitochondrial potential. It was only when either VDAC1 or VDAC2 (but not both) was knocked down that modulation of the concentrations of free tubulin had an influence on mitochondrial potential. Taken together, we concluded that both VDAC1 and VDAC2 are constitutively blocked by tubulin in HepG2 cells, while VDAC3 serves as a leak channel, not influenced by tubulin interaction. By serving as a leak channel, VDAC 3 would plausibly remain open allowing for the maintenance of the mitochondrial gradient even when VDAC1 and VDAC2 are blocked. Again, this supports our findings suggesting that VDAC3 is not influenced as much by the local tubulin concentration due to its inherent tubulin insensitivity.

VDAC1, VDAC2, and VDAC3 all display anion selectivity in open state, and cation selectivity in the tubulin blocked state. The voltage-dependent anion channel, as the name suggests, has an anionic selectivity in its open state, whereby the reversal potential of VDAC isolated from mouse liver fractions was previously described as 12 +/- 1 mV. When the channel was blocked by tubulin, the selectivity changed to -14 +/- 4 mV as reported by (Rostovtseva, Sheldon et al. 2008). Ideally, the open state of the channel is known to favor the flux of negatively charged metabolites, notably ATP and ADP, into and out of the mitochondria. To test whether the three VDAC isoforms may be essential for transporting different metabolites and respiratory substrates, each VDAC isoform selectivity was experimentally calculated. Surprisingly, all three isoforms displayed a similar open state reversal potential (Fig. 11), where VDAC1 is 8.0 +/- 0.27, VDAC2 is

8.0 +/- 0.72 and VDAC3 is 9.3 +/- 2.31. Another remarkable feature of each isoform is the switch in reversal potential when blocked by tubulin. Each isoform changed from anion selective in open state to cation selective in the tubulin blocked state: VDAC1 -5.9 +/- 2.66, VDAC2 -10.2 +/- 0.14 and finally VDAC3 -14.2 +/- 3.25. As previously mentioned, VDAC3 is the most difficult channel to reconstitute and, generally, once reconstituted, loses stability, which in part could explain the larger standard deviation seen for VDAC3 than those for both VDAC1 and VDAC2. Additionally, VDAC3 is tubulin insensitive, as previously mentioned, so the concentrations of tubulin needed to induce channel closure are much higher than used with VDAC1 and VDAC2. Even with this, there is still the possibility that the closure events seen with VDAC3 could be a mix between tubulin blockage events, and voltage induced closure events. Future work will elucidate selectivity of all three isoform in the closed states, without tubulin present, but this will not be a trivial set of experiments. All three VDACs voltage gate to multiple closed states, and each closed state could possibly and quite likely have a different selectivity. Even with this taken into account, we can conclude that all three isoforms are anion selective in their open states, and that each channel reverses its selectivity in the tubulin-blocked state.

VDAC isoforms display differing closed states in the presence of tubulin. It was previously reported that dimeric tubulin strongly interacts with VDAC isolated from mouse liver, causing rapid and highly reversible channel closures to one characteristic closed state of about 40% residual conductance (Rostovtseva, Sheldon et al. 2008). To test if this closed state conductance is conserved between all three isoforms, statistical

analysis was performed on all single channel data. Surprisingly, VDAC2 displays one characteristic closed state to 40% residual conductance as seen in (Fig. 12B). VDAC1 (Fig 12A) and VDAC3 (Fig. 12C) however, display multiple closed states induced by tubulin interaction. VDAC1 displays at least two characteristic tubulin-induced closed states, one of which is 40% residual conductance and the other 20% residual conductance, and VDAC3 display multiple (at least three) closed states of 60%, 40% and 20% residual conductance, comprising the majority of events (Fig. 12C). These data are still quite preliminary, but may prove to have major implications in ascertaining the mechanisms of tubulin interaction with the three VDAC isoforms. Dimeric tubulin is comprised of a globular body of an alpha and beta subunit of nearly equal size and charge, and each alpha-beta subunit have a unique alpha and beta C-terminal tail (CTT). As previously mentioned, evolutionarily, these tails have a conserved tail length and charge for all organisms that require mitochondria for energy production. Could it be that the alpha tail interacts specifically with one VDAC isoform, while the beta tail interacts with another? VDAC3 from HepG2 cells appears to be tubulin insensitive, whereby the presence of nanomolar concentrations only seems to induce channel voltage gating, seen by the induction of multiple closed states. This too may be true with VDAC1, where we see the presence of the characteristic 40% residual conductance closed state, but also see the prevalence of a deeper closure or blockage of about 20% residual conductance. To speculate, this additional closed state level is likely due to tubulin-facilitated voltage gating, as previously discussed in (Rostovtseva, Sheldon et al. 2008). However, it is possible that each C-terminal tail of the tubulin dimer may interact quite differently with the topography of the VDAC inner lumen. One of the directions of

our ongoing work is aimed at elucidating the roles of the individual CTTs in VDAC interaction. Briefly, we are developing a construct comprised of amino-terminated dendrimers roughly the size of the tubulin body, in which we will chemically affix one specific CTT (either alpha or beta). This will allow us to test the functional interaction of each separate tail with all three VDAC isoforms and conclude which tail is responsible for VDAC blockage. Additionally, we, in collaboration with Dan Sackett (NICHD, NIH), are developing a recombinant construct of maltose-binding protein (similar size and roughly similar charge to that of the tubulin body) engineered with one alpha or beta CTT from tubulin attached to the C-terminus. Interestingly, the distance between the amino and carboxyl ends of maltose-binding protein is remarkably similar to the distance between the alpha and beta CTTs of tubulin. If we are able to get interaction with the maltose-binding protein construct with one single CTT, future research will be to attach both alpha and beta tails from tubulin onto the C- and N-termni of maltose binding protein, allowing us to study the functional role of the tubulin body and CTTs with the VDAC channel.

Small molecular weight compound erastin reverses VDAC closure by dimeric tubulin. There is an intense field of study focused primarily on finding compounds that are able to distinguish between the genetic phenotype of normal and cancerous cells. Erasin, a small molecular weight compound discovered recently, interacts by selectively targeting and killing mutant Ras/Raf cancer cells as reported by (Yagoda, von Rechenberg et al. 2007). Originally, the mechanism of erastin interaction was unknown, but the authors did mention that VDAC was specifically one of its targets. To test the

possibility that erastin interaction with VDAC may compete with tubulin interaction with VDAC, we used VDAC isolated from untreated HepG2 cells reconstituted into multichannel membranes to study both the effect of tubulin and erastin specifically on channel behavior. Erastin itself has no effect on channel gating properties. It should be noted that although the erastin compound does not alter channel gating, we are hindered by the membrane activity of erastin, whereby when we increase to concentrations greater than 1 μM, erastin causes the membrane to become leaky and eventually rupture forcing us to use sub-μM concentrations.

When tubulin is added to the membrane first, we see the characteristic induction of channel closure shifted to lower potentials (Fig. 13A and B). Remarkably, subsequent addition of erastin reverses this tubulin-induced closure, and eventually restores channel gating to that of the control trace (Fig. 13C). Additional collaborative work with John Lemasters on erastin treatment of whole HepG2 cells supports our findings: HepG2 cells treated with erastin, display mitochondria hyperpolarization allowing us to conclude that erastin promotes VDAC open state, and inhibits tubulin interaction with the channel even after subsequent treatment of cells with colchicine that increases the concentration of dimeric tubulin (Maldonado, Sheldon et al. 2013).

Another hallmark of erastin addition was the induction of channel insertion into the membrane (*data not shown)*. Erastin is composed of three aromatic rings, likely adding to the hydrophobic nature of this compound. It can be inferred that erastin prefers to be imbedded into the hydrophobic core of the lipid membrane, likely altering membrane

mechanics, which may explain the high channel insertion rate after erastin addition. Moreover, this too may explain the competition between erastin and tubulin. As previously published (Rostovtseva, Gurnev et al. 2012), tubulin interaction with VDAC is at least a three-step process: (1) tubulin body interaction with the lipid membrane, (2) tubulin body interaction with the cytosolic loops of the VDAC channel, and (3) CTT permeation into the lumen of the VDAC pore. Although erastin interference with steps 2 and 3 cannot be discounted, likely, erastin is likely interfering with step 1, altering membrane mechanics and inhibiting tubulin binding of the membrane. Additional work will need to be conducted on a single channel level to ascertain the exact mechanism of erastin competition with dimeric tubulin. Additionally, erastin should be used to probe all three VDAC isoforms to establish if erastin may distinguish between them. One final note should be made concerning the specificity of this compound. It was published to interact with VDAC, but only in mutated Ras/Raf cells, suggesting that erastin may recognize VDAC only after some form of VDAC modification by upstream Ras/Raf dependent signaling events. This is an exciting possibility that could link VDAC post-translational modifications to cell signaling through the activation of the Raf/Ras pathway. Preliminary studies should be aimed at comparing VDAC modifications from non-cancerous tissue to VDAC from Ras/Raf dependent cancerous tissue.

Discussion

Most of the early publications concerning VDAC did not discriminate between the three VDAC isoforms. However, with the mounting evidence of the important role that VDAC

plays in normal cell homeostasis, apoptosis, calcium signaling, etc, there is an increasing need to thoroughly differentiate between each VDAC isoform. Tissue expression levels of each isoform, and now selectivity, sensitivity to tubulin interaction, and sensitivity to voltage induced closure provides strong evidence that there are unique functional differences between each isoform.

As shown for the first time, VDAC isolated and purified from cell culture is viable and able to be reconstituted into planar lipid bilayers. Interestingly, VDAC isolated from untreated HepG2 cells is almost indistinguishable from VDAC isolated from mouse liver. The vast differences arise when each individual VDAC isoform is isolated and studied. siRNA targeting two of the three VDAC isoforms was applied to HepG2 cells, allowing for the isolation and reconstitution of "single isoform-enriched" VDAC populations. Multichannel studies of each isoform demonstrated that VDAC1 and VDAC2 sensitivity to voltage induced closure are quite similar, but that VDAC3 is almost insensitive to voltage induced closure even at potentials of +/- 60 mV. Moreover, there is a striking difference in the sensitivities of each of the isoforms to blockage by tubulin. VDAC1 is highly sensitive to tubulin interaction, followed by VDAC2 and finally VDAC3, which is almost tubulin insensitive. Even at tubulin concentrations five-times those used for VDAC1/2 interaction, VDAC3 blockage by tubulin remained only slightly altered, which, in its own turn, may be a byproduct of tubulin-induced voltage sensitivity rather than direct blockage by tubulin. Indeed, these results were confirmed when each isoform was studied at the single-channel level. Single VDAC channel experiments with each isoform showed that both VDAC1 and VDAC2 are more sensitive to voltage induced

channel closures, and that VDAC3 requires a much greater applied potential to induce gating. Additionally, VDAC1 and VDAC2 are the most sensitive to tubulin interaction, both having an on-rate nearly two orders of magnitude greater than that of VDAC3. Interestingly, conductance and selectivity of the open state of the channels remain consistent among isoforms. Selectivity of each channel reverses from anionic in the open state to cationic in the tubulin blocked state, though to varying degrees. Tubulin – previously described to cause channel blockage to one clearly defined characteristic state described by a 40% residual conductance for channels isolated form mouse liver – induces multiple closed states in both VDAC1 (2 primary closed states) and VDAC3 (displaying a broad distribution of closed states) (Fig.12). These additional closed states may be a result of tubulin enhanced voltage sensitivity of the channel, or could be the outcome of specific CTT interaction with the inner lumen of each channel. Erastin, a small molecular weight quinazolinone that specifically targets cancer cells expressing oncogenic Ras, has no detectable influence on VDAC isolated and reconstituted into planar lipid bilayers. It does, however, compete with tubulin interaction with VDAC, promoting the fully open state of VDAC. These results were supported by the work of our collaborators with whole HepG2 cultured cells. Mitochondrial potential as measured by TMRM uptake sustain that VDAC1 and VDAC2 knockdown by siRNA have little influence on mitochondrial potential. Knockdown of VDAC3, however, greatly depolarizes mitochondria, supporting the conjecture that in HepG2 cells, VDAC1 and VDAC2 are most probably constitutively blocked by tubulin, while VDAC3 remains open serving as a "leak" channel. Erastin treatment of HepG2 cells proved to

hyperpolarize mitochondria, suggesting that erastin may compete with tubulin for VDAC binding (primarily VDAC1 and VDAC2).

It has been reported that there is an intricate balance between MOM permeability and mitochondrial health. I propose that there is an optimal mitochondrial state in which some VDACs are blocked (VDAC1 and VDAC2) while some VDACs remain open (VDAC3), allowing for the flux of metabolites into and out of the mitochondria, thus supporting respiration as seen in Fig. 14. However, if all VDACs are blocked and/or closed, the mitochondrial potential becomes hindered, leading to a maximal suppression of the flux of metabolites into and out of the mitochondria, resulting in mitochondrial defects. Conversely, if all VDACs are open or unblocked, the MOM permeability becomes too great, leading to an oxidative bust and the production of highly reactive oxygen species (which may be modeled by erastin treatment of HepG2 cells) leading to cell death. There are still many questions that remain concerning the need of the three unique VDAC isoforms, but this work begins to provide, for the first time, a better understanding of the importance of the similarities and differences between each VDAC isoform.

Figure 8

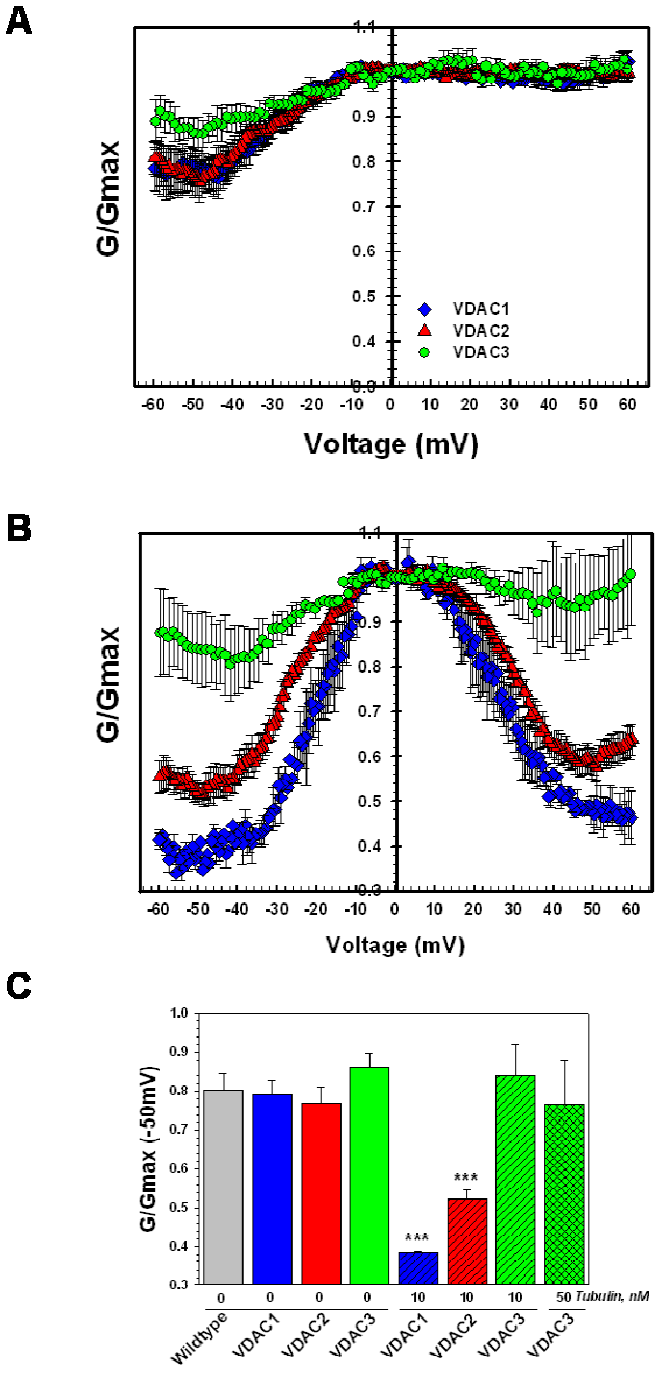

VDAC isoforms display differing sensitivities to blockage by tubulin. Double knock-downs of VDAC isoforms (1/2, 1/3, and 2/3) were performed on HepG2 cells and the remaining VDAC isoform was isolated and reconstituted into lipid bilayers. (A)

Normalize conductance (G/Gmax) is plotted verses applied potential for all three isoforms (VDAC1 in blue, VDAC2 in red, and VDAC3 in green) in the absence of tubulin. (B) 10 nM tubulin was added to both the *cis* and *trans* sides of the membrane, which increased channel closure at lower potentials as seen by the altering of the minimum conductance at potentials greater than 40 mV for VDAC1 and VDAC2 but not VDAC3. (C) Normalized conductance values at a potential of -50 mV with both 10 nM and 50 nM of tubulin present as indicated. *** $p < 0.001$ compared to no tubulin from 3-6 independent experiments for each group. (Maldonado, Sheldon et al., 2013)

Figure 9

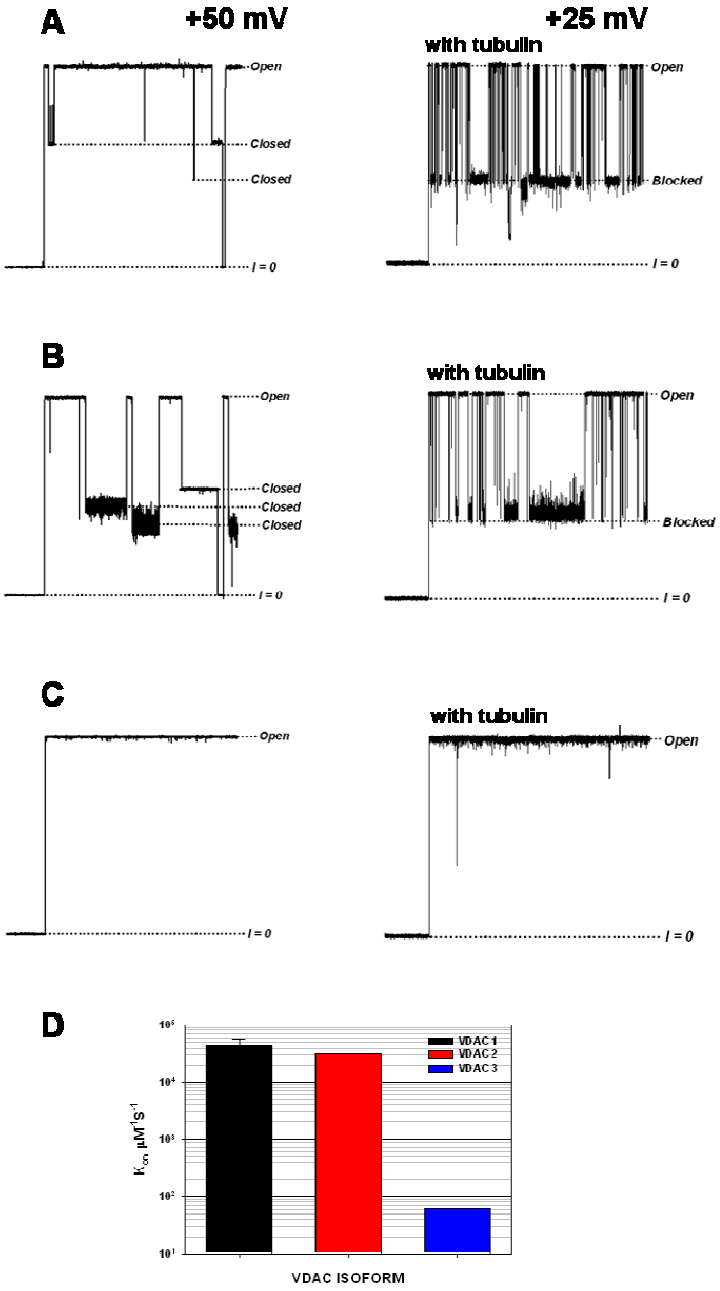

Each isoform displays a differing sensitivity to both applied potential and tubulin. Characteristic single channel current records through (A) VDAC1, (B) VDAC2 and (C) VDAC3 with (right panels) and without (left panels) 10 nM tubulin present. The left panels show voltage induced (50 mV) channel closures where VDAC2 is the most sensitive to voltage induced gating, followed by VDAC1 and then VDAC3, which is almost voltage insensitive. The right panels display the responses of each isoform to 10

nM tubulin where VDAC1 is the most sensitive, followed by VDAC2, while VDAC3 remains almost tubulin insensitive. (D) On-rate for VDAC1 (black), VDAC2 (red), and VDAC3 (blue) calculated from averaging the kinetic analysis of three independent experiments with each individual isoform.

Figure 10

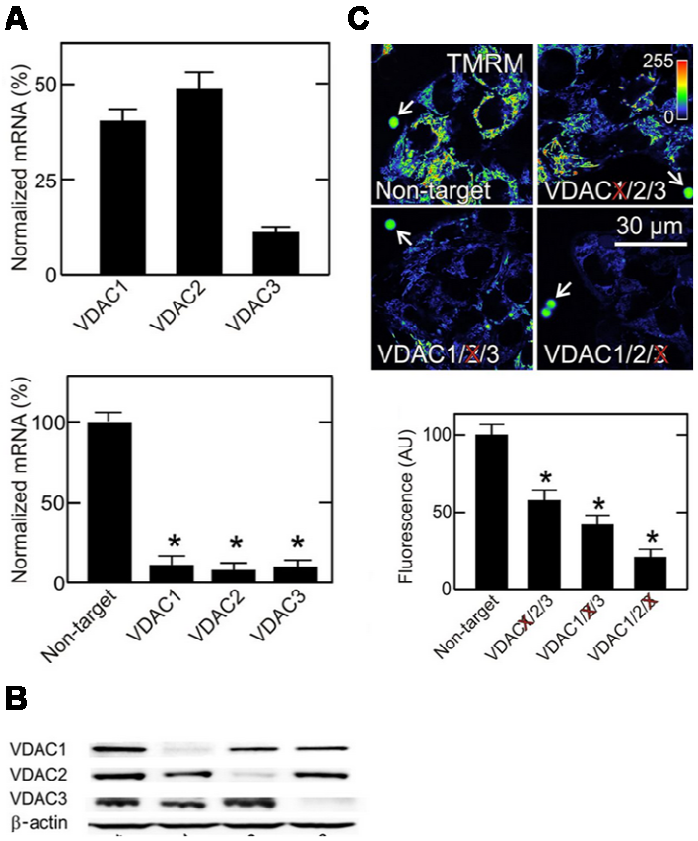

Knockdown of VDAC isoforms decreases mitochondrial membrane potential in HepG2 cells. As conducted by our collaborators, (A) the relative concentrations of VDAC1, VDAC2, and VDAC3 as measured by qPCR with and without siRNA treatment. (B) HepG2 cells were treated with either non-target siRNA or siRNA targeting VDAC21, VDAC2, or VDAC3. After 48 hours of treatment, protein expression of all three isoforms was assayed by immunoblotting. (C) HepG2 cells were loaded with TMRM and imaged after treatment with either non-target siRNA, or siRNA targeting VDAC1, VDAC2, or VDAC3. Image intensity was pseudocolored according to the reference bar and white arrows indicate fiduciary fluorescent beads. Intensities were

averaged (* $p < 0.05$) from five independent experiments analyzing 4-5 random fields with at least 5-10 cells. (Maldonado, Sheldon et al., 2013)

Figure 11

	VDAC1	VDAC2	VDAC3
Erev Open	+8.00 ± 0.27	+8.12 ± 0.72	+9.26 ± 2.31
Erev Tubulin	-5.91 ± 2.66	-10.19± 0.14	-14.23 ± 3.25

Reversal potential of the open state of each VDAC isoform remains unaltered. The reversal potentials of VDAC1, VDAC2 and VDAC3 are shown with standard errors averaged over at least three independent experiments. The reversal potentials of the tubulin blocked states show a general change of each isoform from positive Erev to negative Erev.

Figure 12

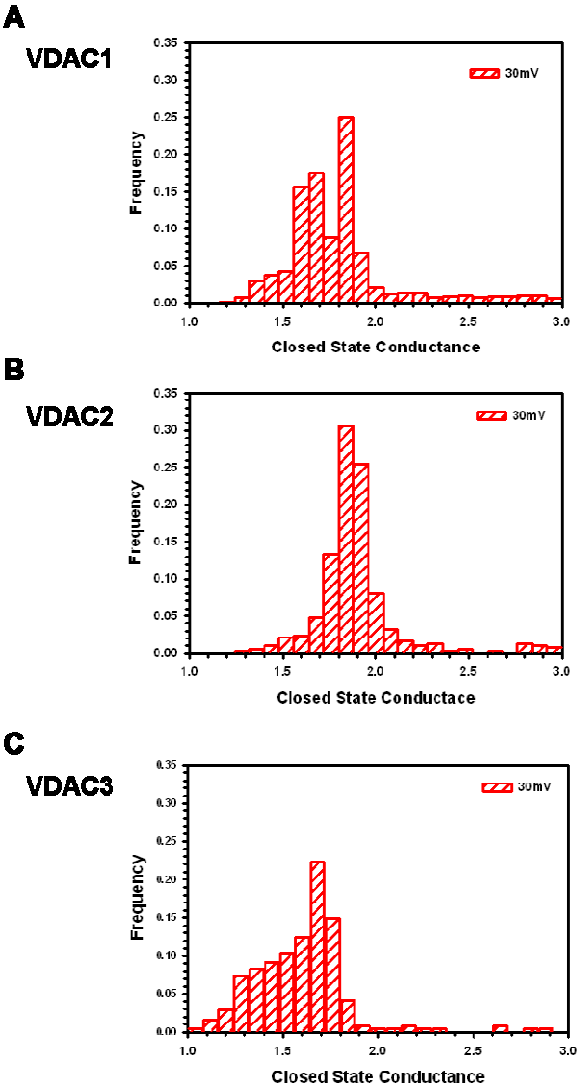

VDAC isoforms display different tubulin induced closed-state conductances. Histograms compiled from at least 500 tubulin events with each isoform. (A) VDAC1 displays at least two closed states, one at the typical 60% blockage and a second deeper closure to about 80% blockage. (B) VDAC2 displays one unique and characteristic 60% closed state, while (C) VDAC3 displays multiple closed states seen in the wider distribution of states.

Figure 13

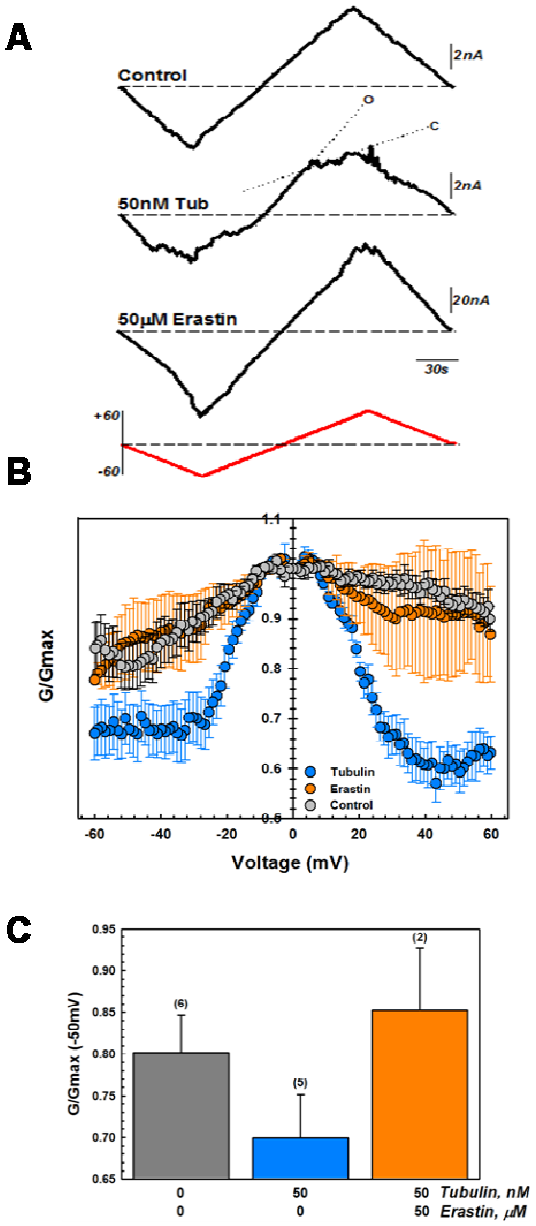

Erastin treatment of multichannel VDAC membranes reverses tubulin-induced blockage of VDAC. (A) Representative current traces through the same multichannel membrane in response to periodic triangular voltage waves with a potential between +60 and -60 mV at 5 mHz. Open state slope is depicted by a dashed line and "O" while channel closure slope is indicated by a dashed line and "C". (B) The normalized average

conductance (G/Gmax) versus voltage is plotted from at least three independent experiments as shown in (A), where tubulin addition induces channel closure. Subsequent treatment with erastin restores channel gating to levels observed without tubulin present. Each data point represents the average of 3-6 experiments +/- standard error. (Maldonado, Sheldon et al., 2013)

Figure 14

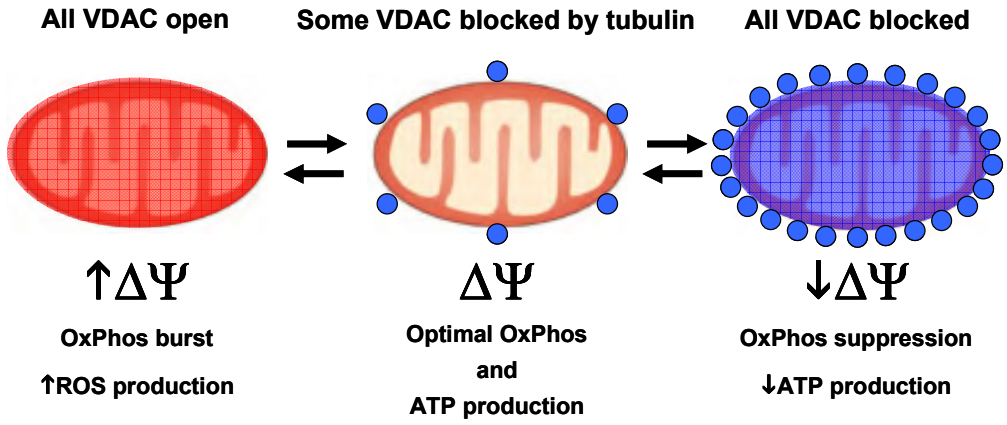

Mitochondrial health as defined by mitochondrial membrane potential is modulated by VDAC blockage. Scheme displaying the correlation between mitochondrial outer membrane remobilization and mitochondrial potential. When all channels are blocked by tubulin, oxidative phosphorylation becomes suppressed and leads to a decrease in ATP production, and mitochondrial depolarization. Conversely, if all VDAC channels become open, there is a burst of oxidative phosphorylation leading to an increase in mitochondrial polarization, and a production of reactive oxygen species.

CHAPTER 4: PRELIMINARY RESULTS AND FUTURE DIRECTIONS IN THE STUDY OF THE VOLTAGE DEPENDENT ANION CHANNEL

PART I: NEUROGLOBIN BINDS THE VOLTAGE DEPENDENT ANION CHANNEL CAUSING UNIQUE CHANNEL BLOCKAGES

Introduction

Until recently, the globulin super-family was considered to contain two sub-families: (1) myoglobin and (2) hemoglobin. Both proteins are classically known for their ability to bind and store oxygen in either muscle tissue or in red blood cells, respectively. Recently, a third sub-family of globin was discovered, found primarily expressed in neural tissues and termed neuroglobin (Ngb) (Burmester, Weich et al. 2000; Burmester and Hankeln 2009). Although Ngb was discovered more than ten years ago, its function still remains elusive. Even so, there is much speculation as to the function of Ngb: (1) as the promoter and maintainer of proper neuron function under hypoxic stress (Pesce, Dewilde et al. 2003), (2) as the reducer of cytochrome c leading to apoptosis inhibition, (3) as a reactive oxygen species (ROS) scavenger, and (4) as a carrier of oxygen to the mitochondria in the support of proper electron transport chain function (Burmester and Hankeln 2009). The crystal structure of Ngb was solved and revealed 151 amino acids (17 kDa) comprising 6 alpha-helices folded in a fashion similar to other globin-family proteins, with the presence of short N- and C-terminals (Pesce, Dewilde et al. 2003). Several publications have shown the close association of Ngb with mitochondria,

especially in neurons under hypoxic stress (Lechauve, Augustin et al. 2012; Yu, Xu et al. 2012). Moreover, Ngb has been linked to neuroprotection against both Alzheimer's disease and stroke (Greenberg, Jin et al. 2008).

The voltage-dependent anion channel (VDAC) is the most abundant protein of the mitochondrial outer membrane (MOM), where it spans the thickness of MOM and serves as a passageway for metabolite flux. Very recently, it was shown by co-immunoprecipitation that Ngb targets and binds VDAC in cultured mouse neurons, and that this interaction was up-regulated upon oxygen-glucose deprivation (Yu, Liu et al. 2013). The aim of the present work was to verify the interaction of Ngb and VDAC on the single channel level, and to further explore the consequences that Ngb-VDAC binding may have on the VDAC channel properties. We show that the addition of nanomolar concentrations of recombinant human neuroglobin to a single VDAC reconstituted into a planar lipid bilayer induces high frequency noise as well as channel closure or blockage.

Materials and methods

VDAC isolation and reconstitution

VDAC was isolated from mouse liver fractions that were a generous gift of Marco Colombini. Isolation was conducted according to the previously published method: briefly, after incubation of the membranes with buffer containing Triton-X100, the samples were run over a 2:1 hydroxyappatite/celite column (Rostovtseva, Kazemi et al.

2006). Fractions were collected and stored at -20°C for subsequent use. Planar lipid bilayers were formed from monolayers composed of diphytanoyl phosphatidylcholine (DPhPC) 5 mg/mL dissolved in pentane. A thin Teflon partition separating two compartments filled with buffer (1 M KCl, 5 mM HEPES, pH 7.4) contained a thin aperture with a diameter roughly 50-60 μm treated with hexadecane in pentane (1% vol/vol). VDAC was reconstituted according to previously described methods with a minor modification of applying a steady state voltage of 150 mV to induce single channel insertion. Once inserted, recombinant human Ngb, which was a generous gift from Zhanyang Yu (Massachusetts General Hospital, Charlestown, MA), was added to either one or both sides of the channel under constant stirring for 1 min. All data were collected and analyzed as previously described.

Results

Nanomolar concentrations of Ngb induce high frequency channel noise and channel closure. To study functional interaction of Ngb with VDAC isolated from mouse liver, nanomolar concentrations of Ngb were added to either one or both sides of a single reconstituted VDAC channel. At 50 mV applied potential, 10 nM of Ngb induces both high-frequency channel noise and channel gating shown in Fig. 15. These characteristics are heavily dependent on both Ngb concentration and applied potential as seen in panels B through D. It is possible that Ngb interaction with VDAC is through the N- and C-terminal tails of Ngb, which consist of 5 residues with a net charge of -1, and 7 residues with a net charge of -1, respectively, and is similar to the model for tubulin interaction

with VDAC (Rostovtseva, Sheldon et al. 2008). Although the net charge of Ngb is only -1 (19 negative residues and 18 positive residues), there are regions of negative charge on the protein body as well as on the bend that connects two of the alpha-helicies. Interestingly, Ngb induction of channel noise is very reminiscent of the noise induced upon addition of Tub-S as reported (Rostovtseva, Sheldon et al. 2008). Likely, this high-frequency noise is created by Ngb interaction with the mouth of the VDAC channel, obstructing the path of flow of ions through the channel. Moreover, it is this interaction with the mouth of the channel that is likely responsible for inducing voltage sensitivity of VDAC. Another characteristic of Ngb interaction with VDAC is inducing channel closure to multiple closed states as seen in Fig. 15. Whereas tubulin is known to induce ~60% channel closure, Ngb induces a wide distribution of closed-state conductance more typically seen with voltage gating of the channel. One final note should be made concerning *cis* (cytosolic) and *trans* (inner-mitochondrial) interaction of Ngb with VDAC. Indeed, Ngb interacts with both sides of the channel, however, the *cis* side of VDAC seems to be much more sensitive to Ngb than the *trans* side. Interestingly, it has been noted that Ngb is found both associated with the MOM and also found inside of the mitochondria (Lechauve, Augustin et al. 2012; Yu, Xu et al. 2012), and that the concentration of Ngb inside of the mitochondria markedly increases after oxygen-glucose deprivation. It was reported that Ngb does not contain the 'typical' mitochondrial targeting pre-sequence strongly suggesting that it does not undergo the typical mitochondrial import mechanism through the translocase of the outer membrane (Tom) that ~ 50% of mitochondrial proteins do (Lechauve, Augustin et al. 2012).

Much of the focus of recent work concerning Ngb has been in its neuroprotective role by inhibiting the formation of the mitochondrial permeability transition pore (Mptp) as published in (Yu, Xu et al. 2012; Yu, Liu et al. 2013). Another possibility is Ngb competition with dimeric tubulin, maintaining VDAC in its open state. More specifically, Ngb will be studied with each of the three VDAC isoforms to ascertain if there is any channel specificity of Ngb interaction.

PART 2: TAT-HEXOKINASE PEPTIDE AND FULL LENGTH HEXOKINASE COMPETITION WITH DIMERIC TUBULIN FOR BINDING TO THE VOLTAGE DEPENDENT ANION CHANNEL

Introduction

The Warburg Effect is classically defined as the propensity of cancerous cells to undergo respiration via glycolysis, even in the presence of oxygen (Warburg, Wind et al. 1927; Warburg 1956). Ultimately, oxygen – in relation to oxidative respiration via the electron transport chain located in the inner mitochondrial membrane – is the last electron acceptor whereby it combines with H^+ in the formation of water, a byproduct of respiration. In non-cancerous cells, under normoxic conditions, energy in the form of ATP is generated by ATP synthase in response to a proton-motive force maintained across the inner mitochondrial membrane as long as oxygen is present. Under conditions where oxygen may not be readily available (intense or prolonged exercise), the electron transport chain function is toned down and there is a cellular switch to ATP formation via glycolysis.

Classically speaking, oxidative respiration as compared to anaerobic respiration generates ATP at a ratio of roughly 15:1 respectively (Porter and Brand 1995; Rich 2003). An immediate question arises. Cancerous cells are known to be high-energy demanding cells, likely due to the need to grow and divide. So why would cancerous cells favor respiration via glycolysis to respiration via aerobic respiration? Recent evidence suggests

that the answer may be in the speed of ATP production, whereby glycolysis produces ATP at a much faster rate (Lopez-Lazaro 2008; Lunt and Vander Heiden 2011). But this hypothesis only partially explains the switch.

Interestingly, another hallmark of many cancers is the up-regulation and targeting of hexokinase to the mitochondrial membrane (Mathupala, Ko et al. 2006). Hexokinase is responsible for the phosphorylation of glucose at the sixth carbon, producing glucose-6-phosphate (G6P), thereby inhibiting the export of glucose from the cell via the glucose transporter (GLUT4). The mammalian hexokinase family is comprised of four isoforms, HK1, HK2, HK3 and glucokinase. Because glucokinase is only expressed in the liver, and currently very little is known about HK3, both will not be discussed in this chapter. Additionally, HK1 is relatively unaffected by most physiological functions and serves as a "house-keeping" enzyme maintaining a balance of cellular glucose levels. HK2 however, is classically up-regulated in cancerous cells where it translocates from the cytosol to the mitochondrial outer membrane (MOM). Recent evidence suggests that HK2 docks to the MOM through VDAC (Pastorino and Hoek 2008; Pedersen 2008). However, there is a long standing disagreement as to its outcome. It was reported that when HK2 binds VDAC, it greatly decreased the open probability of the channel (Azoulay-Zohar, Israelson et al. 2004). However, there is also evidence that when HK2 binds VDAC, it locks the channel in an open conformation (Gogvadze 2011).

Recent work has demonstrated that HK2 expression is also cardio-protective. Under induced ischemia and subsequent reperfusion of whole mouse hearts, it was shown that

the cytosolic concentration of HK2 greatly decreased and the concentration of mitochondrial-bound HK2 significantly increased (Zuurbier, Smeele et al. 2009). TAT-HK2 has been shown to selectively compete with native Hxk2 for mitochondrial binding (Gurel, Smeele et al. 2009). More specifically, the application of TAT-HK2 (hydrophobic TAT peptide affixed to 16 amino acid residues of the N-terminus of HK2) at low dose demonstrated the same outcome of cardioprotection. However, the application of high concentrations of TAT-HK2 displaced native HK2 from the mitochondria, and eventually led to cell death (*unpublished data, Zuurbier)*.

Recently, work from our lab and our collaborators' lab demonstrated that mitochondrial respiration, as indicated by isolated mitochondria respiration, mitochondrial potential via TMRE, and VDAC reconstitution experiments, is modulated by both local tubulin concentrations and phosphorylation state of the VDAC channel (Lemasters and Ramshesh 2007; Maldonado, Patnaik et al. 2010; Sheldon, Maldonado et al. 2011; Lemasters, Holmuhamedov et al. 2012; Maldonado, Sheldon et al. 2013). VDAC is the most abundant protein of the MOM and serves as the channel that facilitates the flux of metabolites, namely ADP and ATP, into and out of the mitochondria. Since previous work demonstrated that VDAC was possibly a target of HK2 interaction, we sought to explore the functional interaction of (1) TAT-HK2 and (2) full length isolated and recombinant HK2 with VDAC.

Materials and methods

Isolation of recombinant hexokinase 2. rhHexokinase2 (rhHK2) B-PER 6xHis Fusion Protein plasmid was transfected and expressed in One Shot BL21 competent cells according to company recommendations (Invitrogen, Grand Island, NY). All cell media and subsequent isolation materials and protocols were obtained from Invitrogen. Each isolated and purified protein sample was stored in glycerol (10%) at -20^{o}C. Protein concentration was analyzed with Pierce BCA Protein Assay Kit according to company recommendations (Thermo Scientific, Rockford, IL). Hexokinase activity was determined by an assay that is based upon the reduction of NAD^{+} coupled to the reaction of glucose-6-phosphate (G6P) dehydrogenase as published by Worthington (Lakewood, NJ). A unit of hexokinase activity was defined as the reduction of one micromole of NAD^{+} per minute at 30^{o}C. rhHexokinase2 was also purchased from GenWay Bio (San Diego, CA) for use as a control.

Isolation of hexokinase 2 from mouse skeletal muscle. Isolation of native mouse hexokinase from whole brains was carried out according to (Zelenina, Avramova et al. 1991) as translated from Russian to English by Philip Gurnev. Purification of the final hexokinase preps was carried out on a suspension of diethylaminoethyl (DEAE)-cellulose in a buffer containing 10 mM K-phosphate at pH 7.0. All hexokinase samples were run on SDS page (Invitrogen) and probed with anti-hxk2 #2106 (Cell Signaling, Danvers, MA).

Results

TAT-HK2 binds to VDAC and inhibits tubulin interaction. For whole heart perfusion experiments, the concentration of TAT-HK2 was roughly in the micromolar range. To begin, I first tested the interaction of the peptide with VDAC reconstituted from mouse liver. TAT-HK2 has no apparent interaction with VDAC as seen by an unaltered channel conductance, absence of high frequency channel noise, and unchanged channel selectivity. This did not discount the possibility that TAT-HK2 could indeed be binding to the channel loops away from the mouth of the VDAC channel. To test for this, nanomolar concentrations of dimeric tubulin were added to the bath to check for the tubulin induced blockage of VDAC channel conductance. Surprisingly, no interaction of tubulin was seen with VDAC. Moreover, tubulin added to the same channel, but at the *trans* side which did not contain TAT-HK2, induced characteristic channel closure verifying channel integrity. As seen in Fig. 16, to test if TAT-HK2 competes with tubulin in a dose dependent manner, 20 nM tubulin was added to the *cis* side of a reconstituted VDAC channel without TAT-HK2 present (16A). The tubulin was allowed to interact with VDAC for roughly 10 mins to reach equilibrium in tubulin binding to VDAC. This was followed by subsequent additions of TAT-control to the *cis* side of VDAC and, as seen in Fig. 16A, had no influence on tubulin binding. This was followed by the addition of 3 and then 10 micromolar Tat-HK as seen in Fig. 16B. Increasing concentrations of TAT-Hxk2 decreased tubulin interaction, and at 10 μM concentration the channel was maintained in an open state. Surprisingly, TAT-HK2 does compete with tubulin interaction with VDAC from both sides of the channel, both *cis* and *trans*,

however, *trans* side interaction requires a much greater concentration of TAT-HK2 (roughly 3-5 times). Additionally, when TAT was used without the addition of the 16 amino acids from HK2 (TAT-Con), it had no effect on the basic channel properties and moreover, no effect on tubulin-VDAC interaction.

Thus, according to the preliminary data, TAT-HK2 competes with dimeric tubulin for specific VDAC binding. Logically, the next step was to test if this interaction was conserved in full length HK2. For these experiments, both rhHK2, HK2 isolated from mouse skeletal muscle, and commercially available rhHK2 were employed. All three forms of HK2 were run on SDS page and probed with a commercially available anti-HK antibody and each sample showed an approximate band at 100 kDa, the molecular weight of hexokinase as previously published. However, when subjected to an activity assay that monitored the rate at which the enzymes were able to convert glucose into G6P, both the isolated and rhHK2 failed to show an enzyme activity. The only HK that displayed catalytic activity was the commercially available HK2. All subsequent experiments were conducted with the commercially available HK2 (referred heretofore as HK2).

To begin, HK2 was added to the bath on the *cis* and/or *trans* side of VDAC. Interestingly, unlike TAT-HK2, HK2 induced both high frequency channel noise, and at high (micromolar) concentrations sensitized VDAC to voltage induced gating as seen in Fig. 17. The difference between TAT-HK2 and HK2 induced noise may be due to the bulky body of the full length HK2. Even if the N-terminal region of full length HK2 binds to the loops of the channel, the body of the protein is large enough to partially

obstruct the flow of ions through the mouth of the channel, resulting in the high frequency channel noise. Additionally, this channel noise was voltage dependent, whereby noise induction was seen at lower applied potentials with increasing HK2 concentrations. Subsequent addition of TAT-HK2 competed with HK2 and reduced channel noise in a dose dependent manner as seen in Fig. 17. This adds support for our claim that HK2 does indeed bind specifically to VDAC. One interesting note to make is that at no concentration (nanomolar to micromolar) of HK2 or HK1 did the enzyme induce channel closure as previously published (Azoulay-Zohar, Israelson et al. 2004). In fact, even with the increased voltage sensitivity of the channel after HK2 addition, potentials of 70 mV or greater were needed to begin to see highly reversible voltage gating. And, although micromolar concentrations of HK2 were added to VDAC both *cis* and *trans* side, VDAC was never closed.

To test if HK2 competes with tubulin as did the TAT-HK2 peptide, tubulin was subsequently added (10-100 nM) to test for the interaction. HK2 did inhibit tubulin from binding and blocking VDAC as seen in Fig. 18B. However, surprisingly, if tubulin was added to VDAC first, HK2 did not compete with tubulin binding to VDAC as seen with TAT-HK2. There is the possibility that the concentrations of tubulin at which we are working are higher than physiological, where the best estimates of dimeric tubulin concentration span the order of sub-nanomolar to micromolar depending on the cell activity. More work will be conducted regarding the mechanism by which the competition of tubulin and HxK2 for VDAC binding depends on the order of addition.

Discussion

There has been a long standing question in the field concerning the role of HK2-VDAC interaction in context of the Warburg Effect. We add support to a previously posed model, whereby HK2 binds VDAC and maintains the channel in its open state. We add to this model by showing for the first time, that HK2 bound to VDAC does not influence much its voltage gating but rather inhibits tubulin blockage of VDAC. This would theoretically allow for HK2 preferential access to the ATP that is fluxing through VDAC, to be used in the conversion of glucose to G6P in support of increased glycolysis, a hallmark of many cancers. In addition, this would allow for the maintenance of the low-grade electron transport chain function, which has been known to be functional in cancerous mitochondria, just at altered rates (Weinhouse 1976). Additionally, low-dose TAT-HK2 has been shown to be cardioprotective during ischemia and reperfusion of whole mouse hearts while high-dose TAT-HK2 is lethal (Nederlof, Xie et al. 2013). Although the mechanisms of protection and lethality are still in question, we showed that at nanomolar concentrations, TAT-HK2 inhibited tubulin from binding and blocking VDAC in a dose dependent manner. We further consider an intricate balance of open and closed VDAC channels in the regulation of mitochondrial health as seen in Fig. 19. We hypothesize that at high concentrations of HK2, all tubulin is displaced from the mitochondrial membrane allowing all VDAC to maintain open state conformations leading to an increased concentration of glucose-6-phosphate supporting glycolysis as classically described by the Warburg effect. HK2 would have preferential access to

mitochondrial generated ATP, maintaining proper electron transport chain function, supporting mitochondrial health, but promoting the glycolytic pathway.

Future work will focus primarily on specifically testing for both TAT-HK2 and full length HK2 interaction on each of the three VDAC isoforms. As previously mentioned, we concluded that in HepG2 cells, VDAC1 and VDAC2 are constitutively blocked by tubulin while VDAC3 served as a "leak" channel for maintenance of the flux of metabolites and electron transport chain integrity. Additionally, each isoform of VDAC isolated from HepG2 cells displays a high variability to tubulin interaction where VDAC1 is the most sensitive, followed by VDAC2, and finally VDAC3 which is almost tubulin insensitive. It is possible that there is also specificity in HK2 binding to VDAC isoforms.

PART III: SMALL MOLECULAR WEIGHT COMPOUND ERASTIN INTERACTION WITH THE VOLTAGE DEPENDENT ANION CHANNEL

Introduction

Erastin is a small molecular weight compound that has been shown to selectively target and kill RAS/RAF mutated cancer cells (Dolma, Lessnick et al. 2003). Specifically, erastin was shown to target VDAC2 and VDAC3, as detected by a reduced impact of erastin on cells that had either VDAC2 or VDAC3 knocked-down (Yagoda, von Rechenberg et al. 2007). When further studied by affinity purification and mass spectrometry, and a filter binding assay that used a radiolabeled analogue of erastin, it was concluded that VDAC2 is the primary isoform that erastin binds, inducing non-apoptotic cell death (Bauer, Gieschler et al. 2011). Subsequent work from the same group established that the mechanism by which erastin leads to non-apoptotic cell death is highly dependent on intercellular iron concentrations, describing this form of cell death as ferropotosis (Dixon, Lemberg et al. 2012). In both reports, erastin strongly targeted VDAC2, leading to iron dependent reactive oxygen species (ROS) production, which caused downstream signaling events promoting cell death by ferropotosis. Recently, it was shown that in VDAC reconstituted into planar lipid bilayers, erastin is able to interfere with VDAC blockage by tubulin and restore channel conductance to that of the control (Maldonado, Sheldon et al. 2013).

Here, we aim to test the specificity of erastin on VDAC isolated from multiple sources (*N. crassa*, mouse spinal cord, mouse liver, rmVDAC1 and rmVDAC2). We show that even at micromolar concentrations, erastin has seemingly no influence on VDAC channel behavior. Additionally, at concentrations higher than 1 μM, erastin induces stress on the planar lipid bilayer leading to membrane rupture. Moreover, in contrast to previously published results showing erastin inhibition of tubulin interaction with VDAC on multichannel membranes, erastin shows no competition with tubulin-VDAC interaction on the single channel level.

Materials and methods

Erastin was purchased from Sigma-Aldrich (St. Louis, MO).

Results

Erastin does not interact with a single reconstituted VDAC channel. To test if erastin influenced VDAC channel behavior, concentrations of erastin, first diluted either in DMSO or ethanol due to its hydrophobic nature, were added to the bath either on the *cis* or *trans* side of the channel (*data not* shown). Even at concentrations in the micromolar range, erastin had no detectable effect on VDAC channel conductance or noise of the open state of the channel of VDAC isolated from mouse liver. This suggests that if the small molecule does interact with VDAC, it must do so at a region of the channel that is out of the path of the flow of ions. Interestingly, it should be noted that although it is difficult to quantify, erastin seems to have a large impact on the lipid bilayer. As

concentrations increased, erastin induced membrane leakiage as revealed by a large induction of unstable conductance, before eventually causing the membrane to rupture. It should also be noted that erastin contains several aromatic rings adding to the compounds hydrophobic nature, so it would not be surprising if erastin partitioned into the lipid bilayer altering its properties.

As previously mentioned, on multichannel membranes, erastin was able to reverse channel closure induced by the addition of dimeric tubulin to the bath. To test if this competition was conserved on the single channel level, one VDAC channel was reconstituted and tubulin was added to the *cis* side of the channel. After roughly 10 mins, erastin was added to both the *cis* and *trans* side of the channel. Surprisingly, erastin had no detectable effect on tubulin interaction with VDAC isolated from mouse liver. Moreover, at high concentrations, erastin appeared to enhance tubulin blockage of VDAC (*data not shown*). Although there is a possibility that erastin may increase tubulin interaction with VDAC, it is more likely that the vehicle (DMSO, ethanol) is responsible for the increase of tubulin interaction. In data not shown, both the addition of DMSO or ethanol was enough to induce a greater tubulin interaction with VDAC, presumably by dehydrating the surface of VDAC and/or the membrane allowing for increased sensitivity to tubulin binding. More work will need to be conducted to find a vehicle for erastin that does not interfere with the tubulin-VDAC interaction.

One possibility explaining the discrepancy between our multichannel and single channel data might be through the type of VDAC in the membrane. Although it was previously

published that erastin targets VDAC2 specifically, it does not explain the ability of erastin to discriminate between wild type VDAC2 and VDAC2 from RAS/RAF mutated cells. This may suggest that VDAC could be modified by post-translational modifications due to upstream signaling resulting from RAS/RAF activation. Indeed, RAS/RAF activation is known to activate a large number of kinases, one of which may target VDAC, more specifically VDAC2. Although erastin was shown to interact with rVDAC2 reconstituted into liposomes, in my experiments, erastin had no influence on rVDAC2 channel behavior.

Additionally, we tested VDAC isolated from many sources: mouse brain, mouse liver, mouse heart, *N. crassa*, mouse spinal cord, HepG2 mitochondrial fractions and rVDAC1/rVDAC2 to name a few. With each of these VDACs, erastin had no effect on basic channel properties or tubulin interaction with the channel. This suggests two likely possibilities: (1) VDAC must be modified to become sensitive to erastin interaction or (2) erastin is indeed isoform specific. There is a possibility that in our multichannel membranes of VDAC isolated from HepG2 cells, the channels were a heterogeneous mix primarily of VDAC1 and VDAC2. It is likely though that VDAC1 is the primary isoform expressed in all other sources mentioned. However, even when HepG2 VDAC single channels were reconstituted, erastin still had no effect.

Discussion

Although the idea of a small molecular weight compound that can selectively distinguish cancerous from noncancerous cells is provocative, there is still a great amount of work to be conducted with erastin to prove and verify its activity. Current studies suggest that VDAC, more specifically VDAC2, is a direct target of erastin interaction. What is not known is the outcome of this specific interaction, other than erastin treatment leading to cell death in RAS/RAF mutated cell lines. We previously showed that on multichannel membranes comprised of VDAC isolated from HepG2 cells, erastin was able to compete with tubulin for VDAC binding. Although this was quite exciting, further work with erastin on single VDAC channels isolated from HepG2 proved to complicate our findings. There does, however, seem to be some dependence of the interaction on both VDAC isoform and the source of VDAC isolation. VDAC isolated from mouse liver, even in multichannel membranes, was seemingly unaffected by erastin in our system. VDAC isolated from HepG2 proved to interact with erastin, but only on a multichannel membrane. Future work will need to be conducted to deduce both the role of post-translational modification as well as isoform type on the specificity of erastin interaction.

Moreover, VDAC channel properties have been reported to be highly dependent on membrane lipid composition (Campbell and Chan 2008; Rostovtseva and Bezrukov 2008; Mlayeh, Chatkaew et al. 2010). Tubulin interaction with VDAC was shown to be at least a three-step process: (a) tubulin binding the membrane, (b) tubulin binding the VDAC channel loops, and (c) tubulin C-terminal tail permeation into the inner lumen of

VDAC leading to the characteristic channel block. Could the competition between erastin and tubulin actually be through erastin modification of lipid mechanics impacting step (a)? The hydrophobic nature of erastin would suggest that it may penetrate into the lipid leaflets. This could be enough to locally influence VDAC properties; however this would not explain the RAS/RAF specificity.

Figure 15

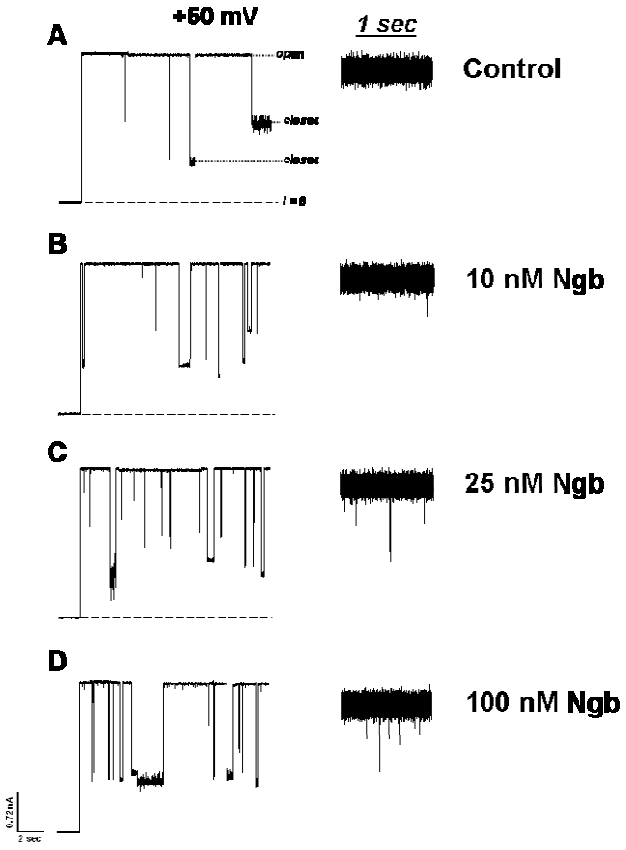

Neuroglobin induces characteristic VDAC current noise and increases VDAC voltage sensitivity. (A) A characteristic current record through a single VDAC channel with an applied potential of 50 mV. (B-D) The subsequent addition of increasing concentrations of neuroglobin induces both VDAC current noise as well as channel closure in a dose dependent manner.

Figure 16

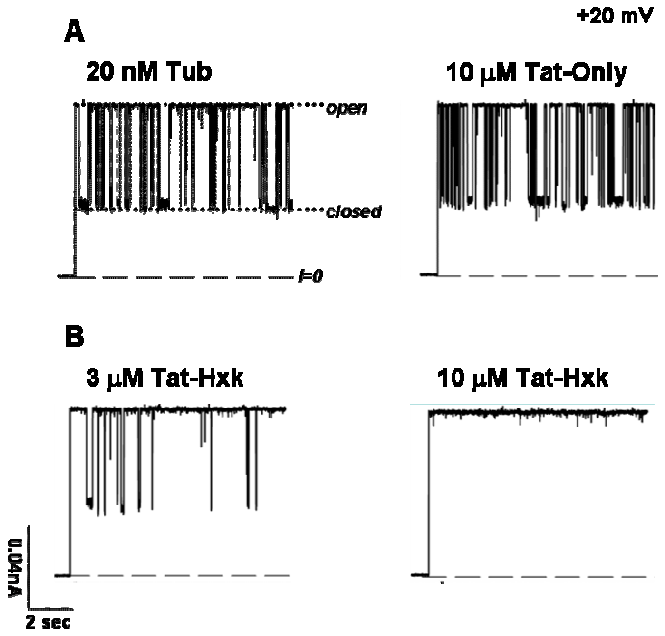

Tat-HK competes with tubulin for VDAC binding. Fig. 16 displays the current record through one single VDAC channel of the same experiment. The addition of 20 nM of tubulin induces characteristic channel blockage events. Subsequent addition of 10 μM of Tat peptide has no influence (A); however following additions of increasing concentrations of Tat-HK (3 μM and 10 μM) compete with tubulin and lock VDAC in its fully conducting state (B).

Figure 17

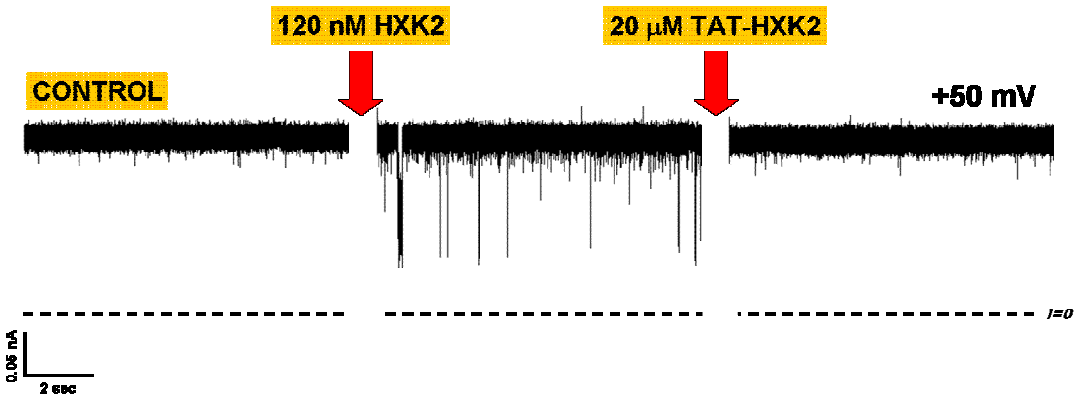

Full length HK2 induces high frequency channel noise that is inhibited by the addition of competing Tat-HK2. Fig. 17 displays the current record of the open state of VDAC at 50 mV. As compared with the control, the addition of 120 nM HK2 induces high frequency channel noise. Subsequent addition of 20 μM of competing Tat-HK2 inhibits HK2 binding of VDAC as displayed by the suppression of this high frequency noise.

Figure 18

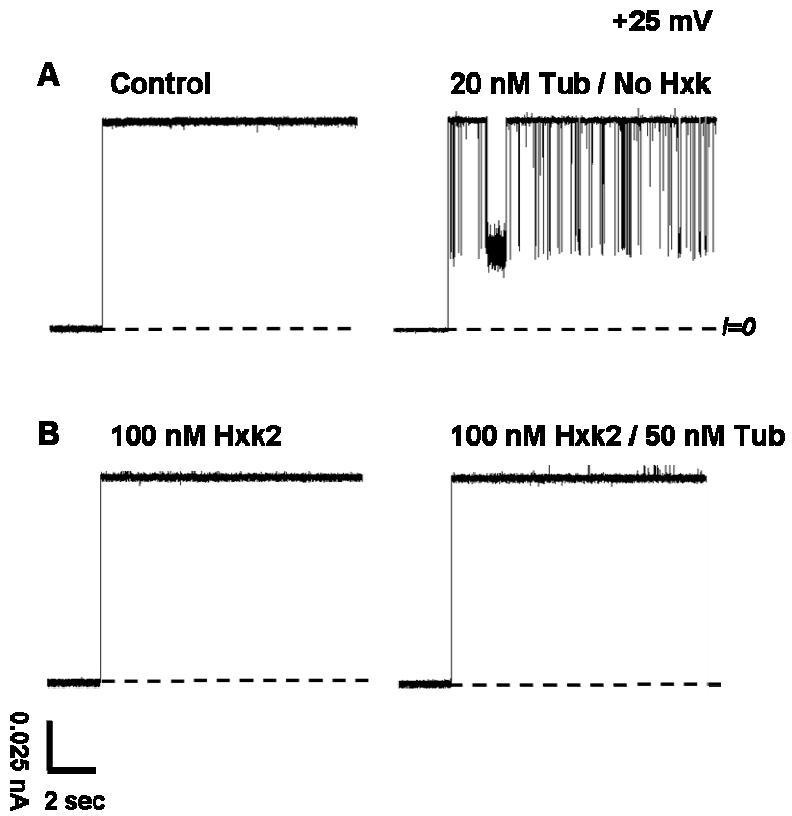

Full length HK competes with tubulin-VDAC interaction. Fig. 18 depicts the current record through one single VDAC channel (A) with and without 20 nM of tubulin present. When the channel is first treated with 100 nM HK2, we see no changes from the control. However, subsequent tubulin addition induces no channel blockages even with 50 nM tubulin present (B).

Figure 19

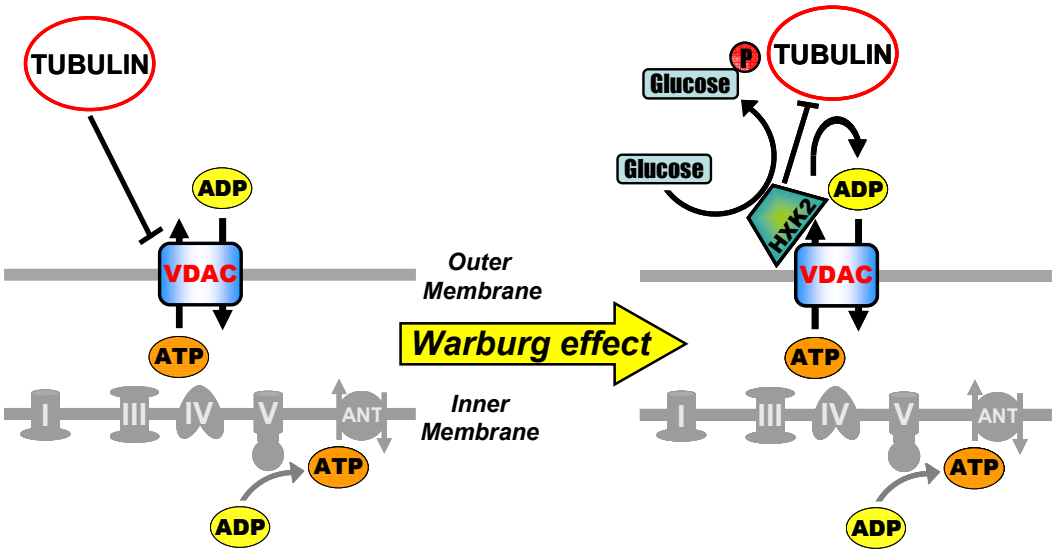

HK2 competition with tubulin for VDAC binding could be a hallmark of the Warburg effect. Here, we propose a scheme in which HK2 competition with tubulin for VDAC binding leads to the promotion of the classically defined Warburg effect. When HK2 binds VDAC, it blocks tubulin from binding VDAC, maintaining VDAC in its open conformation. HK2 has preferential access to ATP flux, promoting the phosphorylation of glucose in support of glycolysis.

REFERENCES

Abu-Hamad, S., H. Zaid, et al. (2008). "Hexokinase-I protection against apoptotic cell death is mediated via interaction with the voltage-dependent anion channel-1: mapping the site of binding." J Biol Chem **283**(19): 13482-13490.

Aliev, G., M. E. Obrenovich, et al. (2013). "Link between cancer and Alzheimer disease via oxidative stress induced by nitric oxide-dependent mitochondrial DNA overproliferation and deletion." Oxid Med Cell Longev **2013**: 962984.

Amos, L. A. and D. Schlieper (2005). "Microtubules and maps." Adv Protein Chem **71**: 257-298.

Anflous, K., O. Blondel, et al. (1998). "Characterization of rat porin isoforms: cloning of a cardiac type-3 variant encoding an additional methionine at its putative N-terminal region." Biochim Biophys Acta **1399**(1): 47-50.

Angeles, R., J. Devine, et al. (1999). "Mutations in the voltage-dependent anion channel of the mitochondrial outer membrane cause a dominant nonlethal growth impairment." J Bioenerg Biomembr **31**(2): 143-151.

Appaix, F., A. V. Kuznetsov, et al. (2003). "Possible role of cytoskeleton in intracellular arrangement and regulation of mitochondria." Exp Physiol **88**(1): 175-190.

Azoulay-Zohar, H., A. Israelson, et al. (2004). "In self-defence: hexokinase promotes voltage-dependent anion channel closure and prevents mitochondria-mediated apoptotic cell death." Biochem J **377**(Pt 2): 347-355.

Bahamonde, M. I., J. M. Fernandez-Fernandez, et al. (2003). "Plasma membrane voltage-dependent anion channel mediates antiestrogen-activated maxi Cl- currents in C1300 neuroblastoma cells." J Biol Chem **278**(35): 33284-33289.

Bahamonde, M. I. and M. A. Valverde (2003). "Voltage-dependent anion channel localises to the plasma membrane and peripheral but not perinuclear mitochondria." Pflugers Arch **446**(3): 309-313.

Baines, C. P., R. A. Kaiser, et al. (2007). "Voltage-dependent anion channels are dispensable for mitochondrial-dependent cell death." Nat Cell Biol **9**(5): 550-555.

Banerjee, J. and S. Ghosh (2006). "Phosphorylation of rat brain mitochondrial voltage-dependent anion as a potential tool to control leakage of cytochrome c." J Neurochem **98**(3): 670-676.

Basanez, G., L. Soane, et al. (2012). "A new view of the lethal apoptotic pore." PLoS Biol **10**(9): e1001399.

Bauer, A. J., S. Gieschler, et al. (2011). "Functional model of metabolite gating by human voltage-dependent anion channel 2." Biochemistry **50**(17): 3408-3410.

Bayrhuber, M., T. Meins, et al. (2008). "Structure of the human voltage-dependent anion channel." Proc Natl Acad Sci U S A **105**(40): 15370-15375.

Bera, A. K. and S. Ghosh (2001). "Dual mode of gating of voltage-dependent anion channel as revealed by phosphorylation." J Struct Biol **135**(1): 67-72.

Bera, A. K., S. Ghosh, et al. (1995). "Mitochondrial VDAC can be phosphorylated by cyclic AMP-dependent protein kinase." Biochem Biophys Res Commun **209**(1): 213-217.

Bernier-Valentin, F. and B. Rousset (1982). "Interaction of tubulin with rat liver mitochondria." J Biol Chem **257**(12): 7092-7099.

Blachly-Dyson, E. and M. Forte (2001). "VDAC channels." IUBMB Life **52**(3-5): 113-

118.
Blachly-Dyson, E., S. Peng, et al. (1990). "Selectivity changes in site-directed mutants of the VDAC ion channel: structural implications." Science **247**(4947): 1233-1236.
Blachly-Dyson, E., S. Z. Peng, et al. (1989). "Probing the structure of the mitochondrial channel, VDAC, by site-directed mutagenesis: a progress report." J Bioenerg Biomembr **21**(4): 471-483.
Bradbury, J. (2004). "Parkinson's disease in the PINK." Drug Discov Today **9**(12): 508-509.
Brustovetsky, N., J. M. Dubinsky, et al. (2003). "Two pathways for tBID-induced cytochrome c release from rat brain mitochondria: BAK- versus BAX-dependence." J Neurochem **84**(1): 196-207.
Burmester, T. and T. Hankeln (2009). "What is the function of neuroglobin?" J Exp Biol **212**(Pt 10): 1423-1428.
Burmester, T., B. Weich, et al. (2000). "A vertebrate globin expressed in the brain." Nature **407**(6803): 520-523.
Campbell, A. M. and S. H. Chan (2008). "Mitochondrial membrane cholesterol, the voltage dependent anion channel (VDAC), and the Warburg effect." J Bioenerg Biomembr **40**(3): 193-197.
Carre, M., N. Andre, et al. (2002). "Tubulin is an inherent component of mitochondrial membranes that interacts with the voltage-dependent anion channel." J Biol Chem **277**(37): 33664-33669.
Casadio, R., I. Jacoboni, et al. (2002). "A 3D model of the voltage-dependent anion channel (VDAC)." FEBS Lett **520**(1-3): 1-7.
Chiara, F., D. Castellaro, et al. (2008). "Hexokinase II detachment from mitochondria triggers apoptosis through the permeability transition pore independent of voltage-dependent anion channels." PLoS One **3**(3): e1852.
Colombini, M. (1989). "Voltage gating in the mitochondrial channel, VDAC." J Membr Biol **111**(2): 103-111.
Colombini, M. (2009). "The published 3D structure of the VDAC channel: native or not?" Trends Biochem Sci **34**(8): 382-389.
Cortese, J. D., A. L. Voglino, et al. (1992). "The ionic strength of the intermembrane space of intact mitochondria is not affected by the pH or volume of the intermembrane space." Biochim Biophys Acta **1100**(2): 189-197.
Craddock, T. J., J. A. Tuszynski, et al. (2012). "Cytoskeletal signaling: is memory encoded in microtubule lattices by CaMKII phosphorylation?" PLoS Comput Biol **8**(3): e1002421.
Crompton, M., S. Virji, et al. (1998). "Cyclophilin-D binds strongly to complexes of the voltage-dependent anion channel and the adenine nucleotide translocase to form the permeability transition pore." Eur J Biochem **258**(2): 729-735.
Cuadrado-Tejedor, M., M. Vilarino, et al. (2011). "Enhanced expression of the voltage-dependent anion channel 1 (VDAC1) in Alzheimer's disease transgenic mice: an insight into the pathogenic effects of amyloid-beta." J Alzheimers Dis **23**(2): 195-206.
Das, S. and C. Steenbergen (2012). "Mitochondrial adenine nucleotide transport and cardioprotection." J Mol Cell Cardiol **52**(2): 448-453.
Davies, S. P., H. Reddy, et al. (2000). "Specificity and mechanism of action of some

commonly used protein kinase inhibitors." Biochem J **351**(Pt 1): 95-105.
De Pinto, V., F. Guarino, et al. (2010). "Characterization of human VDAC isoforms: a peculiar function for VDAC3?" Biochim Biophys Acta **1797**(6-7): 1268-1275.
De Pinto, V., A. Messina, et al. (2010). "Voltage-dependent anion-selective channel (VDAC) in the plasma membrane." FEBS Lett **584**(9): 1793-1799.
Desagher, S., A. Osen-Sand, et al. (1999). "Bid-induced conformational change of Bax is responsible for mitochondrial cytochrome c release during apoptosis." J Cell Biol **144**(5): 891-901.
Desai, A. and T. J. Mitchison (1997). "Microtubule polymerization dynamics." Annu Rev Cell Dev Biol **13**: 83-117.
Distler, A. M., J. Kerner, et al. (2007). "Post-translational modifications of rat liver mitochondrial outer membrane proteins identified by mass spectrometry." Biochim Biophys Acta **1774**(5): 628-636.
Dixon, S. J., K. M. Lemberg, et al. (2012). "Ferroptosis: an iron-dependent form of nonapoptotic cell death." Cell **149**(5): 1060-1072.
Dolma, S., S. L. Lessnick, et al. (2003). "Identification of genotype-selective antitumor agents using synthetic lethal chemical screening in engineered human tumor cells." Cancer Cell **3**(3): 285-296.
Dominguez, R. and K. C. Holmes (2011). "Actin structure and function." Annu Rev Biophys **40**: 169-186.
Duchen, M. R. (1999). "Contributions of mitochondria to animal physiology: from homeostatic sensor to calcium signalling and cell death." J Physiol **516 (Pt 1)**: 1-17.
Elinder, F., N. Akanda, et al. (2005). "Opening of plasma membrane voltage-dependent anion channels (VDAC) precedes caspase activation in neuronal apoptosis induced by toxic stimuli." Cell Death Differ **12**(8): 1134-1140.
Flamholz, A., E. Noor, et al. (2013). "Glycolytic strategy as a tradeoff between energy yield and protein cost." Proc Natl Acad Sci U S A **110**(24): 10039-10044.
Fong, D. and B. Lee (1988). "Beta tubulin gene of the parasitic protozoan Leishmania mexicana." Mol Biochem Parasitol **31**(1): 97-106.
Gard, D. L. and M. W. Kirschner (1987). "Microtubule assembly in cytoplasmic extracts of Xenopus oocytes and eggs." J Cell Biol **105**(5): 2191-2201.
Geisler, S., K. M. Holmstrom, et al. (2010). "PINK1/Parkin-mediated mitophagy is dependent on VDAC1 and p62/SQSTM1." Nat Cell Biol **12**(2): 119-131.
Glass, D. B., H. C. Cheng, et al. (1986). "Differential and common recognition of the catalytic sites of the cGMP-dependent and cAMP-dependent protein kinases by inhibitory peptides derived from the heat-stable inhibitor protein." J Biol Chem **261**(26): 12166-12171.
Gogvadze, V. (2011). "Targeting mitochondria in fighting cancer." Curr Pharm Des **17**(36): 4034-4046.
Greenberg, D. A., K. Jin, et al. (2008). "Neuroglobin: an endogenous neuroprotectant." Curr Opin Pharmacol **8**(1): 20-24.
Gross, A., K. Pilcher, et al. (2000). "Biochemical and genetic analysis of the mitochondrial response of yeast to BAX and BCL-X(L)." Mol Cell Biol **20**(9): 3125-3136.
Guerrero, K., C. Monge, et al. (2010). "Study of possible interactions of tubulin,

microtubular network, and STOP protein with mitochondria in muscle cells." Mol Cell Biochem **337**(1-2): 239-249.
Gurel, E., K. M. Smeele, et al. (2009). "Ischemic preconditioning affects hexokinase activity and HKII in different subcellular compartments throughout cardiac ischemia-reperfusion." J Appl Physiol **106**(6): 1909-1916.
Gurnev, P. A., T. K. Rostovtseva, et al. (2011). "Tubulin-blocked state of VDAC studied by polymer and ATP partitioning." FEBS Lett **585**(14): 2363-2366.
Guzun, R., M. Gonzalez-Granillo, et al. (2012). "Regulation of respiration in muscle cells in vivo by VDAC through interaction with the cytoskeleton and MtCK within Mitochondrial Interactosome." Biochim Biophys Acta **1818**(6): 1545-1554.
Hanks, S. K. and T. Hunter (1995). "Protein kinases 6. The eukaryotic protein kinase superfamily: kinase (catalytic) domain structure and classification." FASEB J **9**(8): 576-596.
Hardwick, J. M., Y. B. Chen, et al. (2012). "Multipolar functions of BCL-2 proteins link energetics to apoptosis." Trends Cell Biol **22**(6): 318-328.
Hardwick, J. M. and L. Soane (2013). "Multiple functions of BCL-2 family proteins." Cold Spring Harb Perspect Biol **5**(2).
Hebert, L. E., J. Weuve, et al. (2013). "Alzheimer disease in the United States (2010-2050) estimated using the 2010 census." Neurology **80**(19): 1778-1783.
Heggeness, M. H., M. Simon, et al. (1978). "Association of mitochondria with microtubules in cultured cells." Proc Natl Acad Sci U S A **75**(8): 3863-3866.
Herman, W. H. (2013). "The economic costs of diabetes: is it time for a new treatment paradigm?" Diabetes Care **36**(4): 775-776.
Hiller, S., R. G. Garces, et al. (2008). "Solution structure of the integral human membrane protein VDAC-1 in detergent micelles." Science **321**(5893): 1206-1210.
Hoppins, S. and J. Nunnari (2012). "Cell Biology. Mitochondrial dynamics and apoptosis--the ER connection." Science **337**(6098): 1052-1054.
Hsu, P. P. and D. M. Sabatini (2008). "Cancer cell metabolism: Warburg and beyond." Cell **134**(5): 703-707.
Hsu, Y. T. and R. J. Youle (1998). "Bax in murine thymus is a soluble monomeric protein that displays differential detergent-induced conformations." J Biol Chem **273**(17): 10777-10783.
Hunter, T. (1995). "Protein kinases and phosphatases: the yin and yang of protein phosphorylation and signaling." Cell **80**(2): 225-236.
Janke, C. and M. Kneussel (2010). "Tubulin post-translational modifications: encoding functions on the neuronal microtubule cytoskeleton." Trends Neurosci **33**(8): 362-372.
Jonas, E. A., J. M. Hardwick, et al. (2005). "Actions of BAX on mitochondrial channel activity and on synaptic transmission." Antioxid Redox Signal **7**(9-10): 1092-1100.
Kerner, J., K. Lee, et al. (2012). "VDAC proteomics: Post-translation modifications." Biochim Biophys Acta **1818**(6): 1520-1525.
Kirschner, M. and E. Schulze (1986). "Morphogenesis and the control of microtubule dynamics in cells." J Cell Sci Suppl **5**: 293-310.
Kowal, S. L., T. M. Dall, et al. (2013). "The current and projected economic burden of

Parkinson's disease in the United States." Mov Disord **28**(3): 311-318.
Krauskopf, A., O. Eriksson, et al. (2006). "Properties of the permeability transition in VDAC1(-/-) mitochondria." Biochim Biophys Acta **1757**(5-6): 590-595.
Krendel, M., G. Sgourdas, et al. (1998). "Disassembly of actin filaments leads to increased rate and frequency of mitochondrial movement along microtubules." Cell Motil Cytoskeleton **40**(4): 368-378.
Lechauve, C., S. Augustin, et al. (2012). "Neuroglobin involvement in respiratory chain function and retinal ganglion cell integrity." Biochim Biophys Acta **1823**(12): 2261-2273.
Lemasters, J. J., E. L. Holmuhamedov, et al. (2012). "Regulation of mitochondrial function by voltage dependent anion channels in ethanol metabolism and the Warburg effect." Biochim Biophys Acta **1818**(6): 1536-1544.
Lemasters, J. J. and V. K. Ramshesh (2007). "Imaging of mitochondrial polarization and depolarization with cationic fluorophores." Methods Cell Biol **80**: 283-295.
Lemeshko, V. V. (2006). "Theoretical evaluation of a possible nature of the outer membrane potential of mitochondria." Eur Biophys J **36**(1): 57-66.
Li, H., H. Zhu, et al. (1998). "Cleavage of BID by caspase 8 mediates the mitochondrial damage in the Fas pathway of apoptosis." Cell **94**(4): 491-501.
Ligon, L. A. and O. Steward (2000). "Role of microtubules and actin filaments in the movement of mitochondria in the axons and dendrites of cultured hippocampal neurons." J Comp Neurol **427**(3): 351-361.
Lopez-Lazaro, M. (2008). "The warburg effect: why and how do cancer cells activate glycolysis in the presence of oxygen?" Anticancer Agents Med Chem **8**(3): 305-312.
Lu, L., C. Zhang, et al. (2013). "Voltage-dependent anion channel involved in the alpha-synuclein-induced dopaminergic neuron toxicity in rats." Acta Biochim Biophys Sin (Shanghai) **45**(3): 170-178.
Lunt, S. Y. and M. G. Vander Heiden (2011). "Aerobic glycolysis: meeting the metabolic requirements of cell proliferation." Annu Rev Cell Dev Biol **27**: 441-464.
Maldonado, E. N. and J. J. Lemasters (2012). "Warburg revisited: regulation of mitochondrial metabolism by voltage-dependent anion channels in cancer cells." J Pharmacol Exp Ther **342**(3): 637-641.
Maldonado, E. N., J. Patnaik, et al. (2010). "Free tubulin modulates mitochondrial membrane potential in cancer cells." Cancer Res **70**(24): 10192-10201.
Maldonado, E. N., K. L. Sheldon, et al. (2013). "Voltage dependent anion channels modulate mitochondrial metabolism in cancer cells: regulation by free tubulin and erastin." Journal of Biological Chemistry.
Maldonado, E. N., K. L. Sheldon, et al. (2013). "Voltage-dependent Anion Channels Modulate Mitochondrial Metabolism in Cancer Cells: REGULATION BY FREE TUBULIN AND ERASTIN." J Biol Chem **288**(17): 11920-11929.
Manczak, M. and P. H. Reddy (2012). "Abnormal interaction of VDAC1 with amyloid beta and phosphorylated tau causes mitochondrial dysfunction in Alzheimer's disease." Hum Mol Genet **21**(23): 5131-5146.
Mannella, C. A., M. Forte, et al. (1992). "Toward the molecular structure of the mitochondrial channel, VDAC." J Bioenerg Biomembr **24**(1): 7-19.
Mannella, C. A., A. F. Neuwald, et al. (1996). "Detection of likely transmembrane beta

strand regions in sequences of mitochondrial pore proteins using the Gibbs sampler." J Bioenerg Biomembr **28**(2): 163-169.
Margulis, L. (1975). "Symbiotic theory of the origin of eukaryotic organelles; criteria for proof." Symp Soc Exp Biol(29): 21-38.
Margulis, L., M. Chapman, et al. (2006). "The last eukaryotic common ancestor (LECA): acquisition of cytoskeletal motility from aerotolerant spirochetes in the Proterozoic Eon." Proc Natl Acad Sci U S A **103**(35): 13080-13085.
Martel, C., M. Allouche, et al. (2013). "Glycogen synthase kinase 3-mediated voltage-dependent anion channel phosphorylation controls outer mitochondrial membrane permeability during lipid accumulation." Hepatology **57**(1): 93-102.
Martinez, A., M. Alonso, et al. (2002). "First non-ATP competitive glycogen synthase kinase 3 beta (GSK-3beta) inhibitors: thiadiazolidinones (TDZD) as potential drugs for the treatment of Alzheimer's disease." J Med Chem **45**(6): 1292-1299.
Martinez, A., A. Castro, et al. (2002). "Glycogen synthase kinase 3 (GSK-3) inhibitors as new promising drugs for diabetes, neurodegeneration, cancer, and inflammation." Med Res Rev **22**(4): 373-384.
Massa, R., L. N. Marliera, et al. (2000). "Intracellular localization and isoform expression of the voltage-dependent anion channel (VDAC) in normal and dystrophic skeletal muscle." J Muscle Res Cell Motil **21**(5): 433-442.
Mathupala, S. P., Y. H. Ko, et al. (2006). "Hexokinase II: cancer's double-edged sword acting as both facilitator and gatekeeper of malignancy when bound to mitochondria." Oncogene **25**(34): 4777-4786.
Mathupala, S. P., Y. H. Ko, et al. (2009). "Hexokinase-2 bound to mitochondria: cancer's stygian link to the "Warburg Effect" and a pivotal target for effective therapy." Semin Cancer Biol **19**(1): 17-24.
Mathupala, S. P. and P. L. Pedersen (2010). "Voltage dependent anion channel-1 (VDAC-1) as an anti-cancer target." Cancer Biol Ther **9**(12): 1053-1056.
McGhee, D. J., P. L. Royle, et al. (2013). "A systematic review of biomarkers for disease progression in Parkinson's disease." BMC Neurol **13**: 35.
Menzel, V. A., M. C. Cassara, et al. (2009). "Molecular and functional characterization of VDAC2 purified from mammal spermatozoa." Biosci Rep **29**(6): 351-362.
Mertins, B., G. Psakis, et al. (2012). "Flexibility of the N-terminal mVDAC1 segment controls the channel's gating behavior." PLoS One **7**(10): e47938.
Messina, A., S. Reina, et al. (2012). "VDAC isoforms in mammals." Biochim Biophys Acta **1818**(6): 1466-1476.
Miller, W. R. (2002). "Regulatory subunits of PKA and breast cancer." Ann N Y Acad Sci **968**: 37-48.
Mlayeh, L., S. Chatkaew, et al. (2010). "Modulation of plant mitochondrial VDAC by phytosterols." Biophys J **99**(7): 2097-2106.
Morrison, K. E. (2003). "Parkin mutations and early onset parkinsonism." Brain **126**(Pt 6): 1250-1251.
Nederlof, R., C. Xie, et al. (2013). "Pathophysiological consequences of TAT-HKII peptide administration are independent of impaired vascular function and ensuing ischemia." Circ Res **112**(2): e8-13.
Neumann, D., J. Buckers, et al. (2010). "Two-color STED microscopy reveals different degrees of colocalization between hexokinase-I and the three human VDAC

isoforms." PMC Biophys **3**(1): 4.
Nogales, E., S. G. Wolf, et al. (1998). "Structure of the alpha beta tubulin dimer by electron crystallography." Nature **391**(6663): 199-203.
Noskov, S. Y., T. K. Rostovtseva, et al. (2013). "ATP transport through VDAC and VDAC/tubulin complex probed by equilibrium and non-equilibrium MD simulations." Biochemistry.
Ott, M., E. Norberg, et al. (2009). "Mitochondrial targeting of tBid/Bax: a role for the TOM complex?" Cell Death Differ **16**(8): 1075-1082.
Palmieri, F. and V. De Pinto (1989). "Purification and properties of the voltage-dependent anion channel of the outer mitochondrial membrane." J Bioenerg Biomembr **21**(4): 417-425.
Parsons, D. F., W. D. Bonner Jr, et al. (1965). "ELECTRON MICROSCOPY OF ISOLATED PLANT MITOCHONDRIA AND PLASTIDS USING BOTH THE THIN-SECTION AND NEGATIVE-STAINING TECHNIQUES." Canadian Journal of Botany **43**(6): 647-655.
Pastorino, J. G. and J. B. Hoek (2008). "Regulation of hexokinase binding to VDAC." J Bioenerg Biomembr **40**(3): 171-182.
Pastorino, J. G., J. B. Hoek, et al. (2005). "Activation of glycogen synthase kinase 3beta disrupts the binding of hexokinase II to mitochondria by phosphorylating voltage-dependent anion channel and potentiates chemotherapy-induced cytotoxicity." Cancer Res **65**(22): 10545-10554.
Patra, K. C. and N. Hay (2013). "Hexokinase 2 as oncotarget." Oncotarget.
Patra, K. C., Q. Wang, et al. (2013). "Hexokinase 2 is required for tumor initiation and maintenance and its systemic deletion is therapeutic in mouse models of cancer." Cancer Cell **24**(2): 213-228.
Pavlica, R. J., C. B. Hesler, et al. (1990). "Two-dimensional gel electrophoretic resolution of the polypeptides of rat liver mitochondria and the outer membrane." Biochim Biophys Acta **1022**(1): 115-125.
Pedersen, P. L. (1978). "Tumor mitochondria and the bioenergetics of cancer cells." Prog Exp Tumor Res **22**: 190-274.
Pedersen, P. L. (2007). "Warburg, me and Hexokinase 2: Multiple discoveries of key molecular events underlying one of cancers' most common phenotypes, the "Warburg Effect", i.e., elevated glycolysis in the presence of oxygen." J Bioenerg Biomembr **39**(3): 211-222.
Pedersen, P. L. (2008). "Voltage dependent anion channels (VDACs): a brief introduction with a focus on the outer mitochondrial compartment's roles together with hexokinase-2 in the "Warburg effect" in cancer." J Bioenerg Biomembr **40**(3): 123-126.
Pediaditakis, P., J. S. Kim, et al. (2010). "Inhibition of the mitochondrial permeability transition by protein kinase A in rat liver mitochondria and hepatocytes." Biochem J **431**(3): 411-421.
Peng, S., E. Blachly-Dyson, et al. (1992). "Determination of the number of polypeptide subunits in a functional VDAC channel from Saccharomyces cerevisiae." J Bioenerg Biomembr **24**(1): 27-31.
Peng, S., E. Blachly-Dyson, et al. (1992). "Large scale rearrangement of protein domains is associated with voltage gating of the VDAC channel." Biophys J **62**(1): 123-

131; discussion 131-125.
Pesce, A., S. Dewilde, et al. (2003). "Human brain neuroglobin structure reveals a distinct mode of controlling oxygen affinity." Structure **11**(9): 1087-1095.
Poleti, M. D., A. C. Tesch, et al. (2010). "Relationship between expression of voltage-dependent anion channel (VDAC) isoforms and type of hexokinase binding sites on brain mitochondria." J Mol Neurosci **41**(1): 48-54.
Porcelli, A. M., A. Ghelli, et al. (2005). "pH difference across the outer mitochondrial membrane measured with a green fluorescent protein mutant." Biochem Biophys Res Commun **326**(4): 799-804.
Porter, R. K. and M. D. Brand (1995). "Mitochondrial proton conductance and H+/O ratio are independent of electron transport rate in isolated hepatocytes." Biochem J **310 (Pt 2)**: 379-382.
Priault, M., B. Chaudhuri, et al. (1999). "Investigation of bax-induced release of cytochrome c from yeast mitochondria permeability of mitochondrial membranes, role of VDAC and ATP requirement." Eur J Biochem **260**(3): 684-691.
Priel, A., J. A. Tuszynski, et al. (2005). "Transitions in microtubule C-termini conformations as a possible dendritic signaling phenomenon." Eur Biophys J **35**(1): 40-52.
Rahmani, Z., C. Maunoury, et al. (1998). "Isolation of a novel human voltage-dependent anion channel gene." Eur J Hum Genet **6**(4): 337-340.
Rich, P. R. (2003). "The molecular machinery of Keilin's respiratory chain." Biochem Soc Trans **31**(Pt 6): 1095-1105.
Rodionov, V., E. Nadezhdina, et al. (1999). "Centrosomal control of microtubule dynamics." Proc Natl Acad Sci U S A **96**(1): 115-120.
Rostovtseva, T. and M. Colombini (1996). "ATP flux is controlled by a voltage-gated channel from the mitochondrial outer membrane." J Biol Chem **271**(45): 28006-28008.
Rostovtseva, T. and M. Colombini (1997). "VDAC channels mediate and gate the flow of ATP: implications for the regulation of mitochondrial function." Biophys J **72**(5): 1954-1962.
Rostovtseva, T. K., B. Antonsson, et al. (2004). "Bid, but not Bax, regulates VDAC channels." J Biol Chem **279**(14): 13575-13583.
Rostovtseva, T. K. and S. M. Bezrukov (1998). "ATP transport through a single mitochondrial channel, VDAC, studied by current fluctuation analysis." Biophys J **74**(5): 2365-2373.
Rostovtseva, T. K. and S. M. Bezrukov (2008). "VDAC regulation: role of cytosolic proteins and mitochondrial lipids." J Bioenerg Biomembr **40**(3): 163-170.
Rostovtseva, T. K., P. A. Gurnev, et al. (2012). "Membrane lipid composition regulates tubulin interaction with mitochondrial voltage-dependent anion channel." J Biol Chem **287**(35): 29589-29598.
Rostovtseva, T. K., N. Kazemi, et al. (2006). "Voltage gating of VDAC is regulated by nonlamellar lipids of mitochondrial membranes." J Biol Chem **281**(49): 37496-37506.
Rostovtseva, T. K., K. L. Sheldon, et al. (2008). "Tubulin binding blocks mitochondrial voltage-dependent anion channel and regulates respiration." Proc Natl Acad Sci U S A **105**(48): 18746-18751.

Rostovtseva, T. K., W. Tan, et al. (2005). "On the role of VDAC in apoptosis: fact and fiction." J Bioenerg Biomembr **37**(3): 129-142.
Sackett, D. L., B. Bhattacharyya, et al. (1985). "Tubulin subunit carboxyl termini determine polymerization efficiency." J Biol Chem **260**(1): 43-45.
Saetersdal, T., G. Greve, et al. (1990). "Associations between beta-tubulin and mitochondria in adult isolated heart myocytes as shown by immunofluorescence and immunoelectron microscopy." Histochemistry **95**(1): 1-10.
Saks, V. A., A. V. Kuznetsov, et al. (1995). "Control of cellular respiration in vivo by mitochondrial outer membrane and by creatine kinase. A new speculative hypothesis: possible involvement of mitochondrial-cytoskeleton interactions." J Mol Cell Cardiol **27**(1): 625-645.
Sampson, M. J., R. S. Lovell, et al. (1996). "Isolation, characterization, and mapping of two mouse mitochondrial voltage-dependent anion channel isoforms." Genomics **33**(2): 283-288.
Sampson, M. J., R. S. Lovell, et al. (1997). "The murine voltage-dependent anion channel gene family. Conserved structure and function." J Biol Chem **272**(30): 18966-18973.
Schein, S. J., M. Colombini, et al. (1976). "Reconstitution in planar lipid bilayers of a voltage-dependent anion-selective channel obtained from paramecium mitochondria." J Membr Biol **30**(2): 99-120.
Schmidt-Mende, J., E. Hellstrom-Lindberg, et al. (2000). "Freezing induces artificial cleavage of apoptosis-related proteins in human bone marrow cells." J Immunol Methods **245**(1-2): 91-94.
Schwertz, H., J. M. Carter, et al. (2007). "Myocardial ischemia/reperfusion causes VDAC phosphorylation which is reduced by cardioprotection with a p38 MAP kinase inhibitor." Proteomics **7**(24): 4579-4588.
Shah, C., C. Z. Xu, et al. (2001). "Properties of microtubules assembled from mammalian tubulin synthesized in Escherichia coli." Biochemistry **40**(15): 4844-4852.
Sheldon, K. L., E. N. Maldonado, et al. (2011). "Phosphorylation of voltage-dependent anion channel by serine/threonine kinases governs its interaction with tubulin." PLoS One **6**(10): e25539.
Shimizu, S., T. Ide, et al. (2000). "Electrophysiological study of a novel large pore formed by Bax and the voltage-dependent anion channel that is permeable to cytochrome c." J Biol Chem **275**(16): 12321-12325.
Shimizu, S., M. Narita, et al. (1999). "Bcl-2 family proteins regulate the release of apoptogenic cytochrome c by the mitochondrial channel VDAC." Nature **399**(6735): 483-487.
Shimizu, S., Y. Shinohara, et al. (2000). "Bax and Bcl-xL independently regulate apoptotic changes of yeast mitochondria that require VDAC but not adenine nucleotide translocator." Oncogene **19**(38): 4309-4318.
Shinohara, Y., T. Ishida, et al. (2000). "Characterization of porin isoforms expressed in tumor cells." Eur J Biochem **267**(19): 6067-6073.
Shoshan-Barmatz, V., M. Zakar, et al. (2009). "Key regions of VDAC1 functioning in apoptosis induction and regulation by hexokinase." Biochim Biophys Acta **1787**(5): 421-430.
Shulga, N., R. Wilson-Smith, et al. (2009). "Hexokinase II detachment from the

mitochondria potentiates cisplatin induced cytotoxicity through a caspase-2 dependent mechanism." Cell Cycle **8**(20): 3355-3364.
Siegel, R., D. Naishadham, et al. (2013). "Cancer statistics, 2013." CA Cancer J Clin **63**(1): 11-30.
Siekevitz, P. (1957). Powerhouse of the cell. San Francisco, Freeman.
Sigworth, F. J. and S. M. Sine (1987). "Data transformations for improved display and fitting of single-channel dwell time histograms." Biophys J **52**(6): 1047-1054.
Simamura, E., K. Hirai, et al. (2006). "Furanonaphthoquinones cause apoptosis of cancer cells by inducing the production of reactive oxygen species by the mitochondrial voltage-dependent anion channel." Cancer Biol Ther **5**(11): 1523-1529.
Simamura, E., H. Shimada, et al. (2008). "Mitochondrial voltage-dependent anion channels (VDACs) as novel pharmacological targets for anti-cancer agents." J Bioenerg Biomembr **40**(3): 213-217.
Song, J., C. Midson, et al. (1998). "The sensor regions of VDAC are translocated from within the membrane to the surface during the gating processes." Biophys J **74**(6): 2926-2944.
Song, J., C. Midson, et al. (1998). "The topology of VDAC as probed by biotin modification." J Biol Chem **273**(38): 24406-24413.
Sun, Y., A. A. Vashisht, et al. (2012). "Voltage-dependent anion channels (VDACs) recruit Parkin to defective mitochondria to promote mitochondrial autophagy." J Biol Chem **287**(48): 40652-40660.
Szabo, I., V. De Pinto, et al. (1993). "The mitochondrial permeability transition pore may comprise VDAC molecules. II. The electrophysiological properties of VDAC are compatible with those of the mitochondrial megachannel." FEBS Lett **330**(2): 206-210.
Szabo, I. and M. Zoratti (1993). "The mitochondrial permeability transition pore may comprise VDAC molecules. I. Binary structure and voltage dependence of the pore." FEBS Lett **330**(2): 201-205.
Tait, S. W. and D. R. Green (2012). "Mitochondria and cell signalling." J Cell Sci **125**(Pt 4): 807-815.
Tan, W. and M. Colombini (2007). "VDAC closure increases calcium ion flux." Biochim Biophys Acta **1768**(10): 2510-2515.
Teijido, O., R. Ujwal, et al. (2012). "Affixing N-terminal alpha-helix to the wall of the voltage-dependent anion channel does not prevent its voltage gating." J Biol Chem **287**(14): 11437-11445.
Thinnes, F. P. (2011). "Apoptogenic interactions of plasmalemmal type-1 VDAC and Abeta peptides via GxxxG motifs induce Alzheimer's disease - a basic model of apoptosis?" Wien Med Wochenschr **161**(9-10): 274-276.
Tortora, G. and G. Daniele (2006). "[New frontiers in cancer treatment]." Recenti Prog Med **97**(12): 781-786.
Tsujimoto, Y. and S. Shimizu (2000). "VDAC regulation by the Bcl-2 family of proteins." Cell Death Differ **7**(12): 1174-1181.
Tuszynski, J. A., E. J. Carpenter, et al. (2006). "The evolution of the structure of tubulin and its potential consequences for the role and function of microtubules in cells and embryos." Int J Dev Biol **50**(2-3): 341-358.
Ujwal, R., D. Cascio, et al. (2008). "The crystal structure of mouse VDAC1 at 2.3 A

resolution reveals mechanistic insights into metabolite gating." Proc Natl Acad Sci U S A **105**(46): 17742-17747.
Van Damme, P., T. Arnesen, et al. (2011). "Protein alpha-N-acetylation studied by N-terminomics." FEBS J **278**(20): 3822-3834.
Vander Heiden, M. G., N. S. Chandel, et al. (2000). "Outer mitochondrial membrane permeability can regulate coupled respiration and cell survival." Proc Natl Acad Sci U S A **97**(9): 4666-4671.
Verdanis, A. (1977). "Protein kinase activity at the inner membrane of mammalian mitochondria." J Biol Chem **252**(3): 807-813.
Vignais, P. V. (1976). "Molecular and physiological aspects of adenine nucleotide transport in mitochondria." Biochim Biophys Acta **456**(1): 1-38.
Wallace, D. C. (2005). "A mitochondrial paradigm of metabolic and degenerative diseases, aging, and cancer: a dawn for evolutionary medicine." Annu Rev Genet **39**: 359-407.
Wang, G., S. J. Jones, et al. (2006). "Identification of genes targeted by the androgen and PKA signaling pathways in prostate cancer cells." Oncogene **25**(55): 7311-7323.
Warburg, O. (1956). "On the origin of cancer cells." Science **123**(3191): 309-314.
Warburg, O., F. Wind, et al. (1927). "The Metabolism of Tumors in the Body." J Gen Physiol **8**(6): 519-530.
Weinhouse, S. (1976). "The Warburg hypothesis fifty years later." Z Krebsforsch Klin Onkol Cancer Res Clin Oncol **87**(2): 115-126.
Wenner, C. E. (2010). "Cell signaling and cancer-possible targets for therapy." J Cell Physiol **223**(2): 299-308.
Werkheiser, W. C. and W. Bartley (1957). "The study of steady-state concentrations of internal solutes of mitochondria by rapid centrifugal transfer to a fixation medium." Biochem J **66**(1): 79-91.
Wilson, J. E. (2003). "Isozymes of mammalian hexokinase: structure, subcellular localization and metabolic function." J Exp Biol **206**(Pt 12): 2049-2057.
Wolf, A., S. Agnihotri, et al. (2011). "Hexokinase 2 is a key mediator of aerobic glycolysis and promotes tumor growth in human glioblastoma multiforme." J Exp Med **208**(2): 313-326.
Wolff, J., D. L. Sackett, et al. (1996). "Cation selective promotion of tubulin polymerization by alkali metal chlorides." Protein Sci **5**(10): 2020-2028.
Xu, X., W. Decker, et al. (1999). "Mouse VDAC isoforms expressed in yeast: channel properties and their roles in mitochondrial outer membrane permeability." J Membr Biol **170**(2): 89-102.
Xu, X., J. G. Forbes, et al. (2001). "Actin modulates the gating of Neurospora crassa VDAC." J Membr Biol **180**(1): 73-81.
Yagoda, N., M. von Rechenberg, et al. (2007). "RAS-RAF-MEK-dependent oxidative cell death involving voltage-dependent anion channels." Nature **447**(7146): 864-868.
Yamamoto, T., A. Yamada, et al. (2006). "VDAC1, having a shorter N-terminus than VDAC2 but showing the same migration in an SDS-polyacrylamide gel, is the predominant form expressed in mitochondria of various tissues." J Proteome Res **5**(12): 3336-3344.
Yi, C. H., H. Pan, et al. (2011). "Metabolic regulation of protein N-alpha-acetylation by

Bcl-xL promotes cell survival." Cell **146**(4): 607-620.
Yu, Z., N. Liu, et al. (2013). "Neuroglobin overexpression inhibits oxygen-glucose deprivation-induced mitochondrial permeability transition pore opening in primary cultured mouse cortical neurons." Neurobiol Dis **56**: 95-103.
Yu, Z., J. Xu, et al. (2012). "Mitochondrial distribution of neuroglobin and its response to oxygen-glucose deprivation in primary-cultured mouse cortical neurons." Neuroscience **218**: 235-242.
Zelenina, E. V., L. V. Avramova, et al. (1991). "[Preparation of hexokinase isoenzyme II with expressed adsorption properties]." Biokhimiia **56**(6): 1096-1103.
Zhang, X., J. Ye, et al. (2011). "A proteome-scale study on in vivo protein Nalpha-acetylation using an optimized method." Proteomics **11**(1): 81-93.
Zheng, J. (2012). "Energy metabolism of cancer: Glycolysis versus oxidative phosphorylation (Review)." Oncol Lett **4**(6): 1151-1157.
Zizi, M., C. Byrd, et al. (1998). "The voltage-gating process of the voltage-dependent anion channel is sensitive to ion flow." Biophys J **75**(2): 704-713.
Zuurbier, C. J., K. M. Smeele, et al. (2009). "Mitochondrial hexokinase and cardioprotection of the intact heart." J Bioenerg Biomembr **41**(2): 181-185.

Kely L. Sheldon

52 Q Street NE • Washington, DC • 20002 SheldonK@mail.nih.gov • 704.617.1831

EDUCATION

Doctorate of Philosophy, Molecular Microbiology and Immunology, Johns Hopkins, Baltimore, Maryland, National Institutes of Health, Graduate IRTA Fellowship Award Recipient

Bachelor of Science *with honors*, Biology, Clemson University, Clemson, South Carolina, May 2007

LABORATORY EXPERIENCE

Pre Doctorial IRTA Fellow, Laboratory of Physical and Structural Biology, NICHD, NIH, Bethesda, Maryland in partnership with

The Johns Hopkins School of Public Health, The Johns Hopkins University, Baltimore, Maryland Under Dr. Sergey Bezrukov and Dr. Tatiana Rostovtseva, Fall 2009 -Present Elucidating the regulation of interaction between dimeric tubulin and VDAC by phosphorylation: control of cellular respiration

IRTA Fellow, Laboratory of Physical and Structural Biology, NICHD, NIH, Bethesda, Maryland Under Dr. Sergey Bezrukov and Dr. Tatiana Rostovtseva, Spring 2007 – Fall 2009 Exploring the role of cytosolic protein tubulin and its interaction with the mitochondrial outer membrane voltage dependent anion channel, VDAC

Undergraduate Staff Scientist, Clemson University Center for Bioelectronics, Biosensors and Biochips, Clemson University Under Dr. Anthony Guiseppi-Elie, Fall 2006 -Spring 2007 Studying the biotechnical applications of chemically responsive electroconductive hydrogels which will subsequently be used for molecular biosensor, biochip, and tissue biosensor applications

Research Assistant, Department of Biochemistry and Molecular Biology, The Medical University of South Carolina Under Dr. Yusuf A. Hannun, Summers of 2006 *and* 2007 Determining a possible mechanism for elevated interleukin-6 generation seen in breast cancer patients reported in several clinical studies
PROFICIENT IN: Cell culture, sterile technique, gel electrophoresis, thin-layer chromatography, RNA interference, shRNA design and manipulation, transient transfection, polymerase chain reaction, bacterial transformation, yeast transformation, electrophysiology, patch clamp technique, protein isolation and purification

HONORS AND ACHIEVEMENTS

FEB Mitochondrial Biochemistry, *Physiology and Pathology Conference*, Cambridge, UK 2012
Travel Award Recipient, and platform speaker at the Mitochondrial Physiology MiP Conference held at Cambridge University

Dr. J Harold Drudge Scholarship, The Johns Hopkins University, Baltimore, MD 2010 This fund was established in 2005 by gifts from the Estate of Harold Drudge and his daughter, Caran C. St. John. Dr. Drudge was a graduate of the School and worked on treatments for intestinal parasites at the University of Kentucky.

Student Research Achievement Award, 53rd Biophysical Society Meeting, Boston, MA 2009 Awarded for my work on the phosphorylation of the voltage dependent anion channel and its control of cellular respiration

Outstanding Scientific Research Award, The National Institutes of Health, Bethesda, MD 2008 Awarded the Outstanding Scientific Research Award for my work on tubulin and its control of respiration at the 2008 Mitochondrial Biology Conference sponsored by Johns Hopkins University and the NIH

Best Poster Award, The National Institutes of Health, Bethesda, MD 2008 Awarded best poster for work dealing with the voltage dependent anion channel and its interaction with tubulin at the 2008 NIH Spring Research Festival

Graduate Mentor, The National Institutes of Health, Bethesda, MD 2009 Mentored and trained two summer interns during their respective internships at the National Institutes of Health

PRESENTATIONS

1 **Sheldon K.L.**, Maldonado E. N., Lemasters J. J., Bezrukov S. M., Rostovtseva T. K. VDAC phosphorylation in control of mitochondrial respiration. Platform presentation, Biophysical Society 56th Annual Meeting, San Diego, CA (2012. 03)

2 **Sheldon K.L.**, Bezrukov S. M., Rostovtseva T. K. VDAC phosphorylation governs the respiration of mitochondria. Program on Physical Biology, Bethesda, MD (2011. 11)

PARTICIPATIONS

1 Maldonado E. N., DeHart D. N., Patnaik J. R., **Sheldon K. L.**, Rostovtseva T. K., Manevich Y., Townsend D., Lemasters J. J. Voltage dependent anion channel-3 (VDAC3) is the major isoform contributing to mitochondrial metabolism in HEPG2 cells and is regulated by free tubulin and erastin. Biophysical Society 56th Annual Meeting (2012. 02)

2 Rostovtseva T. K., **Sheldon K. L**., Gurnev P. A., Bezrukov S. M. VDAC regulation by tubulin and its physiological implications. Biophysical Society 56th Annual Meeting (2012. 02)

3 Rostovtseva T. K., **Sheldon K. L**., Gurnev P. A., Bezrukov S. M. VDAC-tubulin interaction as a missing link in regulation of mitochondrial respiration in health and disease. NICHD, Bethesda, MD (2011. 08)

4 **Sheldon K. L.**, Rostovtseva, T., Bezrukov S. Regulators of Respiration: Interplay between Tubulin, Mitochondrial Porin VDAC, and Cytosolic Kinases NICHD Forum Presentation, Bethesda, MD (2010. 05)

5 **Sheldon K. L.**, Bezrukov S., Rostovtseva, T. VDAC phosphorylation regulates interaction with tubulin Meeting of the Biophysical Society, 54th Annual Meeting, San Francisco, CA (2010. 03)

6 **Sheldon K. L.**, Bezrukov S., Rostovtseva, T. Role of C-terminal tails of tubulin in its interaction with mitochondrial channel VDAC Meeting of the Biophysical Society, 53rd Annual Meeting, Boston, Ma (2009. 02)

7 **Sheldon K. L.**, Dan Sackett, Sergey Bezrukov, Tatiana Rostovtseva Role of C-terminal tails of tubulin in its interaction with mitochondrial channel VDAC National Institutes of Health Spring Research Festival Bethesda, MD, USA. (2008. 09)

8 Kitatani K., **Sheldon K. L.**, Anelli V., Jenkins R.W., Sun Y., Grabowski G.A., Obeid L.M., Sun Y., Grabowski, and Hannun Y.A. "p38δ is a novel target for anti-proinflammation therapy of Gaucher disease."
SphingoTherapy Research Association, Tottori, Japan (2008. 07)

9 Kitatani K., **Sheldon K. L.**, Anelli V., Jenkins R.W., Sun Y., Grabowski G.A., Obeid L.M., Sun Y., Grabowski G.A., and Hannun Y.A. Acid β-glucosidase induces negative-regulation of p38 proinflammatory signaling kinase Lysosomal Diseases and the Brain Conference, Sacramento, CA, USA (2008. 05)

10 Tatiana K. Rostovtseva, Dan L. Sackett, **Kely Sheldon**, Claire Monge, Valdur Saks, Sergey M. Bezrukov. Cytoskeleton Regulates Mitochondria Respiration through a Tubulin-VDAC Direct Interaction. Joint Meeting of the Biophysical Society, 52nd Annual Meeting, Long Beach, CA (2008. 02)

11 Kitatani K., **Sheldon K. L.**, Jenkins R. W., and Hannun Y. A. Acid β-glucosidase (GBA1) counteracts p38 activation and consequent biosynthesis of interleukin-6: new insights for the pathogenesis of Gaucher's disease. Gordon Research Conference (Glycolipid & Sphingolipid Biology), Ciocco, Italy, (2008. 02)

12 **Sheldon K. L.**, Dan Sackett, Sergey Bezrukov, Tatiana Rostovtseva Role of C-terminal tails of tubulin in its interaction with mitochondrial channel VDAC 3rd International Mitochondria Minisymposium, Mitochondria and Their Proteomics Bethesda, MD, USA. (2008. 01)

13 Kitatani K., Jenkins R. W., **Sheldon K. L.**, and Hannun Y. A. Ceramide signaling terminates p38 MAPK signaling. 8th Annual Frontiers in Neuroscience Research Day, Charleston, SC, USA (2007. 03)

14 Kitatani K., Jenkins R. W., **Sheldon K. L.**, and Hannun Y. A. Defect in acid β glucosidase activity impairs ceramide signaling and termination of p38 signaling: New insights for the pathogenesis of Gaucher's disease. 4th International Charleston Ceramide Conference, Asilomar, CA, USA (2007. 03)

15 Jenkins R. W., **Sheldon K. L.**, Kitatani K., and Hannun Y. A. p38d is required for interleukin-6 production in acid Involvement of acid β glucosidase depleted cells: linking impaired ceramide formation to inflammation. 41th Annual Southeastern Regional Lipid Conference, Cashiers, NC, USA. (2006. 11)

16 Kitatani K., **Sheldon K. L.**, Jenkins R. W., and Hannun Y. A. Acid β glucosidase modulates protein

kinase C-dependent signal transduction. Gordon Research Conference (Glycolipid & Sphingolipid Biology), Ventura, CA, (2006. 01)

17 Kitatani K., **Sheldon K. L.**, Jenkins R. W., and Hannun Y. A. Involvement of acid β glucosidase in protein kinase C-dependent ceramide formation. 40th Annual Southeastern Regional Lipid Conference, Cashiers, NC, USA. (2005. 11)

PUBLICATIONS

1 Eduardo N. Maldonado, **Kely L. Sheldon**, David N. DeHart, Jyoti Patnaik, Yefim Manevich, Danyelle M. Townsend, Sergey M. Bezrukov, Tatiana K. Rostovtseva, and John J. Lemasters. Voltage-dependent anion channels modulate mitochondrial metabolism in cancer cells. (2013) *J Biol. Chem*.

2 **Kely L. Sheldon**, Eduardo N. Maldonado, John J. Lemasters, Tatiana K. Rostovtseva, and Sergey M. Bezrukov. VDAC phosphorylation by serine-threonine kinases regulate mitochondria respiration by modulating VDAC interaction with tubulin. (2011) *PLoSONE.*

3 Tatiana K. Rostovtseva, **Kely Sheldon**, Elnaz Hassanzadeh, Claire Monge, Valdur Saks, Sergey M. Bezrukov, and Dan L. Sackett. A "new" role for an old protein: Tubulin binding blocks mitochondrial voltage-dependent anion channel and regulates respiration. (2008) *PNAS*

4 Kazuyuki Kitatani**, Kely Sheldon**, Viviana Anelli, Ying Sun, Gregory A. Grabowski, Lina M. Obeid, and Yusuf A. Hannun. GBA1-dependent salvage pathway of ceramide formation counteracts p38δ and IL-6 biosynthesis. (2009) *J Biol. Chem*.

5 Kazuyuki Kitatani, **Kely Sheldon**, Vinodh Rajagopalan, Viviana Anelli, Russell W. Jenkins, Ying Sun, Gregory A. Grabowski, Lina M. Obeid, and Yusuf A. Hannun Involvement of acid B-glucosidase 1 in the salvage pathway of ceramide formation. (2009) *J Biol. Chem*.